PEPTIDE DRUG CANDIDATES

FOR PATHOGENIC AMYLOIDS

A THESIS SUBMITTED TO

THE GRADUATE SCHOOL OF ENGINEERING AND SCIENCE

OF BILKENT UNIVERSITY

IN PARTIAL FULFILLMENT OF THE REQUIREMENTS FOR

THE DEGREE OF

MASTER OF SCIENCE

IN

MATERIALS SCIENCE AND NANOTECHNOLOGY

By

CEMİLE ELİF ÖZÇELİK

JANUARY 2020

PEPTIDE DRUG CANDIDATES FOR PATHOGENIC AMYLOIDS

By Cemile Elif Özçelik

January 2020

We certify that we have read this dissertation and that in our opinion it is fully adequate, in scope and in quality, as a thesis for the degree of Master of Science.

Urartu Özgür Şafak ŞEKER (Advisor)

Serap DÖKMECİ

Fatih İNCİ

Approved for the Graduate School of Engineering and Science:

Ezhan Karaşan
Director of the Graduate School

ABSTRACT

PEPTIDE DRUG CANDIDATE FOR PATHOGENIC AMYLOIDS

Cemile Elif Özçelik

M.S in Materials Science and Nanotechnology

Advisor: Urartu Özgür Şafak Şeker

January 2020

Amyloid fibrils are very stable, ordered cross-β structured, resistant to protease degradation, proteinaceous composits. All amyloids have different peptide/protein sequences although they express similar structural properties. Some of amyloids possess advantageous functionalities such as protection, cell-cell communication, protein storage. However, most of amyloids are associated with various severe diseases such as neurodegenerative diseases. Although amyloids follow similar formation pathway, pathogenic amyloids are challenging since their formations are supported with secondary pathways. Up to now, there were several therapeutic approaches that are only effective in symptoms of disease conditions by masking or slowing down the symptom developments. Nonetheless, different approaches are developed for inhibiting amyloid aggregation. Today, most of the strategies are aiming to inhibit secondary nucleation, which is not fully understood yet. So, such approaches can be faced with lots of challenge in terms of secondary nucleation kinetics and formation mechanism. Thus, inhibition of monomeric

amyloid units, which are developed into amyloid aggregates, can be another novel approach for halting disease-condition developments. In this thesis, candidate ligand peptides that cease aggregation of huntingtin, α-synuclein and amyloid-β were selected by using different types of display systems, which are bacterial surface display, yeast surface display and phage display. The monomeric amyloid units of these proteins were expressed on surfaces of bacterial cells and yeast cells in order to expressing monomeric units with a proper folding and avoiding aggregation after expression without interacting with each other. Candidate ligand peptides were selected against neurodegenerative amyloids by M13 phage display library. First, M13 phage display library was tried to be produced from using wild type M13 bacteriophage by basic cloning methods as well as commercially available M13 phage display library kit was used for peptide selection since the minor coat protein pIII of M13 is widely used for peptide display and ligand peptide selection studies. Thus, 12 amino acid-long peptides displayed on the minor coat protein pIII were selected against neurodegenerative amyloids for inhibiting protein aggregation purpose in the very first step of aggregation pathway.

Keywords: Amyloid Aggregation, Bacterial Surface Display, Yeast Surface Display, Phage Display Library, Peptide Selection, Biopanning

ÖZET

PATOJENİK AMİLOİDLER İÇİN ADAY İLAÇ PEPTİTLERİ

Cemile Elif Özçelik

Malzeme Bilimi ve Nanoteknoloji, Yüksek Lisans

Danışman: Urartu Özgür Şafak Şeker

Ocak 2020

Amiloid fibriller oldukça dayanıklı, düzenli karşılıklı-β yapılı, proteaz degradasyonuna dayanıklı proteinli çökeltilerdir. Tüm amiloidler farklı peptit/protein sekanslarına sahip olmalarına rağmen benzer yapısal özellikler gösterirler. Bazı amiloidler koruma, hücre-hücre iletişimi, protein depolama gibi avantajlı işlevsellikler göstermektedir. Buna rağmen, çoğu amiloidler nörodejeneratif hastalıklar gibi çeşitli ciddi hastalıklarla ilişkilendirilmektedirler. Amiloidler benzer oluşma yolağını takip etseler bile patojenik amiloidler oldukça zorludurlar çünkü oluşumları ikincil yolaklarla desteklenmektedir. Şu ana kadar sadece hastalık durumlarınn semptomlarını maskeleyen ya da semptom gelişmelerini yavaşlatan çeşitli terapetik yaklaşımlar bulunmaktadır. Bununla beraber, farklı yaklaşımlar amiloid agregasyonunu inhibe etmek için farklı yaklaşımlar geliştirilmektedir. Günümüzde, çoğu stratejiler henüz tamamen anlaşılmamış olan ikincil nükleasyonu inhibe etmeği amaçlamaktadır. Bu yüzden, bu tarz yaklaşımlar, ikincil nükleasyon kinetiği ve oluşma mekanizması açısından

pek çok zorluklarla karşı karşıya kalmaktadır. Bu nedenle, amiloid agregatlarını oluşturan monomerik amiloid birimlerinin inhibisyonu, hastalık durumu gelişmesinin durdurulması için diğer bir özgül yaklaşım olabilir. Bu tezde, huntingtin, α-sinüklein ve amiloid-β aggregasyonunu durduracak aday ligand peptitler, bakteriyel yüzey gösterimi, maya yüzey gösterimi ve faj gösterimi gibi yüzey gösterim sistemlerinin kullanılmasıyla seçilmişlerdir. Monomerik birimlerin doğru bir şekilde katlanması ve ekspiresyon sonrası agregasyonu, birbirleriyle etkileşmeksizin önlemek için, monomerik amiloid birimler, bakteri ve maya yüzeylerinde ifade edildi. Aday ligand peptitler, M13 faj gösterim kütüphanesi kullanılarak, nörodejeneratif amiloidlere karşı seçildi. İlk olarak, M13 fajının minör kılıf proteini peptit gösterimlerinde ve ligand seçim çalışmalarında yaygın bir şekilde kullanıldığı için, M13 faj gösterim kütüphanesi, temel klonlama metodları kullanılarak, doğal fenotipli M13 bakteriyofajından üretilmeye çalışılmasının yanı sıra, ticari olarak uygun olan M13 faj gösterim kütüphanesi kiti peptit seçimi için kullanılmıştır. Sonuç olarak, protein agregasyonunu, agregasyon yolağının en başında inhibe edilmesi için, minör kılıf proteininde gösterimi yapılan 12-amino asit uzunluğundaki peptiler, nörodejeneratif amiloid proteinlerine karşı seçilmişlerdir/

Anahtar Kelimeler: Amiloid Agragasyonu, Bakteriyel Yüzey Gösterimi, Maya Yüzey Gösterimi, Faj Gösterim Kütüphanesi, Peptit Seçimi, Biopanning

Acknowledgements

During my 3 years-long master education, I learnt, experienced ans saw lots of things. Most of the time, I faced with many problems in my project. In such times, I would like to thank everyone who was with me and supported me at these times.

Especially I want to thank my advisor Urartu Özgür Şafak Şeker for opening the door for me to the only lab group I want to be for my master education, was always guiding me and keeping my motivation in high level . Also I am thankful to my jury members, Serap Dökmeci and Fatih İnci.

I feel very luck to be a member in SBL group since being the same working environment with valuable and knowledgeable people has improved me during this 3 years. So, I would like to thank all SBL members, specifically to Ebru Şahin Kehribar. It was a great opportunity for me to work on the project she involved.I would also like to thak to our former lab member Özge Beğli to inducing yeast and sharing the same feelings and fate for our project time to time. Besides, I thank to Nedim Hacıosmanoğlu for inducing yeast cells, helping me modelling and sending me funny videos and memes which cheer me up all the time I received them. Although she is the newest lab member, I would like to thank Anooshay Khan for helping me in the lab during my thesis writing period. Also, I thank to Eray Ulaş Bozkurt for sharing his taste of music with me. Besides, I would like to thank to rest of the SBL members who are Sıla Köse, Julian Ostaku, Çisil Kçksaldı, Gökçe Özkul, Zafer Koşar, Merve Yavuz, Merve Erden and Murat Güngen.

I am also very glad to meet precious people and find my lifelong friends during my master. I would like to thank Onur Rojhat Karasu, Recep Erdem Ahan, Behide Saltepe and Büşra Merve Kırpat for their endless support and friendship. Especially I would like to thank Onur for being such a wonderful person and making me feel well everytime I am with him, Recep for his patience and sharing meals, Behide for endless and deep conversations by whispering, Büşra Merve for sharing coffee and support when I was down. Also I thank to Melis Akdoğan Gün who always supported me, even if she is far away.

Finally, I would like to thank my all family members who support me at every moment of my life and show me the way every time I feel lost. Specifically, I would like to thank my father Ertuğrul for his guidance and support whenever I had a question mark in my head, my mother Menevşe for being a perfect role model with her strong character, my sister Fulya for making me forget all my problems, my brother-in-law Vahit for making me questioning of my future, and my little angel Bade. Besides, I would like to thank to Menekşe ve Mert Taşçılar. Whenever my life was boring and I miss my family, they made me feel I'm home when I'm with them.

This project was supported financially by TUBİTAK with project number 216S127.

Table of Contents

List of Figures

List of Tables

CHAPTER 1

INTRODUCTION

About 400 years ago, amyloids were termed at the first time and amiloids have always attracted the attention of researchers [1]. Although amyloids are emphasized with their functional roles observed in diverse organisms such as bacteria, fungi, insects, silkmoths and even mammalian cells lately, amyloid fibrils are mostly related with numerous conditions that decrease life quality and mostly cause cell death [2].

Up to now, there are about 50 different proteins and peptides that are stated as amyloid forming units associated with life threating diseases [3]. These diseases can be neurodegenerative as observed in Alzheimer's disease, Parkinson's disease and dementia and Huntington's disease, or non-neuropathic amyloidosis such as Type II diabetes. Although most of the diseases related with amyloidosis are caused by different type of amyloid proteins or peptides, they all exhibit similar structural properties and identified by primarily with the amyloid aggregation as proteinaceous plaques in tissues [4-7].

All amyloid fibrils are self-assembled, stabilized with low free energy and express highly ordered structures by forming cross-ß structure as well as having resemblance in interaction with ThT and Congo Red dye which are commonly used as an amyloid indicator[8-10]. Likewise, in order to determine the amyloid fibril structure, first x-ray diffraction analysis was applied in early research of

amyloid structures. As a result of X-ray diffraction analysis, all amyloid fibrils are composed of a core structure made up with the amyloid-forming peptides or proteins in ß-strand conformation. These ß-strands interact with each other via hydrogen bonds between carbonyl and amide group of the neighboring amyloid forming peptide or protein, that are parallel to the fiber axis with 4.7–4.8 Å [11, 12]. In the prefibrillar structure, ß-sheets are positioned parallel to each other owe a distance of 6–12 Å [13]. This structural pattern later was confirmed and detailed by different techniques like electron and atomic force microscopy with a detection of length, width and architecture of the fibril, Fourier transform infrared spectroscopy and circular dichorism by investigating secondary structure with different principles, point mutations and using conjugated probes by determining the region affecting amyloid fibril formation, hydrogen-deuterium exchange by studying ß-sheet structure, X-ray crystallography by using crystallized short peptides to get more detailed amyloid structure, solid-state nuclear magnetic resonance by determining orientation of the ß-sheet structure, and cryoelectron microscopy by secondary structure investigation of a single amyloid particle without a necessity to use of crystallized structure of amyloid or isotope-labelling [14-23]. Hence, applications of different techniques enlighten the basic amyloid structures [24]. Still, different approaches proved that the amyloid fibrils are very complicated with a varied assembly combinations as a result of the differences in the amyloid-forming peptide or protein sequences the existence of numerous small precursors, diversity in condition parameters like salt concentrations, pH, temperature and also rate constants of the fibril formation [1].

There are some terminology adopted for the amyloid fibril structure formation.

One of these is oligomers which represents the aggregated unit composed of two or more monomeric units of amyloid forming peptide or protein with having low growth rate and different structures than a fibril [25, 26]. The other one is critical nucleus, which is the smallest aggregation unit [27]. Critical nucleus occupies high Gibbs free energy that undergoes fast monomer addition than the dissociation to monomeric units [25, 27]. Fibrillar oligomers are used for oligomers having fibrillar structure with a shorter length than a fibrillar structure [25]. For the fibrillar structures, protofilament is a description of the fibril-like structure with a composition of monomers having intermolecular electrostatic interactions lie parallel to the fibril axis [28]. The transient state of twisting two or three protofilaments forms protofibril that act as kinetic precursor for amyloid fibril formation [29]. The amyloid fibril is the final product of the amyloid formation mechanism, that composed of three or more twisting protofilament to each other resulted in higher level of fibrillar structure with 60-120 Å in cross-section dimension, varying the length and unbranching structure (Figure 1). The mature amyloid fibrils are stabilized by dipolar interactions between each protofibrillar structure and van der Waals interactions between monomeric amyloid units, making fibrils more stiff as in like steel and stabilized more via hydrophobic interactions and hydrogen bonds formed between side-chains [30-32].

All amyloid fibrils, especially the ones associated with different disease conditions, shares a ß-sheet structure and closer dimensions, although they express diverse arrangements of protofibrils, in other words, they owe differences in the assembly of protofilaments, even for a single type of amyloid fibrils formed

in the same environment [1].

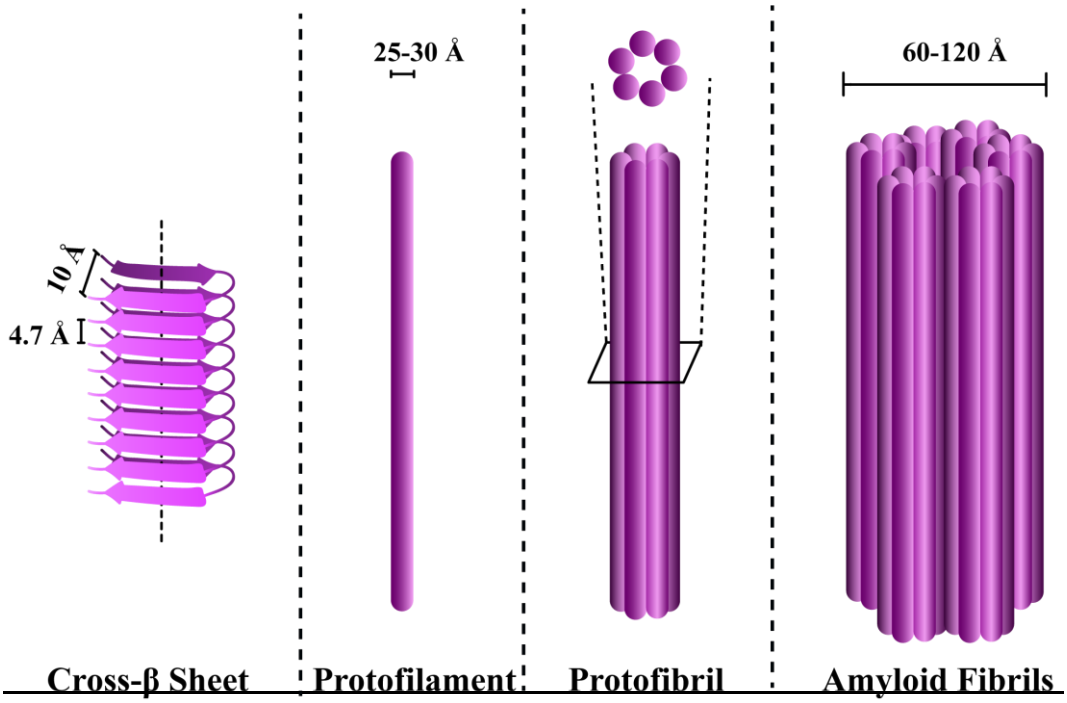

Figure 1: Structures of cross-β sheet, protofilament, protofibril and amyloid fibrils.

These diversifications in protofilament assembly of same amyloid fibrils are the phenomenon known as polymorphism [25, 31]. Amyloid polymorphs are formed for a one type of amyloid fibrils regardless of the amino acid sequence of the amyloid forming peptide or protein by variation of the orientation in the same environment although concentration of the most stable amyloid polymorph increases during amyloid formation since less stable polymorphs lose their amyloid fibril structure by dissociation [25, 31]. This phenomenon makes disease-related amyloid formation studies more complex. Also, conditions of growth environments affect the pathways of amyloid fibril formation, stability of intermediates and assemblies. However, amyloid fibril formation mechanism can

be divided into lag phase, elongation phase and stationary (plateau) phase even if amyloid fibril formation is a dynamic event and cannot be distinctly separated to a single molecular process[32, 33] .In other words, all molecular events show a continuous activity during the whole fibril formation process (Figure 2).

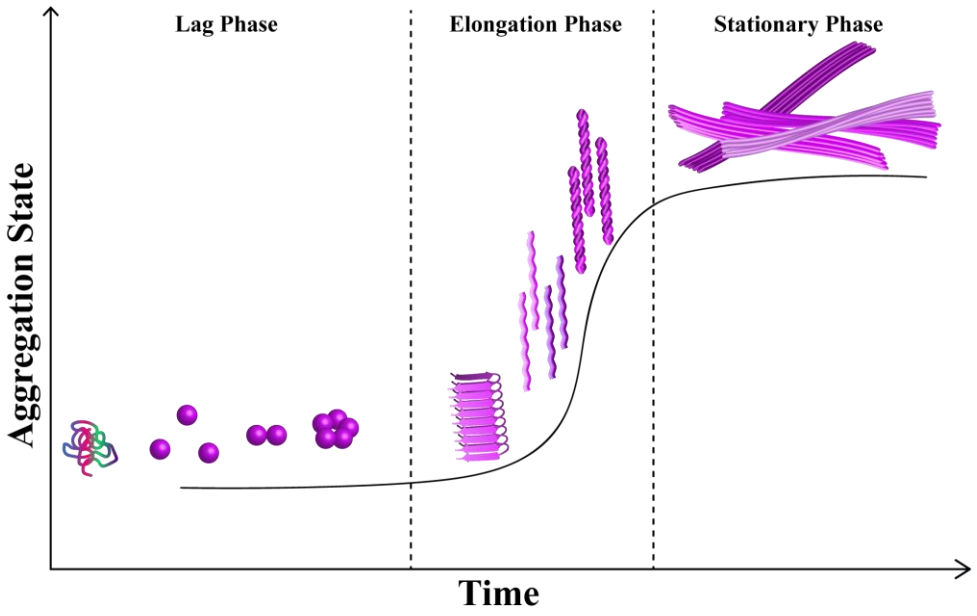

Figure 2: Aggregation phases and amyloid fibril formation mechanism

During the lag phase, primary nucleation and elongation of fibrils and sometimes these events are supported by secondary nucleation and fragmentation events take place, while in the elongation phase, heterogeneous and transient protofibrils are arranged and assembled into mature amyloid fibrils and plaques that are obtained in the stationary phase [33]. In the consideration of lag phase, the amyloid precursor molecule transforms from soluble state to insoluble-aggregating template in the primary nucleation step. Unfolded or misfolded peptides or proteins and also rarely native proteins have a role in the formation of the very first oligomers, which are not persistent and not defined in terms of structural geometry. These oligomers are then involved in amyloid assembly by following

on-pathway fibril formation or they sometimes assembled into proteinaceous complexes that are not formed as fibrils but still they posses a cytotoxicity [1].During oligomerization, a oligomer with high free energy, which is called as critical nucleus, undergoes polymerization fast int order to form amyloid fibril. To do so, precursor oligomers changes their initial assembly structure by organizing secondary structure with ß-strands to form preliminary fibrillar structure in a slow transition event, regardless of the initial structural state [34]. Then, addition of monomers to the free and growing ends of the preliminary amyloid-forming assemblies takes place with a rapid growth, which is happened in elongation phase. The elongation phase is followed by the stationary phase n which complete amyloid fibrils are formed with a lowest free energy, highest stability and insolubility [33].

Also, there are secondary processes that feed the whole pathway in order to form amyloid fibrils. One of these processes is the secondary nucleation which is occurred by autocatalysis of sides of pre-fibrillar assemblies to create new amyloid nuclei, and the other one is fragmentation in which small fragments are created by break off the end of the mature amyloid fibrils to produce fibrillar oligomeric structures [30].

As a whole, the duration of the lag phase is mainly dependent on the formation of amyloid nuclei while the sharp growth observed in elongation phase is affected mainly by the secondary processes [34]. In addition to this, the secondary processes have a high impact on the toxicity and pathogenic effect on the disease conditions such as observed in Alzheimer’s disease, Parkinson’s disease and Huntington’s disease [34].

1.1. The Toxicity of Amyloids

Pathogenicity of amyloids is the most challenging and complicated problem because of the differences in growth conditions, polymorphism, genetic factors and mutations, age, and complex fibril formation mechanism [1].

Each disease related with amyloid formation is originated from the assembly of different types of peptides or proteins. Therefore, the origin of the toxicity of amyloid aggregations and dysfunctionality of the cells producing amyloid aggregates have not been answered clearly, but there are some evidences that oligomeric units of the aggregating amyloid fibrils have high impact on pathogenicity [34]. Besides, it is observed that there is an interaction between amyloid-related diseases as well as non-amyloid diseases affecting the development of amyloid-related disease conditions [1]. For instance, Azheimer's disease condition can be triggered with a high chance in patients having type II diabetes [1], as well as α-synuclein deposition can be observed in the plaques occurred in Alzheimer's disease patients. Also, Parkinson's disease occurrence ratio is relatively high in Gaucher disease patients because of the genetic factor influences [35].

1.2. Association of Amyloids with Alzheimer's Disease

Alzheimer's disease (AD) is the most challenging, progressive and common neurodegenerative disorder that is occurred among population of >65 years old people with a prevalence of 10-30% having a frequency of 1-3% [36]. AD

patients suffer from cognitive decline and irreversible memory loss [37] due to accumulation of amyloid-β plaques in blood vessels and extracellular environments [36, 37]. This then resulted in increased level of phosphorylation of microtubule-associated tau proteins and hyper-phosphorylated tau proteins form insoluble fibrillous aggregates in neuronal cells [36, 37]. Such aggregates cause synaptic dysfunctioning in early stages in AD, which is followed by loss of synaptic interaction then neuronal death leading dementia [37, 38]. This coupled of events is called as amyloid cascade hypothesis [39].

Alzheimer's disease is dependent on amyloid-β clearance in brain cells [40]. Overproduction of amyloid-β and low efficiency in clearance lead to neurodegeneration cascade in patients [41]. The aggregative amyloid-β production is associated with processing of amyloid precursor protein (APP), which is a type, I tarnsmembrane protein expressed from APP gene on chromosome 11 [41]. In normal procession of APP, α-secretase enzyme cleaves at amyloid-β sequence into APPsα. The membrane embedded, remaining part of amyloid-β as well as APPsα is further cleaved by ɣ-secretase to form short peptides called p3 [42]. When the mutations occurred on APP, PS1 and PS2 (genes expressing presenilin 1 and presenilin 2 respectively and these are catalytic subunits of ɣ-secretase) are resulted in overproduction of neurodegenerative amyloid- β proteins. by following different APP processing pathway [41,43]. In this pathway, β-secretase cleaves APP at a position of amyloid-β_1, then ɣ-secretase cleaves the amyloid-β at position of 40 in periphery and at position of 42 in brain, which is developed into senile amyloid-β plaques [40].

1.3. Association of Amyloids with Parkinson's Disease

The second most common neurodegenerative disorder is Parkinson's disease in which symptoms are observed as physically and neuropsychiatrically [44]. The physical symptoms are bradykinesia, hypokinesia, akineasia, hypomimia, hyposmia, hypophonia, drooling, micrograpkia as well as loosing postural reflexes and obesity [45, 48]. For neuropsychiatrical symptoms, decrease in cognitive functioning, depression, and sleep disorders may be given [44]. These symptoms are caused by loss of dopaminergic neurons [46]. This loss of functioning is caused by existence of Lewy bodies whose main component is α-synuclein [46]. α-synuclein is a presynaptic protein and its function is not completely understood. Still, it is thought that synaptic vesicles trafficking and neurotransmitter exocytosis is regulated by α-synuclein [47]. 140 amino acid-long α-synuclein is translated from SNCA gene. 1-60 amino acid residue region of α-synuclein is amphipathic region in which A30P, E46K, H50Q, G51D,A53E and A53T mutations leads to aggregation of α-synuclein [48]. 61-94 amino acid residue region of α-synuclein is called as non-amyloid-β component (NAC) domain that is highly hydrophobic region and formed in β-sheet structure as occurred in amyloid fibrillization [48]. 95-140 amino acid residue region is acidic tail which owe high solubility property [48]. The aggregation of α-synuclein is occurred on presynaptic regions, and this accumulation leads to dysfunctioning, then connection loss between neurons [48].

1.4. Association of Amyloids with Huntington's Disease

Huntington's disease (HD) is the most common inherited neurodegenerative disease occurred by high number of CAG trinucleotide (translated in glutamine amino acid) repeat in IT15 gene, which is called also HTT, located on chromosome 4 [49, 52]. The symptoms of HD are associated with motor dysfunctioning with uncontrolled movement, cognitive and psychiatric problems as well as chorea and dementia [50, 51]. The function of huntingtin protein with 7 to 36 glutamine repeat is not developed in aggregate form and functions in development although the specific role of huntingtin is still not known [53]. Huntingtin protein with more than 36 glutamine repeat with a gain-of-function mutation forms amyloid aggregated which leads to development of the disease condition with progressive neuronal loss [54]. The development of disease condition is dependent to the length of CAG repeat on HTT gene instead of polyglutamine length, which is shown recently [54]. Thus, increase in CAG repeat leads to early development of HD. Also, 10-15 years of onset of HD is concluded to death of patients.

1.5. Therapeutic Strategies for Amyloid-Associated Pathogenicity

The reason of formation of amyloid aggregation is different for all neurodegenerative diseases although amyloid formation pathway is similar for

all. Besides, underlying mechanisms of pathogenic amyloid formation is unclear. Also, the current developed drugs are just masking the symptoms instead of halting the aggregation. Today, researchers are focused on inhibition of amyloid aggregation at different stages of formation with different strategies [34]. One of the strategy is focused on stabilization of amyloid fibrils and inhibiting secondary pathway products by amyloid remodeling [55]. One example for amyloid remodeling is that epigallocatechin-3-gallate (EGCG) compound is shown that it can decrease α-synuclein oligomer toxicity as well as remodel by binding to α-synuclein aggregates leading producing non-toxic oligomers instead of toxic oligomers in vitro [55]. Thus such approach is promising for amyloid toxicity inhibition. Another strategy is immunization of amyloids by binding of antibodies to them in order to clear monomeric units. However, studies depending on amyloid immunization failed at each clinical trial with expressing adverse effects [55]. This might be caused by removal of monomeric amyloids since monomeric amyloids may possess functional role as well as disturbance in protein concentration that may trigger secondary pathways [1, 34].

Still, the studies continue to inhibit amyloid formation by targeting monomeric units, secondary nucleation or amyloid aggregate itself and each result, positive or negative, give information about disease mechanism and amyloid functioning as well as an idea for next strategies like selection of small molecules that interact with precursors of amyloid fibrils at early stages to inhibit amyloid formation, secondary nucleation, or proliferation [1, 34].

1.6. Ligand Peptide Selection by Phage Display Library for Drug Discovery

Drug discovery is a challenging journey where scientist have been faced with variable troubles such as trying different candidates with high amount in variety or failing in clinical trials while in vitro experiments gives promising results. Recently, scientist uses a strategy in which candidate drug molecule is specifically screened against its target, which is called target-based drug discovery strategy [56]. This discovery strategy is applied by using in vitro display techniques which are bacterial surface display, yeast surface display, ribosome display, aptamer display, bead-surface display, cDNA/mRNA display, cis-activity based (CIS) display, covalent antibody display (CAD), SNAP display [57, 58]. Among these display systems, another display technique is phage display that is dominant in use among the other display systems and widely used in drug discovery [56]. In phage display systems, filamentous phages which are M13, f1 and fd, as well as T4, T7 and Lambda phage are used. M13 bacteriophage is the most common bacteriophage used in such system [58]. M13 owes circular ss-DNA encoding 11 genes, two of which are used in phage display technology, *gIII and gVIII.* The major coat protein pVIII and the minor coat protein pIII are used in displaying different types of peptides and proteins [56]. pVIII protein has about 2700 copies in the coat of M13. Thus, it is used for small-sized proteins or peptides with a high efficiency of expression without dissociation of coat proteins [57]. pIII, on the other hand, has 5 copies, having a role in infection of the phage, that is involved in displaying peptides and proteins

with variable length [57].

The selection of candidate ligand from peptide or protein library expressed on phage surface is achieved by 3-4 rounds of biopanning procedure in which target is interacted with phages and bound phages are obtained to identify the peptide sequence for further use [59]. With the power of phage display for selection candidate ligand by biopanning, today several antibody drugs are in use for treatment of severe diseases such as stomach cancer, Chron's disease and ulcerative colitis [59]. In literature, also there are several peptides such as Romiplostim, Ecallantide, and Peginesatide in order to treat idiopathic thrombocytopenic purpura, hereditary angioedema, and chronic kidney disease associated anemia respectively, selected by phage display technology, which makes phage display technology is highly powerful for drug development [59].

1.7. The Aim of Study

There are many different approaches for treatment of neurodegenerative diseases such as Alzheimer's disease, Parkinson's disease and Huntington's disease. However, the lack of knowledge of disease mechanism depending on complex formation pathway of amyloid aggregates is resulted in challenges for drug development. In this thesis, we aimed to select candidate inhibitory peptides by using phage display library against yeast surface displayed-neurodegenerative amyloids. By the power of using monomers expressed on yeast cell surfaces, amyloids are in their monomeric units. Therefore, we select candidate inhibitory peptides for monomeric units by applying biopanning procedure without

immobilizing yeast cells to reach out more surface-displayed peptides. The selected inhibitory peptides may a promising drug candidate and they can inhibit/stabilize the amyloid monomeric units in their environment without clearance of them and disturbing the concentration balance of proteins.

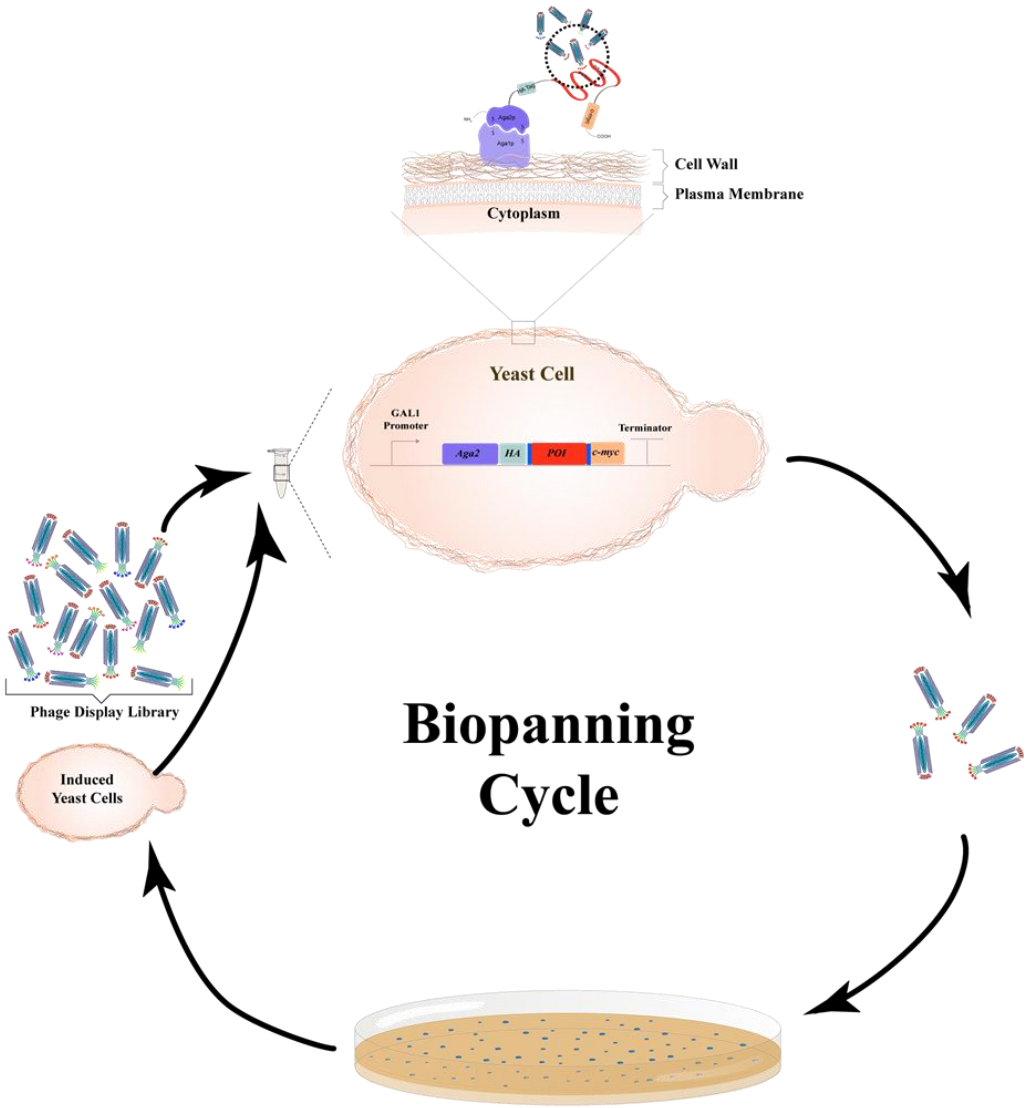

Figure 3: The inhibitory peptide selection by using phage display library and yeast surface display system.

CHAPTER 2

MATERIALS AND METHODS

2.1. Bacterial and Yeast Cell Strains, M13 Bacteriophage, Cell Maintenance and Growth Conditions

For the cloning of the new constructs, *Escherichia coli* (*E.coli)* DH5α PRO strain was used. This strain provides high insert stability and high yield of DNA as a result of mutations in recA1 and endA genes, respectively. For recombinant protein expression, *E.coli* BL21 (DE3) strain was used. BL21 (DE3) strain has high transformation efficiency as well as it is suitable for Isopropyl-β-d-1-thiogalactopyranoside (IPTG) induction of T7 promoter since T7 RNA polymerase gene is expressed with under control of Lac promoter.

In order to store plasmids having repeated nucleotide region for a long time or cloning of new plasmid constructs with high number of repeated nucleotide region, *E.coli* SURE (Stop Unwanted Rearrangement Events) strain was used. *E.coli* SURE strain is deficient in endonuclease A activity and recombination by the expression of recB and recJ. Thus it provides an increased stability to constructs having repeated nucleotide region. Beside, *E.coli* K12 ER2738 strain has been used for bacteriophage propagation. This strain owes F factor that contains a mini-transposon that provides tetracycline resistance. Also, lac Z gene

is deficient in the lac operon, which makes this strain used with M13KE bacteriophage having complementary lacZα gene. Thus, ER2738 strain can be infected with M13KE bacteriophage and selection of infected bacteria can be achieved by blue/white screening with lac operon complementation.

All bacteria strains that were used in this study were stored at -80ºC in Lysogeny Broth (LB) growth medium (recipe given in Appendix E, Table E.1) with the addition of 50% glycerol solution in 1:1 ratio. For *E.coli* ER2738 strain, single-use cell stocks were prepared for each experiment for avoiding lost of F pilus. Before preparing glycerol cell stock, each strain has been streaked to a agar plate having an appropriate antibiotic to get a single colony for stocking.

For biopanning experiments, *Saccharomyces cerevisiae* (*S.cerevisiae)* EBY100 strain was used. EBY100 strain is leucine and tryptophan deficient so these amino acids can be used as marker during cloning. Besides, aga2p gene is knocked out which makes this strain is suitable for surface display studies. This strain can be grown in yeast growth medium at 30ºC with 260 rpm shaking. For a long-term storage, yeast cells were stored with addition of equal volume of ice-cold 30% glycerol at -80ºC.

In order to select ligand peptides for neurodegenerative proteins to inhibit their aggregation, M13 phage display library was used. M13 is a filamentous bacteriophage that infects F+ bacterial cells such as *E.coli* ER2738 and propagates by using such bacterial cells as host. M13 bacteriophages were stored 4ºC for short-term. For long-term storage, 50% glycerol solution with 1:1 ratio was added onto each M13 sample and preserved at -80ºC.

2.2. Chemical Transformation of Bacterial Cells

Plasmids or newly cloned constructs are transformed into bacterial cells with chemical transformation protocol if they are not need to be treated special like necessity of electroporation in order to get high cloning results. For chemical transformation, competent cell was prepared with overnight grown culture of desired cell with the addition of an appropriate antibiotic. The overnight grown culture was diluted with a ratio of 1:100 into fresh LB with an addition of the same antibiotic. The cells were incubated at 37^{o}C and 200 rpm. When OD_{600} value reaches the range of 0.2-0.5, cells are transferred into a new tube and put onto ice for 10 minutes to slow down the metabolism. After ice incubation, cells were centrifuged down at 3000 rpm for 10 minutes at 4^{o}C. After centrifugation step, supernatant was discarded carefully without disrupting the cell pellet, and the cell pellet was resuspended with TSS buffer with a ratio 1:10 of grown culture volume. Then, competent cells were aliquoted into eppendorf tubes with 100 µL volume. The competent cell stocks were stored at -80^{o}C if they were not used immediately. In the case of using stock competent cell, cells were thawed on ice for 30 minutes while freshly prepared competent cells were used directly without thawing step. Then, about 100 ng plasmids or complete Gibson assembly mix or complete T4 ligation mix (given in Appendix E, Table E.11 and Table E.12 respectively) after reaction was completed, were added onto the competent cells. Then cells mixed with plasmids were incubated on ice for 20 minutes. After this incubation, heat-shock step was applied with incubation of cells at 42^{o}C for 45 seconds. Heat-shock step was followed by 5 minutes incubation on ice. After incubation, 500 µL LB was added onto cells and incubation was done at 37^{o}C for

45 minutes at 200 rpm. At the end of the incubation, centrifugation was done at 8000 rpm for 5 minutes. 250 µL of the supernatant was discarded and cell pellet was resuspended with the remaining supernatant. The cells were spreaded onto LB-agar poured with the appropriate antibiotic. The plate then incubated at 37^{o}C overnight if otherwise was not required for the growth of the cell.

2.3. Electrocompetent Cell Preparation and Electroporation of Bacterial Cells

The transformation of double-stranded M13 genome that displays peptides having different sequences on pIII was done by electroporation. To do so, electrocompetent cells were prepared right before electroporation process. Overnight grown bacterial cells were diluted with a ratio of 1:100 into fresh LB medium with the addition of an appropriate antibiotic. The diluted culture incubated at 37^{o}C, 200 rpm until OD_{600} reached to 0.6-0.7. Then, the grown cells were cooled down by incubation on ice for 30 minutes. At the end of the cooling, centrifugation was done at 5000 g, +4^{o}C for 15 minutes. Supernatant was removed and pellet was washed with 1:1 culture volume of ice-cold ddH_2O by gently resuspending the cell pellet. Second centrifugation was done with the same conditions. Supernatant was removed and the second washing was done with 1:2 culture volume of ice-cold ddH_2O. Cells were centrifuged down with the same conditions with the previous ones and supernatant was removed. The third washing was performed with 1:2 culture volume of ice-cold 10% glycerol. Before the final washing step, same centrifugation conditions were applied. For the final washing, supernatant was removed and 1:8 culture volume of ice-cold 10%

glycerol was added to wash the cells. The final centrifugation was done at 8000 g, +4^{o}C for 10 minutes. After centrifugation, supernatant was removed and remaining cell pellet was resuspended with 600 µL ice-cold 10% glycerol. Finally, electrocompetent cells were aliquoted into fresh tubes with the volume of 100 µL for use. Also they can be stored at -80^{o}C for a short-term.

For electroporation, 50 ng plasmid or newly cloned construct with Gibson assembly method or T4 ligation method after clean-up protocol were directly added onto freshly prepared electrocompetent cell or electrocompetent cell stock after thawing competent cells on ice for 30 minutes. Then, mixture of electrocompetent cells and plasmids were transferred to 1 mm electroporation cuvette (VWR, CAT# 58017-890) which was cooled at -20^{0}C for about 20 minutes to increase the efficiency of electroporation. The cuvette having cell-plasmid mixture then put into Bio-Rad Gene Pulser Xcell electroporation machine. Electroporation was done with appropriate parameters which were determined according to cuvette gap-size and cell type (Appendix E, Table E.16). After pulse, 1 mL SOC medium (recipe given in Appendix E, Table E.2) were added onto cells in 5 seconds. Then cells were incubated at 37^{o}C for 30 minutes. At the end of the incubation, cells were centrifuged down at 8000 rpm for 5 minutes. 900 µL of the supernatant was discarded, cell pellet was resuspended with the remaining supernatant. Cells was spreaded onto an LB-agar poured with a proper antibiotic. The plate then incubated at 37^{o}C overnight if different growth parameters were required for the growth of the cell.

2.4. Construction of Plasmid Vectors

For detection of proper folding of proteins displayed on yeast surface, sfGFP gene was inserted into pETcon-Aga2-NDP vector where NDP refers to neurodegenerative proteins (α-synuclein, amyloid β_{40} and amyloid β_{42}, 25Q-Htt, 46Q-Htt, and 103Q-Htt). 1000ng of pETcon-Aga2-25Q-Htt, pETcon-Aga2-46Q-Htt, pETcon-Aga2-103Q-Htt, pETcon-Aga2-Amyloid β_{40}, pETcon-Aga2-Amyloid β_{42} and pETcon-Aga2-α-synuclein vectors were digested with BamHI restriction enzyme digestion reaction. Restriction digestion reaction (recipe given in Appendix E, Table E.5) was performed by incubation at 37ºC for 3 hours. After digestion, samples were loaded on 1% agarose gel containing Sybr™ SAFE stain and electrophoresis was done at 120 V for 30 minutes. The gel was visualized by LED transilluminator (GeneDireX, Inc.). Linearized DNA at the expected region on the gel according to the ladder was separated from rest of the gel and gel extraction was done with NucleoSpin® Gel and PCR clean-up kit (Macherey-Nagel, # 740609.50) by following its own protocol.

For sfGFP cloning into vectors, sfGFP gene was amplified with PCR by using Q5 polymerase. For each type of protein, sfGFP amplification was done with different primers. pCEO3 and pCEO7 primers were used for cloning of sfGFP into pETcon-Aga2-25Q-Htt, pETcon-Aga2-46Q-Htt and pETcon-Aga2-103Q-Htt vectors. pCEO11 and pCEO13 primers were used for cloning of sfGFP into pETcon-Aga2-Amyloid β_{40} vector. pCEO9 and pCEO13 primers were used for cloning of sfGFP into pETcon-Aga2-Amyloid β_{42} vector. pCEO13 and pCEO14 primers were used for cloning of sfGFP into pETcon-Aga2-α-synuclein vector.

PCR was performed with the recommended conditions for the enzyme and the gene. PCR mix was loaded on 1% agarose gel containing Sybr™ SAFE stain, and electrophoresis was performed at 120 V for 30 minutes. At the end of electrophoresis, the gel was visualized by LED transilluminator. The band was observed at expected region and it was cut. DNA was extracted from the gel.

sfGFP and linearized vectors were assembled with Gibson assembly reaction at 50ºC for 1 hour. When assembly was completed, Gibson assembly reaction mix was chemically transformed into *E.coli* DH5α PRO strain. At the end of transformation, cells were spreaded onto LB agar plate poured with appropriate antibiotic (recipe given in Appendix E, Table E.1). The plates were incubated at 37ºC overnight. Next day, colonies were selected and inoculated into 5mL of fresh LB containing appropriate antibiotic. The freshly inoculated cells were incubated at 37ºC, 200 rpm for overnight. Next day, cultures were used for plasmid isolation for preparing sequencing samples.

In order to clone NDPs into bacterial surface display system, pET22b-Ag43-160N-sfGFP vector was used. For the first construct, 25Q-Htt was amplified by using verified pETcon-Aga2-25Q-Htt vector by using pCEO52 and pCEO53 Gibson assembly primers with Q5 polymerase PCR under recommended conditions. For Ag43-160N surface secretion proteins were amplified by pCEO71 and pREA17 Gibson assembly primers with Q5 polymerase PCR under recommended conditions. For backbone preparation, pET22b-Ag43-160N-sfGFP was digested with XhoI and NcoI restriction enzymes (recipe given in Appendix E, Table E.6). Amplified 25Q-Htt was loaded on 2% agarose gel containing Sybr™ SAFE stain and electrophoresis was done at 110 V for 40 minutes while

backbone and amplified Ag43-160N fragment were loaded on 1% agarose gel containing Sybr™ SAFE stain and electrophoresis was done at 120 V for 30 minutes. At the end of electrophoresis, the gels were visualized by LED transilluminator. The bands were observed at expected regions and they were cut. DNAs were extracted from the gel.

The fragments were assembled with Gibson assembly reaction at 50ºC for 1 hour, which was followed by chemical transformation. After transformation, cells were spreaded onto LB agar plate poured with appropriate antibiotic. The plates were incubated at 37ºC overnight. Next day, colonies were selected and inoculated into 5mL of fresh LB containing appropriate antibiotic. The freshly inoculated cells were incubated at 37ºC, 200 rpm for overnight. Next day, cultures were used for plasmid isolation for preparing sequencing samples.

For cloning of α-synuclein into bacterial surface display vector, pCEO54 and pCEO55 Gibson primers were used for amplification of α-synuclein. As backbone, verified pET22b-Ag43-160N-25Q-Htt was digested with BamHI and SpeI to remove previously cloned 25Q-Htt. The fragments were loaded on 1% agarose gel containing Sybr™ SAFE stain and electrophoresis was done at 120 V for 30 minutes. At the end of electrophoresis, the gels were visualized by LED transilluminator. The bands were observed at expected regions and they were cut. DNAs were extracted from the gel. The fragments were assembled with Gibson assembly reaction at 50ºC for 1 hour, which was followed by chemical transformation. After transformation, cells were spreaded onto LB agar plate poured with appropriate antibiotic. The plates were incubated at 37ºC overnight. Next day, colonies were selected and inoculated into 5mL of fresh LB containing

appropriate antibiotic. The freshly inoculated cells were incubated at 37ºC, 200 rpm for overnight. Next day, cultures were used for plasmid isolation for preparing sequencing samples.

For cloning of Amyloid β_{40} into bacterial surface display vector, pCEO65 and pCEO66 Gibson primers were used for amplification of α-synuclein. pET22b-Ag43-160N-25Q-Htt was digested with BamHI and SpeI to remove 25Q-Htt. The fragments were loaded on 1% agarose gel containing Sybr™ SAFE stain and electrophoresis was done at 120 V for 30 minutes. At the end of electrophoresis, the gels were visualized by LED transilluminator. The bands were observed at expected regions and they were cut. DNAs were extracted from the gel. The fragments were assembled with Gibson assembly reaction at 50ºC for 1 hour, which was followed by chemical transformation. After transformation, cells were spreaded onto LB agar plate poured with appropriate antibiotic. The plates were incubated at 37ºC overnight. Next day, colonies were selected and inoculated into 5mL of fresh LB containing appropriate antibiotic. The freshly inoculated cells were incubated at 37ºC, 200 rpm for overnight. Next day, cultures were used for plasmid isolation for preparing sequencing samples.

2.5. Plasmid Isolation, Sanger Sequencing and Sequencing Alignments

After cloning of each new construct, plasmids were isolated from bacterial cells by using Thermo scientific GeneJet® plasmid isolation kit. Isolation was done by following the standard protocol provided with isolation kit. 3 to 10 mL overnight grown bacterial cells having one clone of a plasmid was enough for the kit. The

cell culture was centrifuged down at 8000 rpm for 5 minutes. The supernatant was discarded and cell pellet was resuspended with 250 µL of resuspension buffer having Rnase A provided with the kit. After, cell lysis was done by addition of 250 µL lysis buffer of kit. Cell lysis was done by incubating at room temperature for 4 to 6 minutes. For neutralization the lysis reaction, 300 µL neutralization buffer was added. The mixture was inverted 8 times as up and down slowly. To separate cell debris from supernatant that have plasmids, centrifugation was done at 11000 rpm for 10 minutes. At the end of the centrifugation, supernatant was taken and added to the GeneJet spin filter column. Then the column was centrifuged down at 11000 rpm for 1 minute. Then 2 times washing was done with wash buffer in which 100% ethanol was added as predetermined volume before the first use. For each washing step, 700 µL wash buffer added to the column and centrifugation was done at 11000 rpm for 1 minute. Next, in order to get rid off the remaining ethanol from wash buffer, 3 minutes centrifugation was applied at 11000 rpm. After centrifugation, remaining ethanol was evaporated with heat block at 65^{o}C by incubation for 3 minutes. For elution of plasmid DNA, 20 µL ddH_2O heated up to 65^{o}C was added. The column was incubated for 3 minutes at room temperature to make ddH_2O spreaded to the column filter completely. When 3 minute incubation was completed, column was put into a new micro-centrifuge tube to collect the elution of plasmid DNA. Centrifugation was done at 11000 rpm for 3 minutes. The elution concentration was measured by Thermo Scientific NanoDrop™ 2000 spectrophotometer with 1 µL sample. Plasmids can be stored at -20^{o}C. For sequencing, 800-1000 ng plasmid sample was taken and for sequencing, 0.25 µL of 100 µM

sequencing primer was added to plasmid elution. The volume was completed to 15 µL. The sequencing sample was send to Genewiz company to apply Sanger sequencing. The sequencing result was downloaded from www.genewiz.com as an extension of .ab1 file. Also, the plasmid maps, DNA fragments or a specific gene sequence that have the exact sequence were downloaded as an extension of .gb file from www.benchling.com which is an online tool to design new constructs, primers and to store plasmid maps. The expected sequence file and sequencing result were align with Geneious tool by importing two files to be aligned. The imported two files then selected from the work window and Align/Assemble option>Pairwise align from the upper tab was chosen. Before alignment, some parameters were selected for alignment properties. In general, automatically determine direction option, global alignment with free end gaps as alignment type were selected. For cost matrix option, 65% similarity and 93% similarity were used according to the sequencing results.Beside plasmid isolation and preparing sequencing sample with plasmids, PCR products can also be sequenced. In order to sequencing PCR product, PCR was done with Pfu polymerase with the appropriate forward and reverse primers and recommended conditions(recipe and conditions given in Appendix E, Table E.9 and Table E.10). After PCR and gel electrophoresis and also gel extraction of the band observed in the expected region, about 500 ng of purified PCR product was mixed with 0.25 µL 100 µM sequencing primer. The volume was completed to 15

µL and sequencing sample was send to Genewiz company to get Sanger sequencing result. Alignment of the result with the expected sequence was done as explained above.

2.6. Construction of Combinatorial M13 Phage Display Library by PCR

M13 phage display library can be obtained by following the basic steps explained in the manual of Ph.D.™-12 Phage Display Peptide Library Kit (New England BioLabs® Inc., E8110S). In order to construct and produce our M13 phage display library from using wild type M13 bacteriophages, firstly 81 bp-long oligonucleotide having 36 bp-long degenerate region was designed for cloning into M13 genome with restriction enzyme cut site of KpnI and EagI at near the 5' end and 3' end of the oligonucleotide, respectively. This fragment, then, synthesized by Genewiz Company, in US as 500 nmol scale, and purified by PAGE technique. The delivered oligonucleotide has OD_{260} of 8.41 with annealing temperature of 78.2ºC. The concentration of the oligonucleotide was 100 µL with guaranteed nmol of 10.58.

To start the cloning of the oligonucleotides with random nucleotide regions into *pIII* gene of M13 genome, 5 µg oligonucleotide was annealed with 3 molar equivalents of pCEO85-extension_primer in total volume of 50 µL 1 X Tris-EDTA/ 100mM NaCl buffer. The annealing reaction (recipe given in Table E.13) was done by heating the oligonucleotides and primers from room temperature to 95ºC and reaction was completed by cooling down gradually to room temperature in 30 minutes by using thermal cycler. After annealing the oligonucleotides with

primers, extension was done by using 15 units/reaction Klenow fragment with an appropriate reaction conditions (condition given in Appendix E, Table E.14). After extension, extended double stranded oligonucleotide was digested with KpnI and EagI restriction enzymes to produce the appropriate insert for ligation reaction. The digested duplex was loaded to 8% nondenaturing polyacrylamide gel (recipe given in Appendix E, Table E.15) into 1X TBE running buffer and electrophoresis was applied with 56 V for 2.5 hours. To visualize the gel, gel was placed into 10 mL 1X TBE buffer with an addition of SYBR™ Safe dye. After incubation of gel at dark with shaking gently, the gel was visualized with LED transilluminator.

The digested duplex observed in the expected length according to the ladder was cut and minced finely. The minced gel then was weighted and 'crush & soak buffer' (elution buffer which contains 100 mM sodium acetate, pH 4, 5 mM EDTA, 0.1% SDS) was added with a volume of 3 times more of the weight of the minced gel. Then, gel with buffer was shaken at 37ºC overnight. Next day, gel pieces were centrifuged to separate the gel pieces and elution buffer. Elution buffer was transferred to new tube. In order to purify digested oligomer duplexes from supernatant, phenol/chloroform extraction, chloroform extraction and ethanol precipitation were done. For phenol/chloroform extraction, equal volume of phenol:chloroform (1:1) was added to supernatant. Vortex was done to mix supernatant and phenol:chloroform until the sample got white. Centrifugation was done at 15000 rpm, 4ºC for 1-2 minutes. After centrifugation, sample was settled down at room temperature for 1 minute to make 3 different phase separated completely. Next, the upper aqueous part having DNA was transferred to a new

micro-centrifuge tube without disrupting the interphase or taking sample from the lower organic phase. For chloroform extraction, equal volume of chloroform was added onto the aqueous phase. Vortex was done well and sample was centrifuged down at 15000rpm, 4ºC for 1-2 minutes. The upper phase was transferred to new micro-centrifuge tube. For ethanol precipitation, 1:10 volume of 3 M sodium acetate ($C_2H_3NaO_2$), 1:20 volume of 5 M sodium chloride (NaCl) and 3 volume of 100% ethanol were added onto the transferred upper phase and mixed thoroughly, and next incubated at -20ºC overnight. Next day, sample was centrifuged down at 15000 rpm, 4ºC for 30 minutes. Supernatant was discarded carefully without disrupting the clear pellet containing DNA. Pellet then dried to get rid off remaining ethanol. After drying, pellet was resuspended with 50 µL ddH_2O. Short DNA duplex, then was ready for ligation reaction and was stored at -20ºC.

For preparing the rest of M13 genome for ligation, wild-type M13 bacteriophage was used. In order to prepare the genome as backbone, PCR was applied by using Q5 polymerase under recommended conditions. By this reaction, 7297 bp long M13 genome was amplified by using pCEO49 as forward primer and pCEO36 as reverse primer. PCR was done with 30 reaction cycles. After PCR, reaction mix was loaded on 1% agarose gel prepared with SYBR™ Safe stain. Electroporation was applied with 120 V for 30 minutes by using 1X TAE running buffer. At the end of electroporation, gel was visualized with LED transilluminator, the band at the expected region was cut and separated from the gel. Extraction of PCR product from gel was done with NucleoSpin® Gel and PCR clean-up kit by

following the manual of the product. After DNA extraction from gel was done, DNA elution can be stored at -20ºC for a while until it is used.

When backbone and insert were prepared for ligation reaction, 100 ng of backbone was mixed with insert DNA with a ratio of 1:5 in T4 ligase reaction mix. For ligation reaction to be occurred, the mix was incubated at room temperature for 30 minutes. Then, clean-up protocol was applied same as in NucleoSpin® Gel and PCR clean-up kit manual to remove salts and ions from ligated DNA sample. Next, newly ligated construct was transformed to *E.coli* K12 ER2738 strain by electroporation protocol whose steps are explained in Section 2.3. At the end of the electroporation, cells were mixed 45ºC heated 3 mL top-agar and spreaded onto LB agar plate poured with tetracycline, X-Gal and IPTG. Plate was incubated overnight at 37ºC. Next day, some of the blue plaques were selected and inoculated into 5 mL fresh LB with tetracycline antibiotic and grown at 37ºC, 200 rpm for overnight. After growing the cells having one clone of bacteriophage was centrifuged down at 8000 rpm for 5 minutes. Supernatant was discarded and plasmid isolation was done for purifying M13 genome from the cells. Then isolated DNA elution was send to sequencing to get DNA sequence of the inserted region by using pCEO83_-96_gIII_sequencing_primer.

2.7. Commercially Available Phage Display Library Propagation

In order to select ligand peptide for neurodegenerative proteins, Ph.D.™-12 Phage Display Peptide Library Kit (New England BioLabs® Inc., #E8110S) was used.

To increase the number of phage particle, 1µL of phage stocks having ~ 1 x 10^{13} pfu/ml phage particle provided by the kit was amplified. The overnight growth of *E.coli* ER2738 cells was diluted in 1:100 ratio to 1 L fresh LB into 5 L erlenmayer flask and culture was started to be incubated at 37ºC at 200 rpm. When OD_{600} was in between 0.01-0.05, 1 µL of phage stock was added onto the culture. The culture and phages were incubated at 37ºC at 200 rpm for 4.5 hours. After the incubation, cells were centrifuged with Thermo Scientific Sorvall Evolution RC Superspeed centrifuge at 5500 rpm, 4ºC for 1 hour. Next, supernatant was taken into an erlenmayer flask and 20% (w/v) PEG-8000/2.5 M NaCl solution was added with 1:5 ratio to precipitate phage particles. The supernatant was incubated at 4ºC overnight. Next day, centrifugation was done with superspeed centrifuge at 5500 rpm, 4ºC for 2 hours. Supernatant was removed quickly without disrupting the fingerlike phage precipitates. The phage precipitates were resuspended with 100 mL 1X TBS, then phages were incubated at room temperature by gently rocking for about 3 hours to resuspend the phages throughoutly. After incubation, centrifugation was done at 5000g for 10 minutes at 4ºC to remove residual cells if there is any. The supernatant was transferred into a new tube. For reprecipitating the phages 20% PEG-8000/ 2.5 M NaCl solution was added with a ratio of 1:5 and phages were incubated at 4ºC on ice. At the end of the incubation, phages were centrifuged at 5000g for 20 minutes and supernatant was discarded without disrupting the pellet. To get the final phage library stock, pellet was resuspended with 10 mL 1X TBS by gently rocking for 24 hours at 4ºC. For long term storage, equal volume of 50% sterile glycerol was added onto the phages and stored at -80%.

2.8. ESEM Sample Preparation

The visualization of bacteriophage particles was achieved by environmental scanning electron microscope (ESEM). Bacteriophage samples were added onto small piece of silica wafer and incubated for 5 minutes at room temperature. Fixation was done with 2.5% glutaraldehyde solution prepared in 1X PBS for 1 hour at room temperature. After incubation, silica wafers were washed with 1X PBS 2 times, which was followed by 2 times washing with ddH_2O. During washing with ddH_2O, silica wafers was shaken at 200 rpm at room temperature for 5 minutes. After washing step, 25% EtOH, 50% EtOH, 75% EtOH were added one by one and silica wafers incubated by shaking at 200 rpm at room temperature for 5 minutes for each EtOH addition. Lastly, 100% EtOH was added onto silica wafer and incubation was done at 200 rpm, room temperature for 10 minutes. This step was repeated for 3 times. After removing 100% EtOH completely, Critical Point Dryer (Tousimis) was used for drying silica wafer. Following the drying, silica wafer was covered with Au/Pd alloy with 8 nm thickness. The prepared sample was visualized by ESEM (Tecnia) at 30 kV, 3.5 spot size.

2.9. Protein Expression of Bacterial Surface Displayed Proteins and Characterization

Sequence verified pET22b-Ag43-160N-25Q-Htt, pET22b-Ag43-160N-Amyloid-β_{40} and pET22b-Ag43-160N-α-synuclein vectors were transformed into *E.coli* BL21 (DE3) with chemical transformation method. After colony formation, single

colonies were selected and inoculated into 5 mL LB medium with appropriate antibiotic. Then, cells were incubated at 37ºC, 200 rpm overnight. Next day, overnight grown cell culture was diluted into 10 mL fresh LB with a dilution ratio of 1:100 with addition of appropriate antibiotic and 2% (w/v) glucose. At OD_{600} value reached to the range of 0.4-0.6, induction was started with addition of 1mM IPTG. To induction be occurred, cells were incubated at 18ºC, 200 rpm for overnight.

At the end of the incubation, heat release of displayed proteins and acetone precipitation of protein were done for using in characterization by SDS-PAGE. 1 mL of induced cells was centrifuged at 8000 rpm for 5 minutes. Supernatant was discarded and pellet was resuspended with1 mL 1X PBS. Centrifugation was done with same conditions and supernatant was discarded while pellet was resuspended with 300 µL 1X PBS. Then, heat release was done at 60ºC for 5 minutes. 200 µL of sample was used in acetone precipitation. 20 µL from the remaining sample was saved for SDS-PAGE analysis.

For acetone precipitation, 1 mL acetone was added onto 200 µL of sample and incubated at -20ºC for overnight. At the end of the incubation, centrifugation was done at 14000 rpm, 4ºC for 45 minutes. Supernatant was discarded and pellet was air-dried. Dry pellet was resuspended with 20 µL ddH_2O.

For SDS-PAGE analysis, 12% SDS-PAGE gel was used. For preparing samples for loading, 4 µL of 6X SDS-PAGE loading dye were added onto 20 µL of samples and heated at 95ºC for 5 minutes. SDS-PAGE was performed at 120V for 1.5-2 hours into 1X SDS running buffer. After running, gel was stained with

Coomassie blue by heating gel with the stain at microwave for 30 minutes which was followed by 5-minute incubation at room temperature with gently shaking. After staining, gel was washed with water to remove excess stain, then destaining solution was added onto gel and excessive dye on the gel removed by overnight incubation at room temperature with gently shaking. When destaining was completed and bands were seen clearly, imaging was done by Chemidoc Imaging System (Bio-Rad) and ImageLab software (Bio-Rad).

2.10. Protein Expression of Yeast Surface Displayed Proteins by Galactose Induction

Aga2 fused with neurodegenerative proteins were under control of GAL promoter which was induced with galactose. To do so, EBY100 yeast cell strain was grown in 10 mL selective yeast growth medium (recipe given in Appendix E, Table E.3) at 30ºC, 260 rpm overnight. When OD_{660} measured and cell amount in 1 mL was determined according to the table which is given in http://www.pangloss.com/seidel/Protocols/ODvsCells.html , ~4.63 x 10^6 cells/mL were taken into fresh selective growth medium by completing the volume to 10 mL. Cells were incubated at 30ºC, 260 rpm for 4 hours. During this incubation, OD_{660} reached approximately to 1, which is valid for induction. Then, cells were centrifuged down at 4000 g rof 5 minutes. Supernatant was discarded and cell pellet was resuspended with selective induction medium (recipe given in Appendix E, Table E.4) having galactose. The induction was done by incubating cells at 30ºC, 260 rpm for 16-20 hours. At the end of the incubation, cell amount was determined again for further use.

2.11. Biopanning against Yeast Expressing Neurodegenerative Proteins on the Surface and Bacterial Surface Display System, Phage Amplification and Phage Titering

For ligand peptide selection, EBY100 expressing neurodegenerative proteins on the surface by induction was used separately. The first day of the biopanning, 10^{11} cells were centrifuged down at 3000 g for 3 minutes. The supernatant was discarded and pellet was washed with 1mL 0.1 M $NaHCO_3$, pH 8.6 coating buffer and centrifugation was done at 3000 g for 3 minutes. Supernatant was again discarded and pellet was resuspended with 1 mL of same coating buffer. Then, cell samples was transferred into LoBind eppendorf and volume was completed to 1.5 mL. Cells in the coating buffer was incubated onto rotator at 4ºC overnight. The second day of the biopanning, incubated cells were centrifuged at 3000 g for 3 minutes. Supernatnt was discarded and cell pellet was washed with 1,5 mL 1X TBS-T by resuspending the cells and cells were centrifuged down at 3000 rpm for 3 minutes. Then, 1,5 mL 0.1 M $NaHCO_3$, pH 8.6 containing 5mg/mL BSA blocking buffer was added onto the cell pellet and resuspension was done. For blocking the cells, incubation was done at 4ºC for at 2-4 hours onto rotator. At the end of the blocking step, cells were centrifuged down at 3000 g for 3 minutes. Supernatant was discarded and cells were washed 6 times with 1X TBS-T buffer. After each washing, cells into washing buffer was centrifuged down at 3000 g for 3 minutes and supernatant was discarded after each centrifugation. At the end of the washing, 10^9 phage particle was added onto cell pellet and volume was

completed to 1 mL with 1X TBS. The cells were incubated at room temperature for 1 hour onto rotator for mixing them thoroughly. At the end of the phage binding incubation, cells were centrifuged at 3000 g for 3 minutes and supernatant was discarded. Next cells were washed 10 times with 1.5 mL 1X TBS-T to get rid off the unbound phages. After each addition and resuspension of pellet, centrifugation was done at 3000 g for 3 minutes again. For elution of the unbound phages, 1 mL 0.2 M Glycine-HCl, pH 2.2 elution buffer was added to cells and incubated at room temperature for 7 minutes with gently shaking. At the end of the elution, cells were centrifuged at 3000 g for 3 minutes and supernatant was transferred into fresh tube. To neutralize the elution, 150 µL neutralization buffer was added.

For the amplification of phage elution to increase the amount of phage particle for further use, *E.coli* ER2738 cell strain was grown overnight at 37ºC and 200 rpm. The overnight culture then diluted into 20 mL fresh LB with a dilution ratio of 1:100. The diluted culture was incubated until OD_{600} reached to 0.01-0.05 which takes about 30 minutes. Then eluted phages were added onto the diluted culture and phage propagation was done by incubation at 37ºC, 200 rpm for 4.5 hours. At the end of the propagation, cell culture having amplified phages were centrifuged at 12000 rpm, 4ºC for 10 minutes. Supernatant was transferred into a fresh tube and 5 mL of 20% PEG-8000/ 2.5 M NaCl solution was added to phage precipitation after overnight incubation at 4ºC. Next day, phage was pelleted by centrifugation at 12000 rpm 4ºC for 15 minutes. Supernatant was discarded and finger-like pellet was resuspended with 1 mL 1X TBS. Additional phage precipitation was applied by addition of 200 µL 20% PEG-8000/ 2.5 M NaCl

solution and mixture was incubated on ice for 1 hour which was followed by 14000 rpm, 4ºC centrifugation for 5 minutes. Supernatant was thrown away and pellet was resuspended with 200 µL 1X TBS. The amplified phage was tittered for determination of the amount of phage particle after amplification. This step was critical for further use of the phage during the following biopanning process.

For phage tittering, overnight grown *E.coli* ER2738 cells were diluted in fresh LB containing appropriate antibiotic with a ratio of 1:100. When OD_{600} value reached to approximately 0.5, cells were aliquoted by volume of 200 µL into sterile centrifuge tubes. At the same time, amplified phages were diluted with dilution factors of 10^{-8} to 10^{-12}. 10 µL of each diluted phage sample were added onto 200 µL of cells and they were incubated for 1-5 minutes at room temperature. After incubation, cell-phage samples were mixed with 45ºC, 3 mL top agar, then top agar were spreaded onto LB agar plates poured with X-Gal, IPTG and appropriate antibiotic. The plates were incubated at 37ºC for overnight. Phage tittering was also done for phage elutions after each biopanning procedure in order to calculate enrichment ratio. For phage elutions, dilution factor range was 10^{-2} to 10^{-4}.

Before biopanning for neurodegenerative proteins, preselection was applied with induced EBY100 expressing aga2p without fused with any protein by following the biopanning protocol except unbound phages was collected and amplified for further use in the biopanning of neurodegenerative protein expressing yeast cells.

2.12. M13 Single Plaque Amplification

For the amplification of the plaques representing one phage particle bound to neurodegenerative proteins displayed on yeast surface, phage elutions from fourth

round of biopanning for neurodegenerative proteins were tittered, as explained in Section 2.11. Next day, overnight grown ER2738 cells with tetracycline were diluted into fresh LB with 1:100 dilution factor. For one plaque amplification, 1 ml diluted cell culture was aliquoted into a fresh sterile culture tube. The plaque intent to be amplified was selected from plate via a sterile pipette tip by gently inserting the tip to the plaque. Then the tip is inserted to the diluted culture. The amplification of the plaque was carried out at 37^{o}C for 4.5 hours with shaking at 200 rpm. After the incubation, culture was centrifuged at 14000 rpm for 30 seconds. Supernatant was centrifuged again. Then the upper 800 µL of supernatant was taken gently without disrupting any cell pellets remained. To enrich the amount of the single clone of the phage, 20 µL of the amplified plaque sample was used by following the same amplification protocol explained in Section 2.11. The remaining of 800 µL of amplified phage plaque was stored at -20^{o}C with the addition of 50% glycerol in 1:1 dilution factor.

2.13. Protein Modelling for Prediction of Possible Peptide-Protein Interaction

Amino acid sequences of all neurodegenerative proteins were obtained from www.benchling.com in which the all constructs were stored. To model the neurodegenerative proteins, I-TASSER (Iterative Threading ASSEmbly Refinement), which is an online tool for modeling proteins, were reached from https://zhanglab.ccmb.med.umich.edu/I-TASSER/ and protein models were obtained by using standard parameters [60]. Also, sequenced peptides from biopanning elutions were modeled by using PEP-FOLD, which is an online tool

for predict peptide structures, with standard parameters [61]. For predicted structures of both peptide and protein, files were downloaded with .pdb extension. Then, The prediction the models for interaction of peptides with proteins was achieved by HPEPDOCK server with standard parameters, available in http://huanglab.phys.hust.edu.cn/hpepdock/ [62]. The predicted interaction models and protein models then uploaded to PyMOL software to get the images of the interaction models [63].

2.14. ELISA for Selected Phages Against Yeast Cells Expressing Neurodegenerative Proteins

In order to detect specific interaction of one clone of phage with neurodegenerative proteins expressed on the yeast surface, Enzyme-Linked ImmunoSorbent Assay (ELISA) was performed. For this purpose, the protocol was optimized for the usage of yeast cells by considering the steps of biopanning. 10^7 induced yeast cells expressing neurodegenerative proteins on the surface and yeast cells expressing only Aga2p as control were taken into 1.5 mL Eppendorf® LoBind tube for each phage clone and washed with 1X PBS/1% BSA. After centrifugation at 3000 g for 3 minutes, supernatant was removed carefully without disturbing the pellet and the pellet was again resuspended with 1.5 mL 1X PBS/ 1% BSA. The cells were incubated at room temperature for 3 hours at rotator. At the end of the incubation, cells were washed with 1X PBS/ 0.05% Tween-20 for 3 times. Then, the cells were resuspended with 1X PBS with the addition of 10^{10} single clone phage particle separately to check and to compare the interactions of phage with neurodegenerative proteins. The cells were incubated with the phages

at room temperature for 1 hour at rotator. After the incubation, cells were washed with 1X PBS/ 0.05% Tween-20 for 6 times in order to get rid of the unbound phage particles. Next, cells were resuspended with 1X PBS/ 1% BSA and M13 major coat protein antibody (Santa Cruz Biotechnology, sc-53004) with 1:500 ratio. The incubation was carried out at room temperature for 2 hours at rotator. For the elimination of the noninteracting antibody, cells were washed with 1X PBS/ 0.05% Tween-20 for 3 times. Next, the cell pellet were resuspended with 0.05 M citric acid buffer pH 4.0 including 0.03% H_2O_2 and 200 µL 2,2′-Azino-bis(3-ethylbenzothiazoline-6-sulfonic acid) diammonium salt from 15 mg/mL stock solution. After 30 minutes incubation at room temperature in the dark, cells were centrifuged at 3000 g for 3 minutes. Supernatant was transferred to 96-well plate to measure absorbance at wavelength of 405 nm with the M5 spectrophotometer.

CHAPTER 3

RESULTS AND DISCUSSION

3.1. Construction of pETcon-Aga2-NDP-sfGFP

In order to detect the expression of neurodegenerative proteins (NDPs) which are α-synuclein, amyloid β_{40} and amyloid β_{42}, huntingtin with polyglutamine repeat having 25Q, 46Q and 103Q (25Q-Htt, 46Q-Htt, and 103Q-Htt) in a fast way, superfolder green fluorescent protein (sfGFP) was fused to each pETcon-Aga2-NDP where NDP stands for α-synuclein, amyloid β_{40} and amyloid β_{42}, 25Q-Htt, 46Q-Htt, and 103Q-Htt separately. After cloning of these constructs, our former lab member Ozge Begli was used the constructs to show the expression of neurodegenerative proteins folded properly and expressed on the surface of yeast cell strain EBY100.

The first part of these clonings was the amplification of sfGFP gene by PCR (Figure 4).

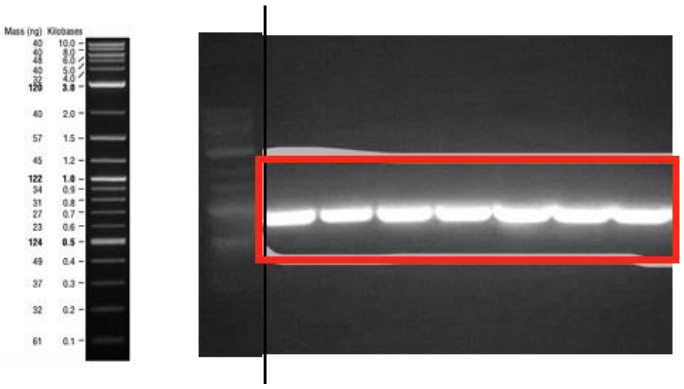

Figure 4: sfGFP PCR product on 1% agarose gel. The lanes were loaded with sfGFP gene amplified by primers for cloning into pETcon_Aga2_25Q-Htt, pETcon-Aga2-46Q-Htt, pETcon-Aga2-103Q-Htt, pETcon-Aga2-Amyloid β_{40}, pETcon-Aga2-Amyloid β_{42} and pETcon-Aga2-α-synuclein respectively.

Preparation of backbone for clonings, pETcon_Aga2_25Q-Htt, pETcon-Aga2-46Q-Htt, pETcon-Aga2-103Q-Htt, pETcon-Aga2-Amyloid β_{40}, pETcon-Aga2-Amyloid β_{42} and pETcon-Aga2-α-synuclein vectors were digested with BamHI restriction enzyme (Figure 5).

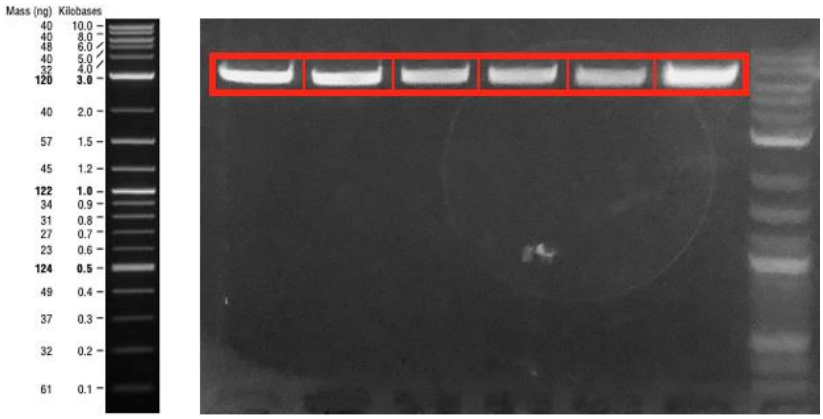

Figure 5: BamHI digestion reactions image. The lane was loaded with digested pETcon vector oh which 25Q-Htt, 46Q-Htt, 103Q-Htt, Amyloid β_{40}, Amyloid β_{42}, α-synuclein genes expressed respectively.

After gel extraction of both sfGFP and backbone for each NDPs, DNA fragments were assembled by Gibson assembly method which was followed by transformation to E.coli DH5α PRO strain. The colonies were selected and after plasmid isolation, plasmids were sequenced by Sanger sequencing method at Genewiz company. According to sequencing results, sfGFP sequence in each construct was verified.

3.2. Neurodegenerative Protein Display by Using Bacterial Surface Display Vector

Until yeast surface display system was optimized for all NDPs, bacterial surface display system was intended to use for all biopanning optimization experiments. To do so, Ag43 autotransporter protein was decided to use for bacterial surface display of NDPs. Ag43 autotransporter protein is a surface protein of bacteria used in secretion systems [63]. Ag43 is composed of a N-terminal signal peptide, N-proximal passenger domain which is also called α-passenger domain and secreted to outer of the membrane, an autochaperone domain which have a role in folding of the α-passenger domain, and β-barrel (β-translocation) domain at C-terminus of the peptide which is a translocator for passenger domain to pass through the outer membrane during secretion. [63].

Ag43 protein was previously engineered our lab member Recep Erdem Ahan to secrete protein of interest to outer membrane of E.coli by replacing the first 160 amino acid region of α-passenger domain with protein of interest in a controlled way [64]. The Ag43 surface display construct is basically shown in Figure 6.

Figure 6: The structure of Ag43 autotransporter-dependent bacterial surface display system

3.2.1. Cloning of 25Q-Htt into pET22b-pelB-Ag43-160N Vector

For surface display, pET22b-pelB-6H-Ag43-160N-sfGFP vector, which was cloned by Recep Erdem Ahan, was used as backbone. For obtain linearized vector without TEV recognition site and sfGFP gene, it was supposed to be digested with NcoI and AflII restriction enzymes. However, 160N α-subunit gene also posses NcoI restriction enzyme cut site. Thus, the complete gene fragment of β-subunit, 160N α-subunit, TEV recognition site and sfGFP was removed by double digestion reaction with NcoI and XhoI restriction enzymes. In the gel image, there was three distinct bands were observed (Figure 7).

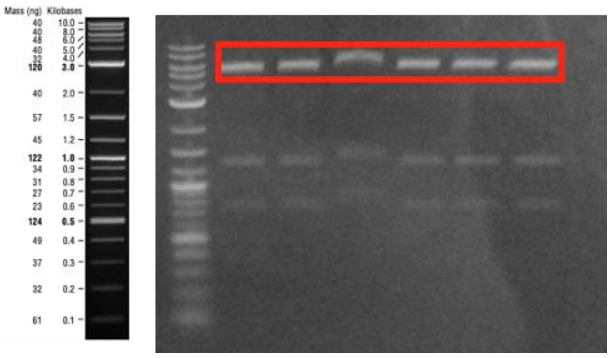

Figure 7: Digestion result of pET22b-pelB-6H-Ag43-160N-sfGFP vector. The backbone was indicated with red rectangle. The expected band size is 7413 bp. The band at the middle of the lane is sfGFP which is 773 bp long after digestion and the band at the bottom is digested part of α-subunit which is 508 bp long after digestion.

For inserting β-subunit and 160N α-subunit again, PCR was applied by using the same vector with Gibson assembly primers, which overhang with 25Q-Htt at N-terminus and digested vector at C-terminus separately (Figure 8).

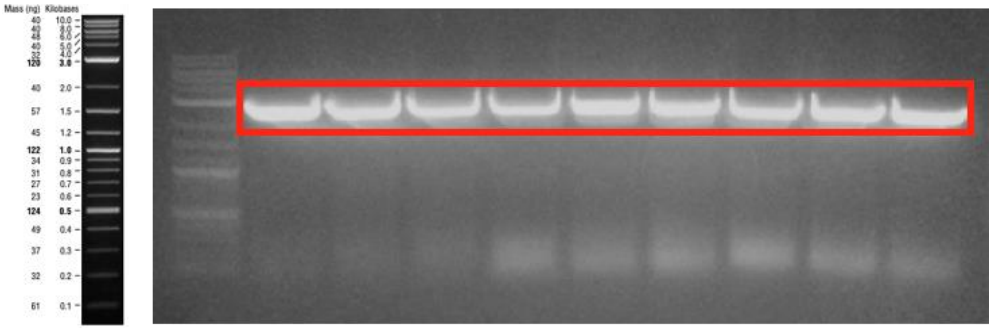

Figure 8: PCR product of β-subunit_160N α-subunit fragment which was amplified by Gibson assembly primers. The expected band size was 2545 bp-long.

25Q-Htt DNA fragment was amplified from pETcon-Aga2-25Q-Htt vector by PCR with Gibson assembly primers, which overhang with vector at N-terminus and α-subunit at C-terminus separately (Figure 9). Also, by using these primers, SpeI restriction enzyme cut site and BamHI restriction enzyme cut site were added to N-terminus and C-terminus of the gene fragment respectively in order to ease the cloning of other NDPs into this vector.

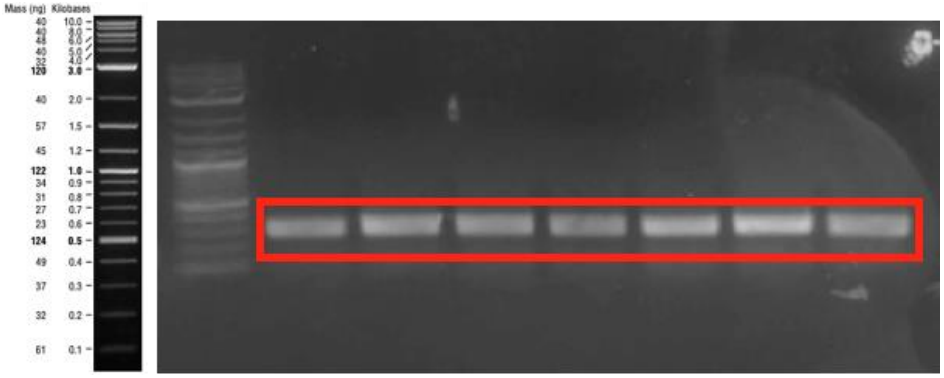

Figure 9: PCR product of 25Q-Htt fragment which was amplified by Gibson assembly primers. The expected band size was 333 bp-long.

The amplified genes, then, were assembled with Gibson assembly method, which was followed by transformation into E.coli DH5α PRO. The colonies were selected and after plasmid isolation, plasmids were digested with SpeI and BamHI for verification and plasmids verified by restriction enzyme digestion were sequenced with Sanger sequencing method by Genewiz Company (Figure 10). According to the sequencing result, the cloned genes were verified.

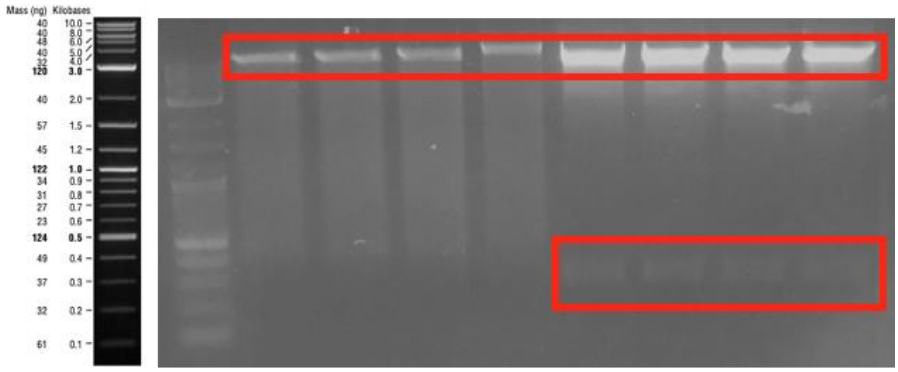

Figure 10: Digestion reaction results of pET22b-pelB-Ag43-160N-25Q-Htt.

The backbone was expected with a size of 7935 bp-long and 25Q-Htt was expected with a size of 294 bp-long. 25Q-Htt band was not obvious in the image since agarose gel was poured as 1%. Thus, small-sized 25Q-Htt was diffused through the gel.

3.2.2. Cloning of α-synuclein into pET22b-pelB-Ag43-160N Vector

For cloning α-synuclein, pET22b-pelB-Ag43-160N-25Q-Htt verified vector was used. By addition of SpeI and BamHI restriction enzyme cut sites, this vector was preferred over pET22b-pelB-Ag43-160N-sfGFP. The vector was digested with SpeI and BamHI restriction enzyme in order to linearize the vector and removing 25Q-Htt gene (Figure 11).

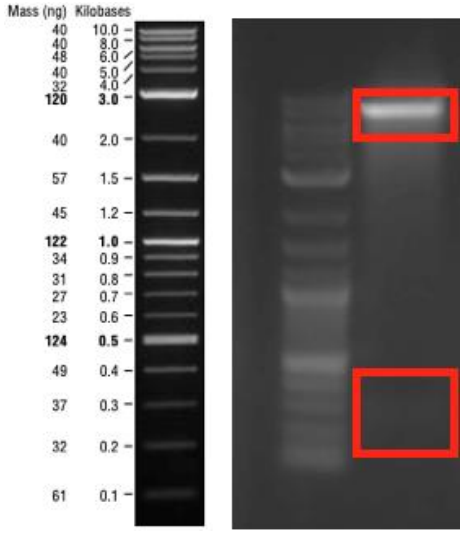

Figure 11: Digestion reaction results of pET22b-pelB-Ag43-160N-25Q-Htt. The backbone was expected with a size of 7935 bp-long and 25Q-Htt was expected with a size of 294 bp-long. 25Q-Htt band was not obvious in the image since agarose gel was poured as 1%. Thus, small-sized 25Q-Htt was diffused through the gel.

α-synuclein was amplified by PCR with Gibson assembly primers (Figure 12).

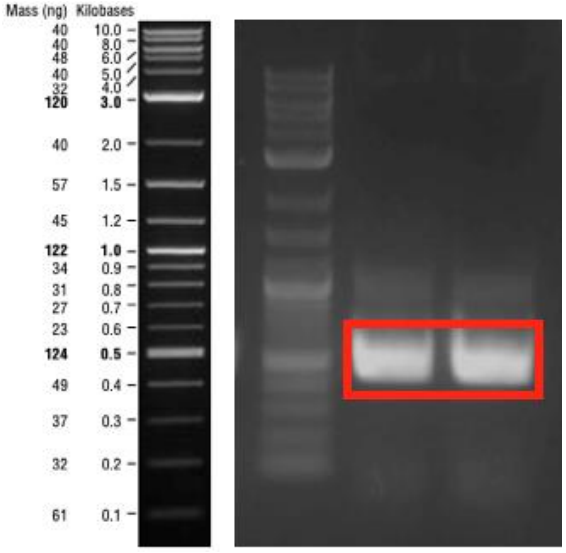

Figure 12: PCR product of α-synuclein fragment which was amplified by Gibson assembly primers. The expected band size was 512 bp-long.

After purifying genes from gel, Gibson assembly method was applied which was followed by transformation, colony selection and plasmid isolation. Isolated plasmids were digested with SpeI and BamHI for verification (Figure 13). Digestion-verified plasmids were send to Genewiz company for Sanger sequencing. After sequencing result was received, the sequence was shown verified.

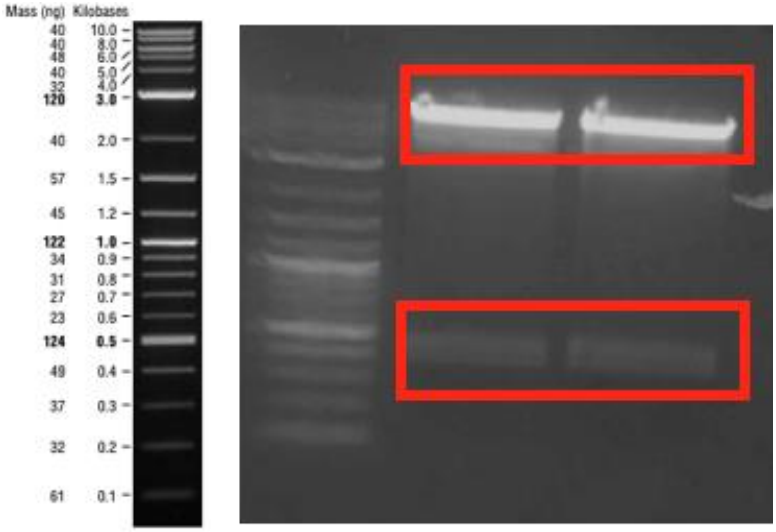

Figure 13: Digestion reaction results of pET22b-pelB-Ag43-160N- α-synuclein. The backbone was expected with a size of 7935 bp-long and α-synuclein was expected with a size of 438 bp-long.

3.2.3. Cloning of Amyloid β_{40} into pET22b-pelB-Ag43-160N Vector

pET22b-pelB-Ag43-160N-25Q-Htt vector was used as backbone. First 25Q-Htt was removed from the vector and vector was linearized with double digestion reaction by using SpeI and BamHI enzymes (Figure 14).

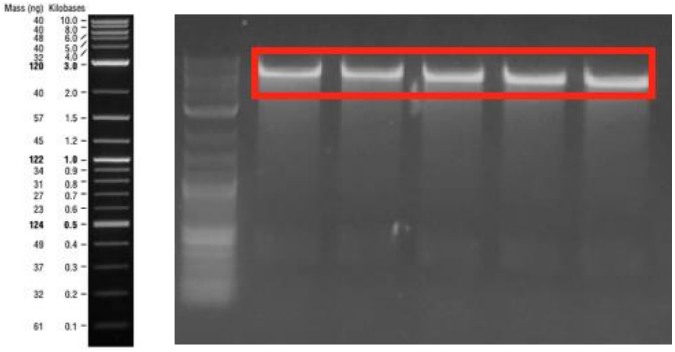

Figure 14: Digestion reaction results of pET22b-pelB-Ag43-160N-25Q-Htt. The backbone was expected with a size of 7935 bp-long and 25Q-Htt was expected with a size of 294 bp-long. 25Q-Htt band was not obvious in the image since agarose gel was poured as 1%. Thus, small-sized 25Q-Htt was diffused through the gel.

Amyloid β_{40} gene was amplified by PCR with Gibson assembly primers (Figure 15).

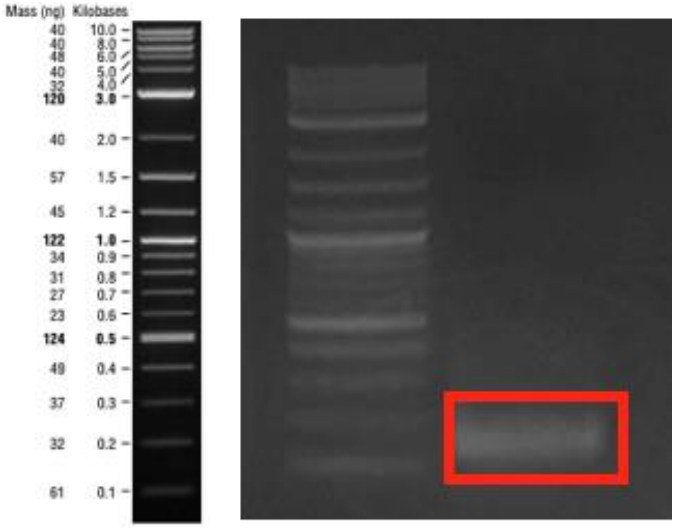

Figure 15: PCR product of amyloid β_{40} fragment which was amplified by Gibson assembly primers. The expected band size was 220 bp-long.

After DNA fragments were purified from gel, Gibson assembly method was applied which was followed by transformation, colony selection and plasmid isolation. Isolated plasmids were digested with SpeI and BamHI restriction enzymes (Figure 16). Then, Sanger sequencing was done for this construct by Genewiz Company. According to sequencing result, verification was completed for this construct.

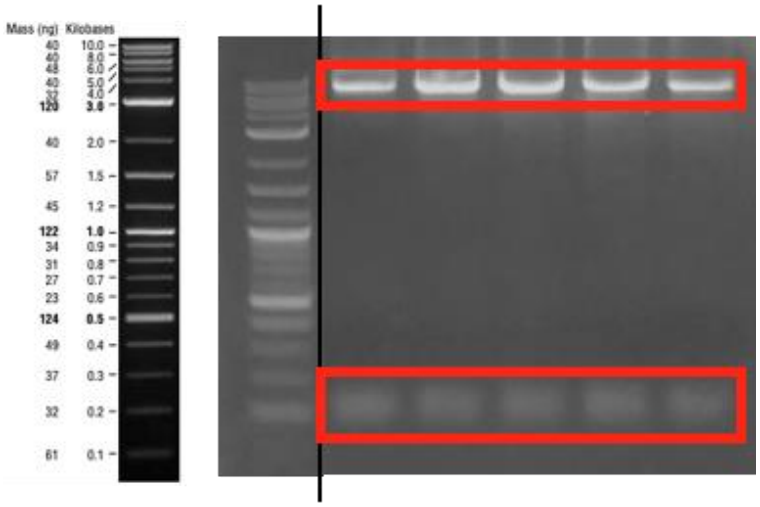

Figure 16: Digestion reaction results of pET22b-pelB-Ag43-160N-Amyloid β_{40}. The backbone was expected with a size of 7935 bp-long and amyloid β_{40} was expected with a size of 141 bp-long.

3.2.4. Surface Displayed 25Q-Htt, α-Synuclein and Amyloid β_{40} with Heat Shock

The expression of protein of interest on outer membrane of E.coli can be verified by heat release of α-subunit, which is attached to β-subunit of Ag43 noncovalently. In order to disruption of noncovalent interaction between these two subunits can be achieved by brief heating [65]. After heat treatment, α-subunit fused with protein of interest is released to extracellular environment. As well as,

acetone precipitation can be applied to concentrate the proteins in the extracellular environment in order to use in characterization studies.

The bacterial surface display constructs were designed without any antibody tags such as 6X His tag since cloning additional tags fused to proteins were supposed to affect the efficiency of binding of M13 during biopanning experiments with possible higher interaction with M13 and additional tags. Hence, verification of expressions and translocations of NDPs with α-subunit to outer membrane of E.coli was achieved only with SDS-PAGE analysis (Figure 17-19).

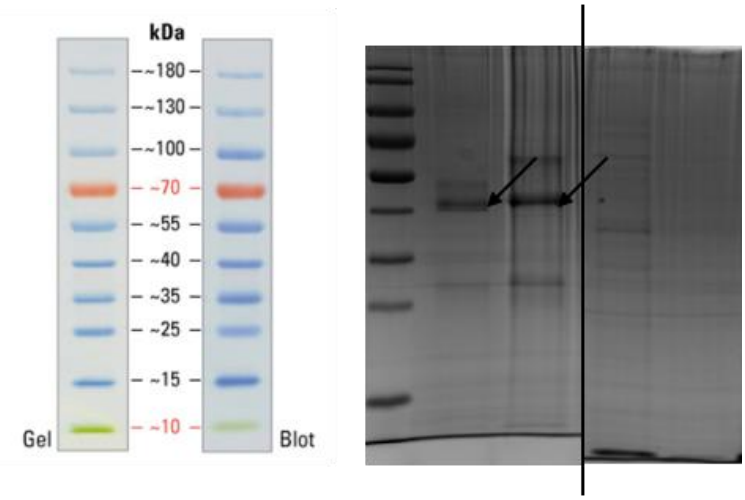

Figure 17: SDS-PAGE gel image result of BL21 cells expressing 25Q-Htt on surface with fusion of Ag43 autotransporter. First indicated band was from heat release-applied sample, second indicated band was from heat release-applied sample which was precipitated with acetone. Third and fourt lanes were loaded with controls prepared with empty BL21 cells by applying same preparation steps for the first sample and the second sample respectively. The expected size was 42 kDa.

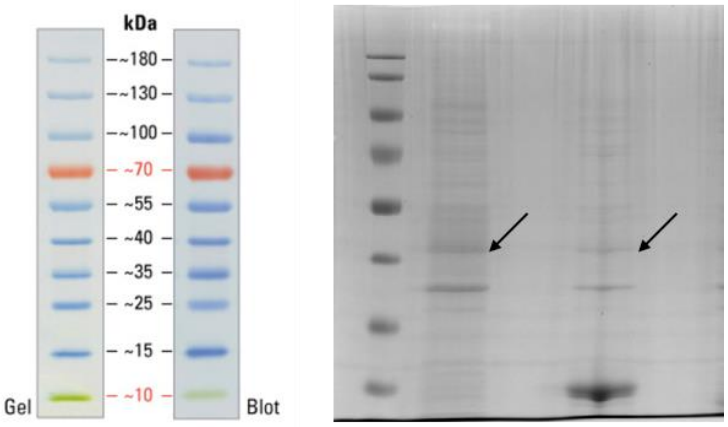

Figure 18: SDS-PAGE gel image result of BL21 cells expressing α-synuclein on surface with fusion of Ag43 autotransporter. First indicated band was from heat release-applied sample which was precipitated with acetone, second indicated band at third lane was from heat release-applied sample. Second and fourt lanes were loaded with controls prepared with empty BL21 cells by applying same preparation steps for the first sample and the second sample respectively. The expected size was 45 kDa.

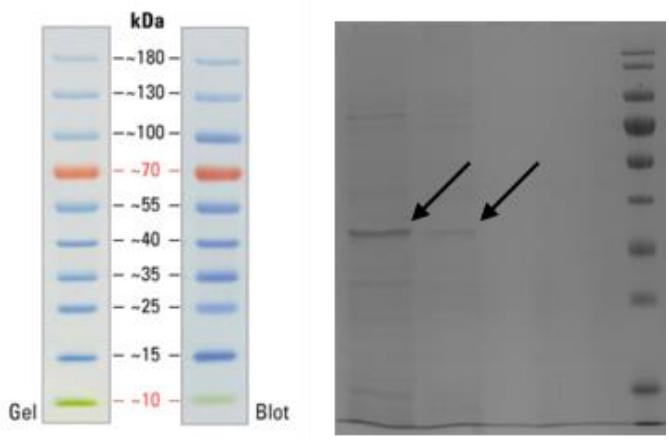

Figure 19: SDS-PAGE gel image result of BL21 cells expressing amyloid-β_{40} on surface with fusion of Ag43 autotransporter. First indicated band was from heat release-applied sample which was precipitated with acetone, second indicated band was from heat release-applied sample. Third and fourt lanes were loaded with controls prepared with empty BL21 cells by applying same preparation steps for the first sample and the second sample respectively. The expected band size was 38 kDa.

According to SDS-PAGE analysis data, the intensities of bands of samples obtained after acetone precipitation of extracellular α-subunit fused with NDPs was higher than the samples obtained from only after heat treatment. Still, for each case, NDPs were expressed on the cell surface well. Thus, bacterial surface display system for NDPs was decided to use in first trial of biopanning experiments.

3.3. Construction of Combinatorial M13 Phage Display Library by PCR and Biopanning against *E.coli* Expressing Neurodegenerative Amyloids as a Fusion of Autotransporter Ag43

M13 phage display technique is highly popular display system since diverse gene fragments, large antibodies and peptides having varied length can be expressed on the surface by insertion of antibodies/peptides within *pIII* gene. Also, M13 is neither lytic nor lysogenic and it can infect only filamentous bacteria resulting in slowing down cell division [65]. So, this system can be used in screening against large number of cell types. Also, M13 phage expressing different types of proteins on the surface serves high number of clones. Thus, this is applicable for screening against our bacterial surface display system and yeast surface display system.

In addition to these, the reason of using synthetic peptide library having random sequences instead of cDNA libraries is to give much more different phage clone after screening. Thus, small-sized peptide displaying gives higher chance to select most interacting peptide with NDPs.

Before all biopanning experiments, first small-scale then large-scale combinatorial M13 phage display library was tried to produce by using single clone of M13 bacteriophage which was a gift from Dr. Ceyda Seker. Increasing the diversity of the number of different 12 amino acid long peptides on pIII gene of M13, PCR was supposed to be applied by using degenerate primer for inserting degenerate region that should be translated 12 amino acid long peptide sequences

randomly during M13 phage replication. Also, primers had KpnI cut site near N-terminus in order to perform T4 ligation (Figure 20).

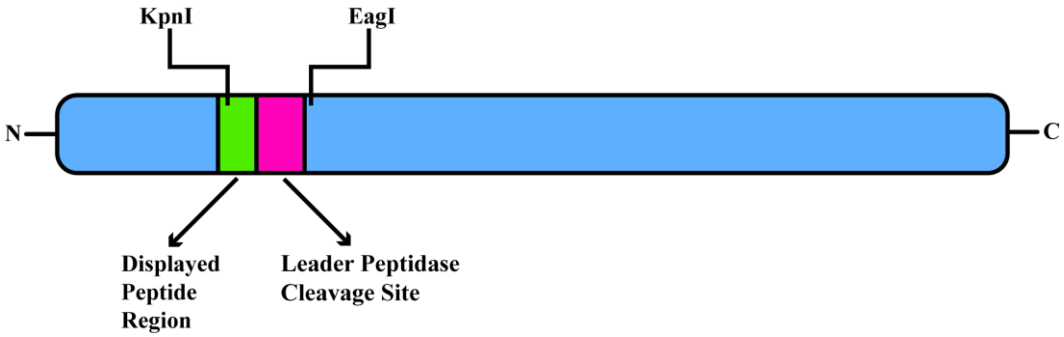

Figure 20: The structure of M13-pIII display system

PCR products gave bands at expected size for M13-KE genome amplification (Figure 21).

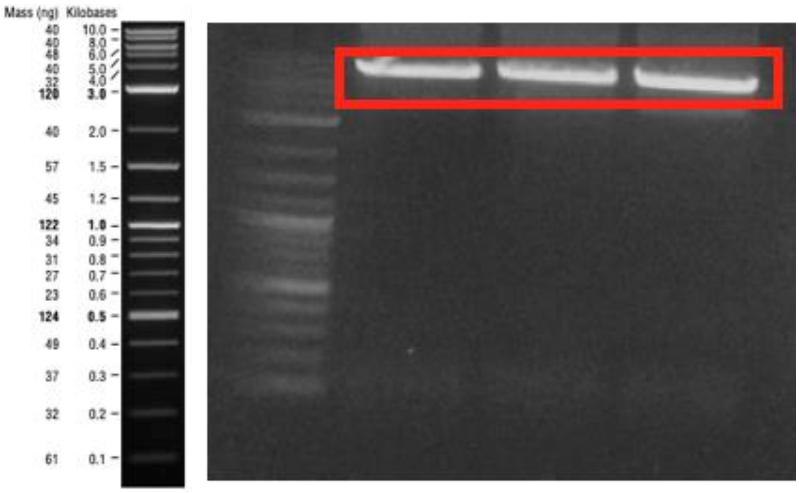

Figure 21: PCR product of M13 genome which was amplified by Gibson assembly primers. The expected band size was 7317 bp-long.

After PCR, which was followed by DNA purification from gel and restriction enzyme digestion with KpnI, and then T4 ligation and electroporation, blue plaques were observed on agar plate (Figure 22).

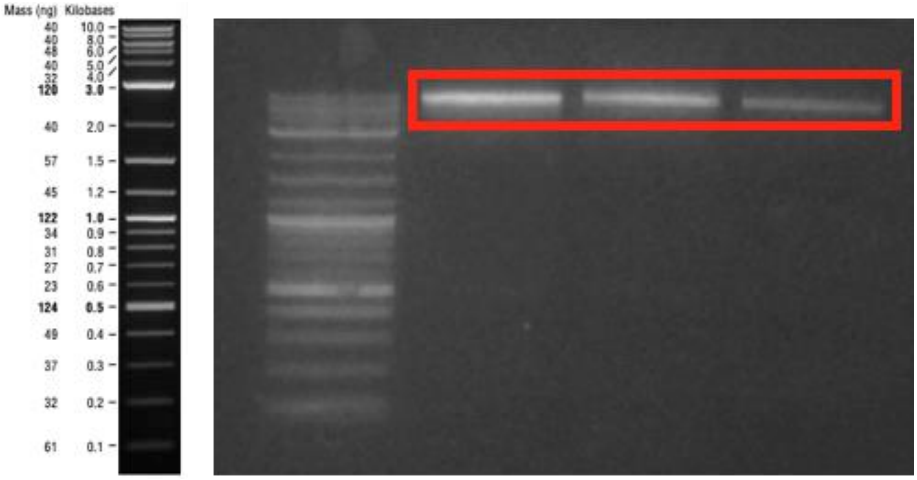

Figure 22: Digestion reaction results of M13 genome PCR product. The expected size was 7282 bp-long

For fast verification of M13 phage cloning, PCR was done to a selected four blue plaques. The gel image gave a positive result by M13 genome amplification (Figure 23).

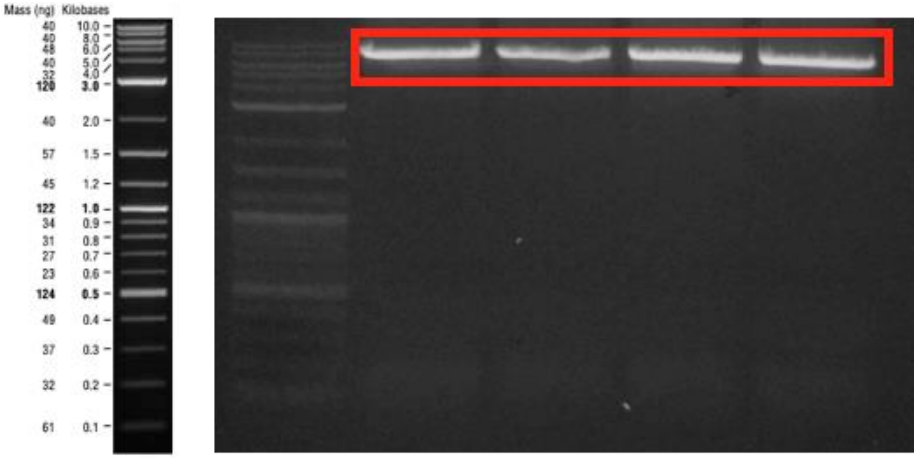

Figure 23: PCR product of M13 genome. The expected band size was 7317 bp-long.

Also, two of the four blue plaques were amplified for sequencing. However, sequencing gave no result because of no priming of the sequencing primer, which

might be occurred due to difficult template of M13 genome or contamination. Still, all steps were followed with large-scale samples and reactions for producing M13 phage display library with large number of clones. According to phage tittering results, library size was only about 6.4 X 10^8 pfu/mL (Figure 24).

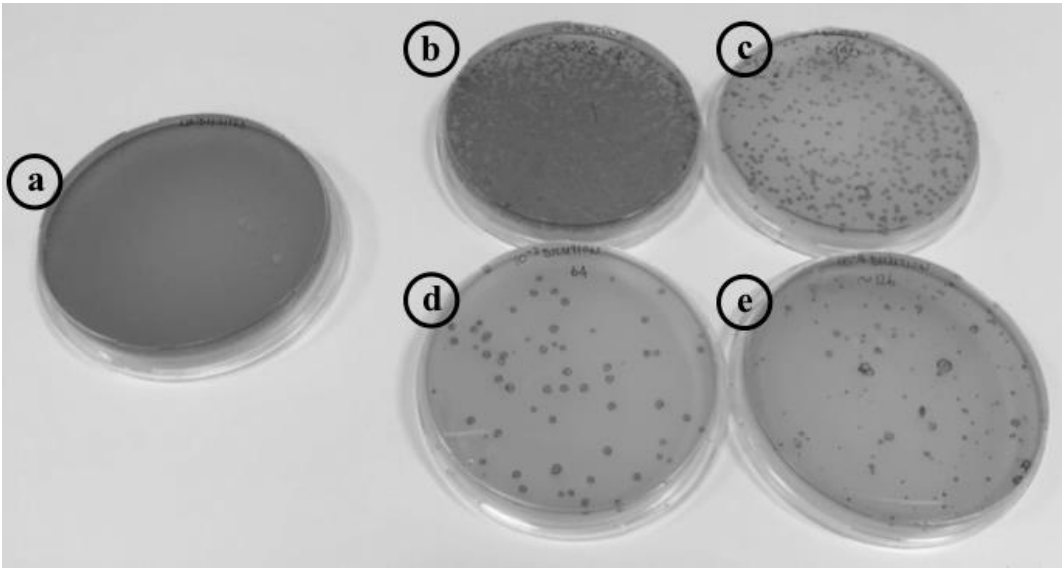

Figure 24: The tittering plates with different dilution factors for determination of library size. a) Phage tittering plate with a dilution factor of 10^{-2}. There were lots of blue plaques that formed smear. b) Phage tittering plate with a dilution factor of 10^{-3}. There were lots of blue plaques that were not countable.) Phage tittering plate with a dilution factor of 10^{-4}. There were more than 300 blue plaques that were not appropriate for determining phage amount. d) Phage tittering plate with a dilution factor of 10^{-5}. There were 64 blue plaques which was relatable with plate c. e) Phage tittering plate with a dilution factor of 10^{-6}. There were 124 blue plaques that were more than expected.

Again, 12 different blue plaques were selected and amplified for sequencing but sequencing result gave no priming error. For verification of M13 existence, PCR was done, and gel image gave positive result for M13 (Figure 25).

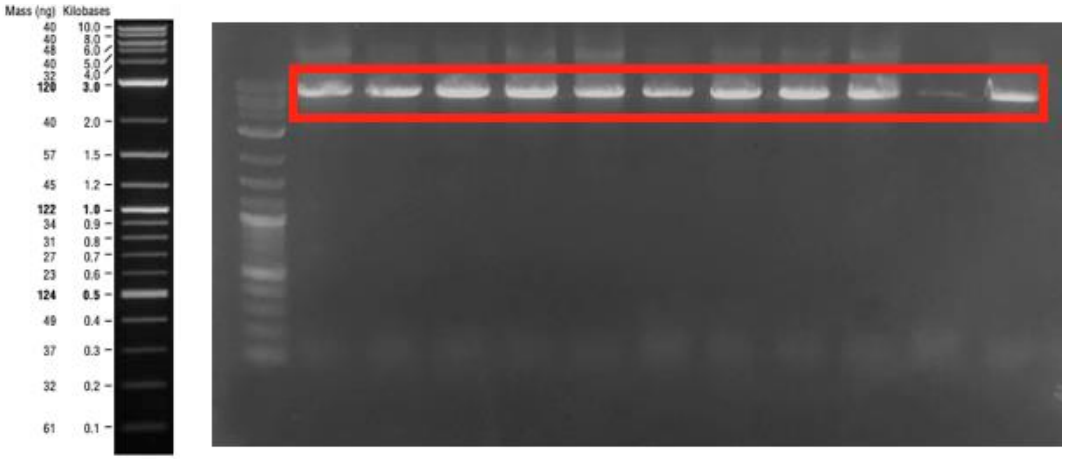

Figure 25: PCR product of M13 genome. The expected band size was 7317 bp-long.

As an additional verification of intact bacteriophage existence, constructed M13 phage display library was analyzed with SEM (Figure 26). M13 bacteriophage is 880 nm long and its diameter is 6nm [66]. Thus, according to this information, SEM image verified that M13 phage display library was not contaminated and full of phage particle. This image was also similar to literatüre [67-70].

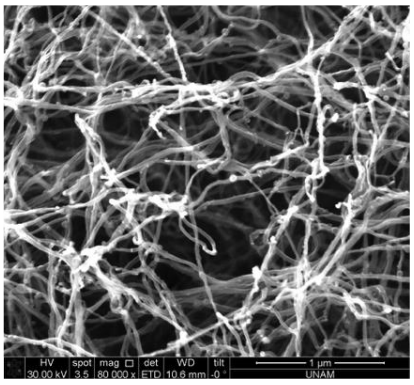

Figure 26: ESEM image of M13 bacteriophages.

After these, biopanning by using PCR-dependently constructed M13 phage display library was performed with E.coli expressing 25Q-Htt on the surface. At the end of 3rd biopanning, 7 blue plaques were selected for sequencing, and isolated directly from ER2738 strain as circular double stranded DNA. According to Sanger sequencing, all of the sequenced phages were cloned as wild-type M13 genome. This was occurred due to failure of the synthesizing of degenerate primer.

Hence, the strategy was changed into oligonucleotide, which has degenerate region, insertion into M13 genome.

3.4. Construction of Combinatorial M13 Phage Display Library by Oligonucleotide Insertion

For construction of M13 phage display library, 2nd strategy was oligonucleotide containing random peptide region insertion into M13 genome by T4 ligation. To do so, oligonucleotide containing degenerate region was synthesized by Genewiz Company as single-stranded DNA fragment. The oligonucleotide, then turned into double-stranded fragment by annealing with extension primers and amplified by Klenow fragment with a small-scale reaction.

To determine the sensitivity of nondenaturing PAGE, Klenow reaction product and KpnI restriction enzyme digestion reaction were loaded to the gel 8% nondenaturing PAGE since small DNA fragments do not diffused during electrophoresis and visualized clearly when it is compared with agarose gel electrophoresis (Figure 27).

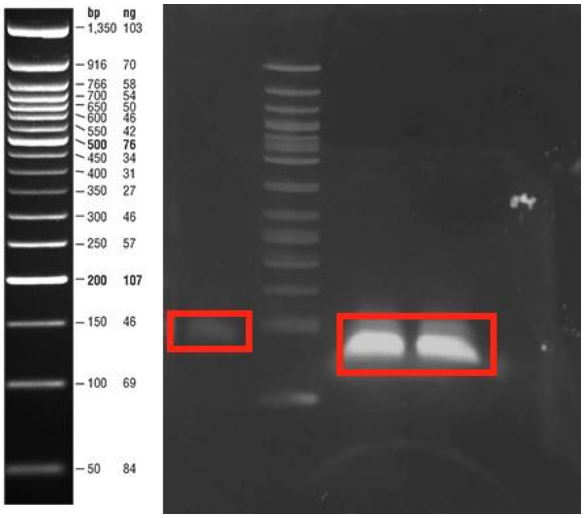

Figure 27: Klenow reaction product and KpnI-digested ds-oligonucleotide. The first lane was Klenow reaction product that is 89 bp-long. The 3rd and 4th lanes were loaded with digestion reaction product that was 72 bp-long.

According to the gel result, small-sized difference can be distinguished clearly as well as the fragment containing neurodegenerative region did not transcribed as having KpnI cut site.

To continue to preparing insert from Klenow fragment amplification reaction, KpnI and EagI restriction cut sites were added to N-terminus and C-terminus respectively. To prepare fragment for ligation reaction, KpnI and EagI restriction enzyme digestion was done. The amplified fragment and digested fragment were visualized by 8% nondenaturing PAGE (Figure 28).

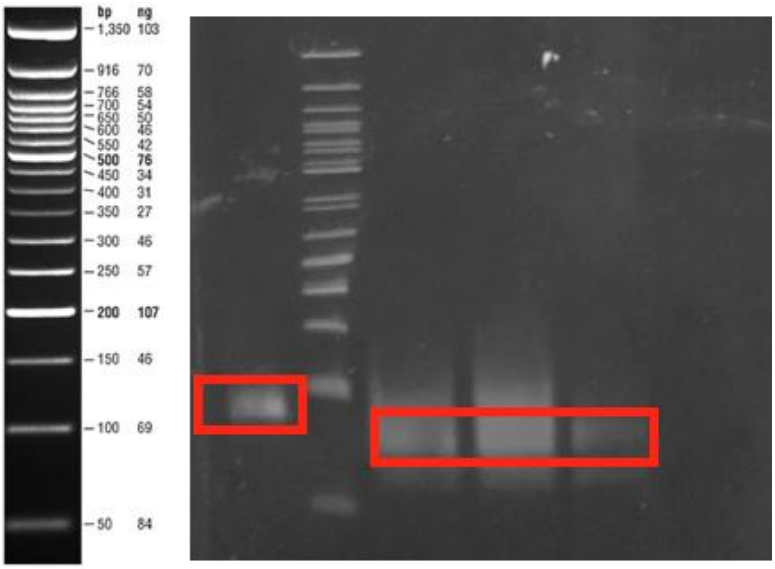

Figure 28: Klenow reaction product and KpnI and EagI digested ds-oligonucleotide. The first lane was Klenow reaction product that is 89 bp-long. The 3rd, 4th and 5th lanes were loaded with digestion reaction product that was 55 bp-long.

Double-stranded DNA fragment was extracted from gel and prepared for ligation by double restriction enzyme digestion with KpnI and EagI restriction enzymes. The reaction product was visualized by nondenaturing PAGE. Digested DNA fragments were observed as smear. Nevertheless, the band was extracted from the region equaled to the expected size.

For construction of the library, M13 genome was amplified as double-stranded DNA by PCR and visualized with agarose gel electrophoresis (Figure 29).

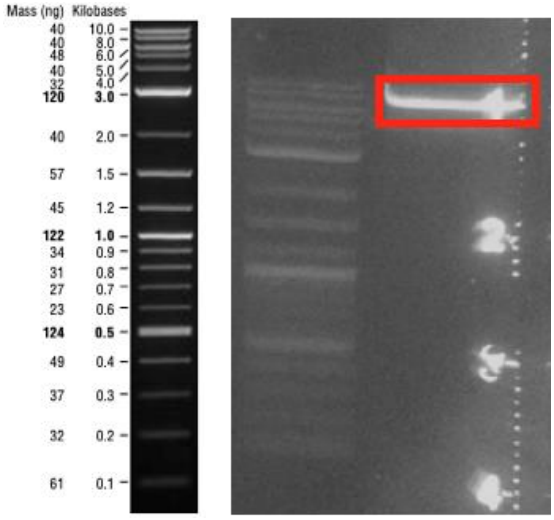

Figure 29: PCR product of M13 genome. The expected band size was 7300 bp-long.

Then, amplified, linearized, double-stranded M13 genome was prepared for T4 ligation by double restriction enzyme digestion with KpnI and EagI. The restriction reaction product was visualized by agarose gel electrophoresis (Figure 30).

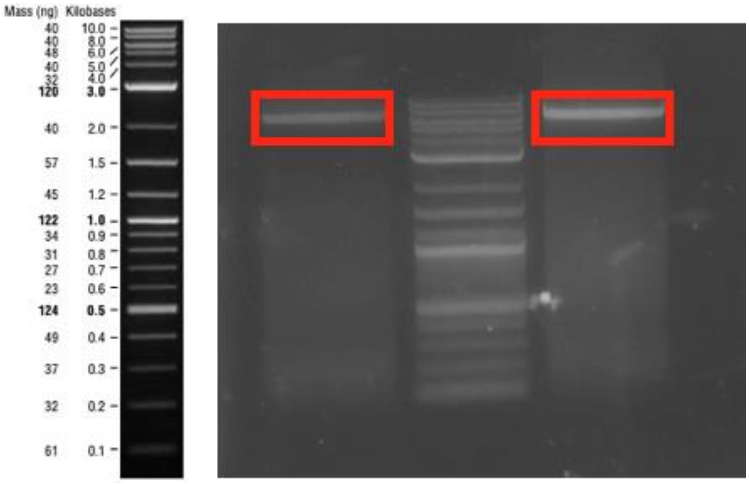

Figure 30: Digestion reaction results of M13 genome PCR product. The expected size was 7227 bp-long.

Both purified double-stranded oligonucleotide and M13 genome were ligated to each other by T4 ligation, which was followed by transformation.

16 blue plaques were selected for phage genome purification by using plasmid isolation kit. Isolated M13 genomes were checked for insertion verification by PCR (Figure 31).

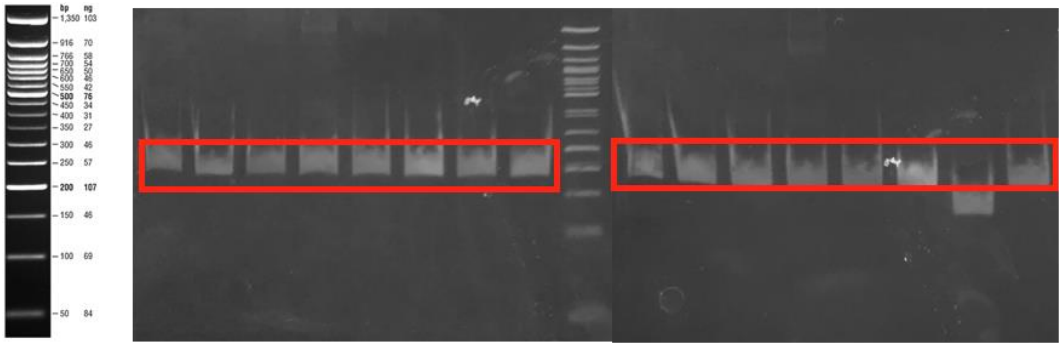

Figure 31: PCR product of M13 pIII. The expected band size was 173 bp-long.

After PCR verification, some of M13 genome samples were send to Genewiz Company for Sanger sequencing. According to sequencing result, both library peptide sequences and lengths were randomized. The reason of undetermined peptide length might be originated from random KpnI and/or EagI cut site insertion on degenerate region during oligonucleotide amplification although only KpnI restriction enzyme digestion result did not give such result. The probable cut site insertion might be occurred randomly.

This problem could be overcame by using high percentage of nondenaturing polyacrylamide gel and separating each of digested oligonucleotide clearly.

This strategy was proper for library construction. However, it required more optimization such as digested fragment separation and producing high number of

phage clones. Therefore, as a 3rd option, the Ph. D. -12 Phage Display Peptide Library kit (NEB) was determined to use in biopanning experiments.

3.5. Biopanning against Neurodegenerative Proteins to Select Inhibitory Ligand Peptides with Yeast Surface Display Systems and Phage Display Technology

In general panning method, target covers ELISA plate surface and phage display library added onto target for selection. In our case, yeast surface display system did not cover the ELISA plate. Instead of this, LoBind eppendorf tubes were used since they have been produced for protein storage with low interaction efficiency between proteins and tube itself. After couple of experiments, biopanning protocol was optimized as explained in Section 2.11.

Before peptide screening against NDPs, preselection of phage display library was done by using yeast cells expressing Aga2 only after galactose induction.

Unbound phages to yeast cells expressing complete surface display system except NDPs is crucial since elimination of phages bound to any surface molecules of yeast cell can give false positive results during biopanning of NDPs. Thus, after preselection, phages bound to surface molecules were separated from phages uninteracted with any yeast surface molecules. So, unbound phages were amplified for biopanning experiments of NDPs with higher chance of interaction and specification.

For the preselection biopanning, 1 X 10^{11} pfu was used against 1 X 10^{9} yeast cells. According to phage tittering results of amplification of unbound phages, new phage display library for NDPs had about 18 X 10^{13} pfu/mL.

Yeast surface display systems were induced with galactose in order to express neurodegenerative proteins on the yeast surface separately for each biopanning experiments. For each round of biopanning, 1 X 10^{9} yeast cell and more or less 1 X 10^{11} pfu was used. In other words, approximately 100 phage particles were used for one yeast cell. For each biopanning round, yeast cell amount and phage particle amount were recorded. Also, at the end of each panning, amount of eluted M13 phages were determined for ratio calculations which is done by dividing output (eluted) phage amount by input phage (used phage during biopanning) amount and the enrichment ratios were determined by dividing the ratio result of 2^{nd} and following pannings with 1^{st} panning ratio result. By applying these formulas, ratio results and enrichment ratio results were obtained for phages that were assummed to bind to 25Q-Htt (Figure 32), 46Q-Htt (Figure 33), 103Q-Htt (Figure 34), amyloid-β_{40} (Figure 35), amyloid-β_{42} (Figure 36), amyloid-β_{40X2} (Figure 37) and α-synuclein (Figure 38).

A)

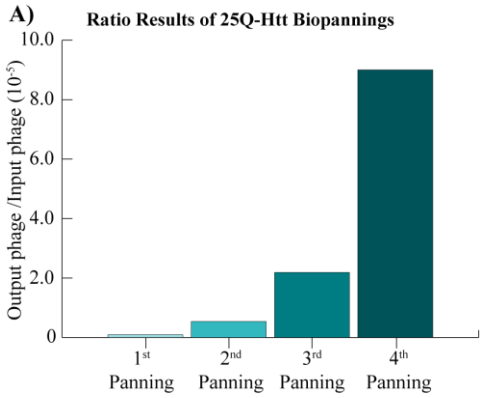

B)

25Q-Htt	1st Round	2nd Round	3rd Round	4th Round
Input Phage (pfu)	1.8×10^{11}	1.28×10^{11}	1.12×10^{11}	0.5×10^{11}
Output Phage (pfu)	1.74×10^{6}	6.9×10^{5}	12.45×10^{6}	4.5×10^{6}
Ratio (Output/Input)	9.66×10^{-7}	5.39×10^{-6}	2.19×10^{-5}	9.0×10^{-5}
Enrichment Ratio	1.0	5.6	22.6	93.2

Figure 32: Phage ratio calculations and enrichment ration results from biopanning of 25Q-Htt. A) Ratio calculations obtained from 'output phage (pfu)/ input phage (pfu)' of 25Q-Htt biopanning results. B) Table for input phage amount, output phage amount, ratio and enrichment ratio obtained from 25Q-Htt biopanning.

By considering this result, enrichment ratio was highly sufficient which means that 25Q-bound phages were eluted and amplified after each biopanning result. However, the quantification of expression level of 25Q-Htt was not done before each biopanning procedure. Thus, if yeast cells used in last biopanning cycle expressed more 25Q-Htt proteins on the surface, phage interaction level might increase. This 93.2 fold increase in enrichment can be analyzed with an optimized ELISA protocol (this is applicable for all other NDP enrichment ratio analysis).

A)

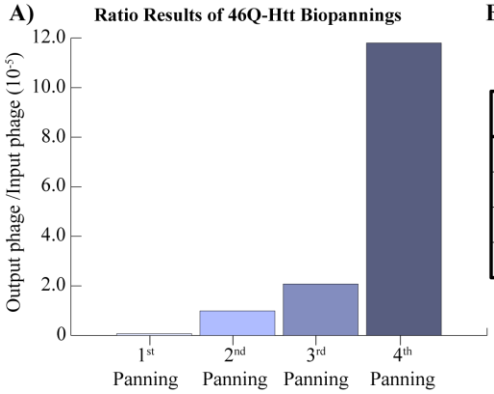

B)

46Q-Htt	1st Round	2nd Round	3rd Round	4th Round
Input Phage (pfu)	1.8×10^{11}	1.42×10^{11}	0.8×10^{11}	0.5×10^{11}
Output Phage (pfu)	1.26×10^{6}	1.41×10^{6}	1.66×10^{6}	5.9×10^{6}
Ratio (Output/Input)	7.0×10^{-7}	9.93×10^{-6}	2.1×10^{-5}	1.18×10^{-4}
Enrichment Ratio	1.0	14.2	30.0	168.6

Figure 33: Phage ratio calculations and enrichment ration results from biopanning of 46-Htt. A) Ratio calculations obtained from 'output phage (pfu)/ input phage (pfu)' of 46Q-Htt biopanning results. B) Table for input phage amount, output phage amount, ratio and enrichment ratio obtained from 46Q-Htt biopanning.

According to this result, there was 168.6-fold increase in enrichment ratio of phages that bound to 46Q-Htt. This result was highly sufficient for selecting phages for further experiments if the expression levels of 46Q-Htt proteins on yeast surface were similar for yeast used in each biopanning cycle.

A)

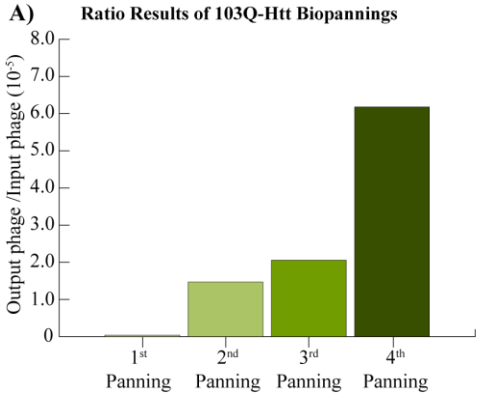

B)

103Q-Htt	1st Round	2nd Round	3rd Round	4th Round
Input Phage (pfu)	1.8×10^{11}	1.28×10^{11}	1.5×10^{11}	0.5×10^{11}
Output Phage (pfu)	7.8×10^{5}	1.88×10^{6}	3.09×10^{6}	2.61×10^{6}
Ratio (Output/Input)	4.33×10^{-7}	1.47×10^{-5}	2.1×10^{-5}	6.18×10^{-5}
Enrichment Ratio	1.0	33.9	47.6	142.7

Figure 34: Phage ratio calculations and enrichment ration results from biopanning of 103-Htt. A) Ratio calculations obtained from 'output phage (pfu)/ input phage (pfu)' of 103Q-Htt biopanning results. B) Table for input phage amount, output phage amount, ratio and enrichment ratio obtained from 103Q-Htt biopanning.

For 103Q-Htt-bound phages, enrichment ratio increased up to142.7 which was highly enough for selecting phages for further experiments. . However, the quantification of expression level of 103Q-Htt was not done before each biopanning procedure. Thus, if yeast cells used in last biopanning cycle expressed more 103Q-Htt proteins on the surface, phage interaction level might increase.

A)

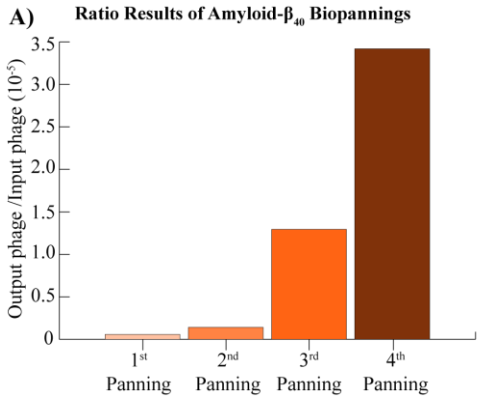

B)

Amyloid β_{40}	1st Round	2nd Round	3rd Round	4th Round
Input Phage (pfu)	1.8×10^{11}	1.9×10^{11}	1.32×10^{11}	0.5×10^{11}
Output Phage (pfu)	1.03×10^{6}	2.5×10^{5}	1.71×10^{6}	3.5×10^{6}
Ratio (Output/Input)	5.72×10^{-7}	1.42×10^{-6}	1.3×10^{-5}	3.42×10^{-5}
Enrichment Ratio	1.0	2.5	22.6	59.8

Figure 35: Phage ratio calculations and enrichment ration results from biopanning of amyloid-β_{40}. A) Ratio calculations obtained from 'output phage (pfu)/ input phage (pfu)' of amyloid-β_{40} biopanning results. B) Table for input phage amount, output phage amount, ratio and enrichment ratio obtained from amyloid-β_{40} biopanning.

These results gave 59.8-fold increase in enrichment ratio of phages that bound to amyloid-β_{40}. This result was sufficient for selecting phages for further experiments if the expression levels of amyloid-β_{40} proteins on yeast surface were similar for yeast used in each biopanning cycle.

A)

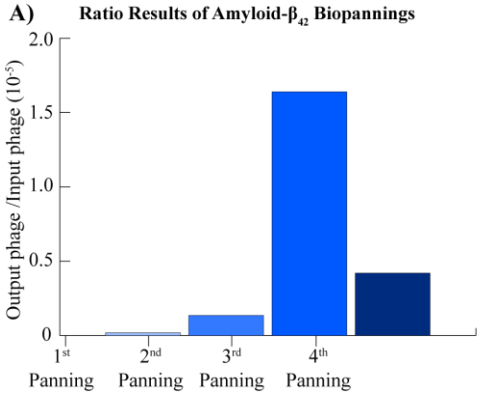

B)

Amyloid β_{42}	1st Round	2nd Round	3rd Round	4th Round
Input Phage (pfu)	1.8×10^{11}	1.54×10^{11}	1.4×10^{11}	0.5×10^{11}
Output Phage (pfu)	3.4×10^{5}	2.1×10^{5}	2.1×10^{5}	4.5×10^{5}
Ratio (Output/Input)	1.89×10^{-7}	1.36×10^{-6}	1.64×10^{-6}	4.2×10^{-6}
Enrichment Ratio	1.0	7.2	8.7	22.2

Figure 36: Phage ratio calculations and enrichment ration results from biopanning of amyloid-β_{42}. A) Ratio calculations obtained from 'output phage (pfu)/ input phage (pfu)' of amyloid-β_{42} biopanning results. B) Table for input phage amount, output phage amount, ratio and enrichment ratio obtained from amyloid-β_{42} biopanning.

In this data, the ratio was decreased after 4th biopanning as well as enrichment ratio was increased slightly less than the others. The reason might be occurred due to the differences in expression level of amyloid-β_{42} on yeast surface after each induction of yeast cells used in biopanning cycles. Also, during biopanning wash steps, some of the yeast cells might be lost and discarded with supernatant as well as some of surface-displayed amyloid-β_{42} might interact with each other during biopanning in order to decrease the free energy of their monomeric state.

A)

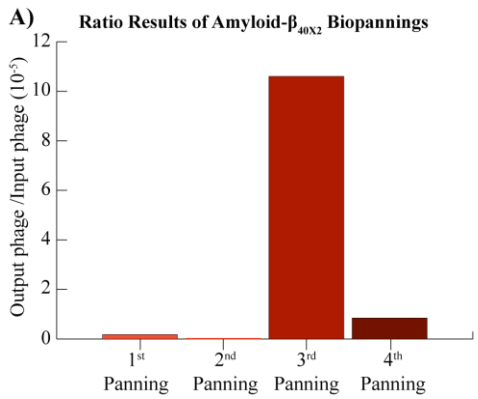

B)

Amyloid β_{40X2}	1st Round	2nd Round	3rd Round	4th Round
Input Phage (pfu)	1.8×10^{11}	2.4×10^{12}	4×10^{10}	0.5×10^{11}
Output Phage (pfu)	3.3×10^{6}	6.6×10^{5}	4.25×10^{6}	6.2×10^{6}
Ratio (Output/Input)	1.83×10^{-6}	2.75×10^{-7}	1.06×10^{-4}	8.5×10^{-6}
Enrichment Ratio	1.0	0.2	57.9	46.5

Figure 37: Phage ratio calculations and enrichment ration results from biopanning of amyloid-β_{40X2}. A) Ratio calculations obtained from 'output phage (pfu)/ input phage (pfu)' of amyloid-β_{40X2} biopanning results. B) Table for input phage amount, output phage amount, ratio and enrichment ratio obtained from amyloid-β_{40X2} biopanning.

According to this data, ratios were fluctuated after all biopanning cycles. Especially there was a decrease in 4th panning ratio and the only significant increase in ratio was observed after 3rd panning. The reason of decrease in might be same as with the reason of decrease in ratio of amyloid-β_{42}-bound phages, which was the differences in expression level of amyloid-β_{40X2} on yeast surface after each induction of yeast cells used in biopanning cycles or lost of yeast cells during biopanning cycle or interaction of amyloid-β_{40X2} expressed on different yeast cell surface.

A)

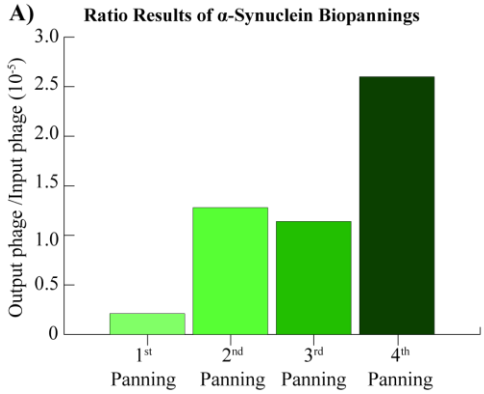

B)

α-Synuclein	1st Round	2nd Round	3rd Round	4th Round
Input Phage (pfu)	1.8×10^{11}	1.48×10^{11}	1.14×10^{11}	0.5×10^{11}
Output Phage (pfu)	3.8×10^{5}	1.9×10^{5}	1.3×10^{5}	1.9×10^{5}
Ratio (Output/Input)	2.11×10^{-7}	1.28×10^{-6}	1.14×10^{-6}	2.6×10^{-6}
Enrichment Ratio	1.0	6.1	5.4	12.3

Figure 38: Phage ratio calculations and enrichment ration results from biopanning of α-synuclein. A) Ratio calculations obtained from 'output phage (pfu)/ input phage (pfu)' of α-synuclein biopanning results. B) Table for input phage amount, output phage amount, ratio and enrichment ratio obtained from α-synuclein biopanning.

According to this result, there was 12.3-fold increase in enrichment ratio of phages that bound to α-synuclein. This result was not significant as occurred in other NDPs with high enrichment ratio. Still, the increase in enrichment ratio was slightly enough for selecting phages for further experiments if the expression levels of α-synuclein proteins on yeast surface were similar for yeast used in each biopanning cycle.

After each round of biopanning, eluted interacting phages were propagated for use in the next panning procedure. For each enrichment ratio after one biopanning cycle should be increased until saturation is occurred. By doing so, every biopanning cycle should give the most interacting phages as well as increased amount of interacting phages for next biopanning and using them should give high amount of phages during elution.

According to enrichment ratio results at the end of 4th cycle of biopanning, ratios of phage enrichment for 25Q-Htt, 46Q-Htt, 103Q-Htt, amyloid-β_{40} and α-synuclein were increased significantly, although ratios were decreased for amyloid-β_{42} and amyloid-β_{40X2}. The reason of decrease in enrichment ratio might be occurred due to the differences in the expression level of surface display of proteins or some of the displayed proteins might interact with each other during panning. Overall, there were fluctuations for each NDP-bound phage ratio results and there was no correlation between them. Thus, difference in dercrease/increase in enrichment ratio, peptide selection was determined to obtained from 4th biopanning elutions of NDPs.

For preparing sequencing samples from phages bound to 25Q-Htt (Figure 39), 46Q-Htt (Figure 40), 103Q-Htt (Figure 41), amyloid β_{40} (Figure 42), amyloid β_{42} (Figure 43) and amyloid β_{40X2} (Figure 44), PCR was done for amplifying about 400 bp region having displayed peptide sequences. For each NDP, 3 sequencing samples were prepared and their sequences were verified by Sanger sequencing.

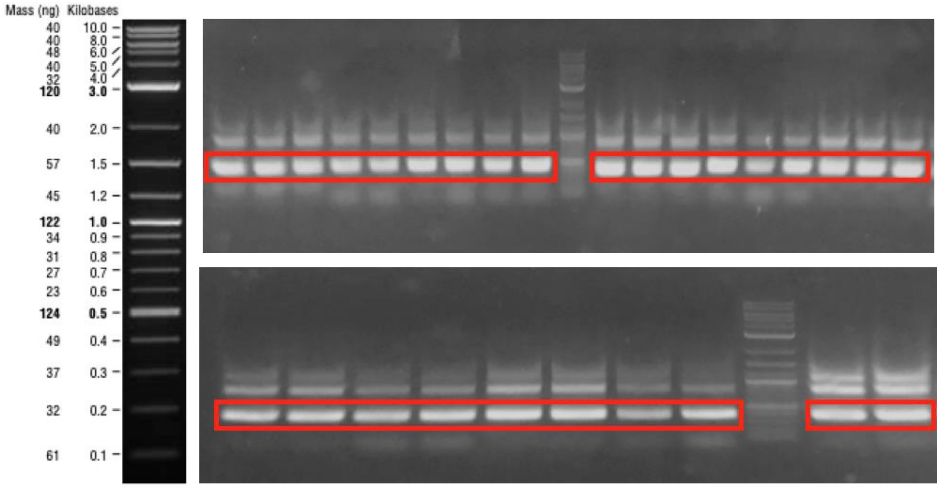

Figure 39: PCR product of M13 pIII genes that were obtained from biopanning of 25Q-Htt for sequencing. The expected size was 433 bp. 10 different samples were loaded and each sample gave same result. The other unexpected bands were originated from unspecific amplification of a region on M13 genome or gemone of remaining ER2738.

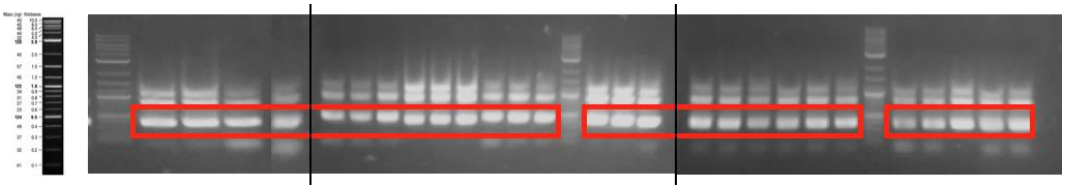

Figure 40: PCR product of M13 pIII genes that were obtained from biopanning of 46Q-Htt for sequencing. The expected size was 433 bp. 10 different samples were loaded and each sample gave same result. The other unexpected bands were originated from unspecific amplification of a region on M13 genome or gemone of remaining ER2738.

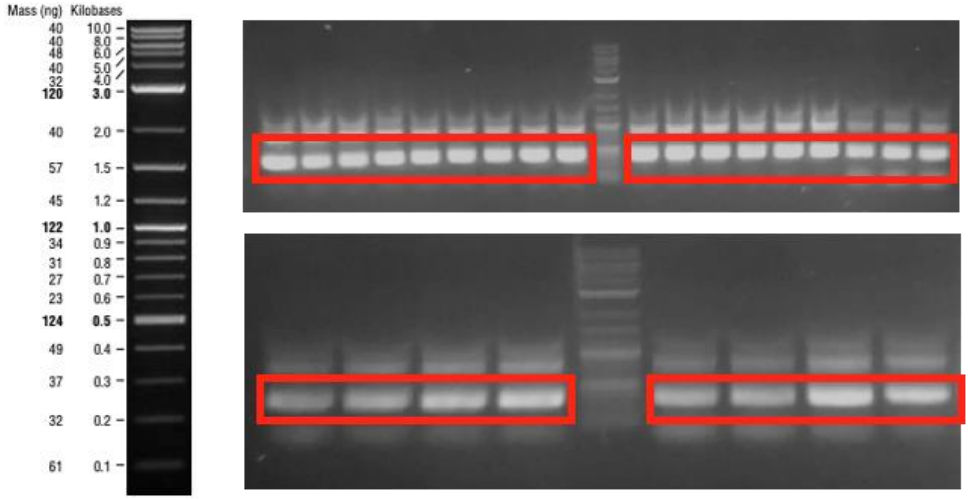

Figure 41: PCR product of M13 pIII genes that were obtained from biopanning of 103Q-Htt for sequencing. The expected size was 433 bp. 10 different samples were loaded and each sample gave same result. The other unexpected bands were originated from unspecific amplification of a region on M13 genome or gemone of remaining ER2738.

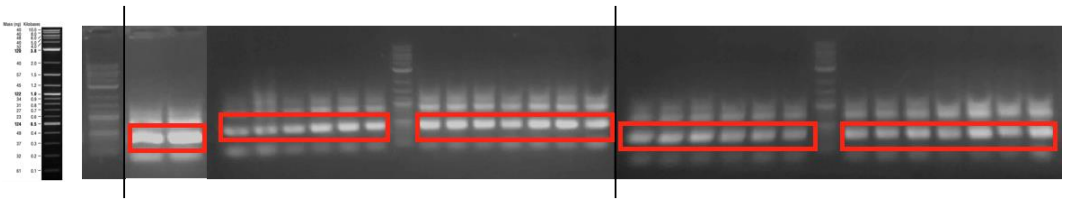

Figure 42: PCR product of M13 pIII genes that were obtained from biopanning of amyloid-β_{40} for sequencing. The expected size was 433 bp. 10 different samples were loaded and each sample gave same result. The other unexpected bands were originated from unspecific amplification of a region on M13 genome or gemone of remaining ER2738.

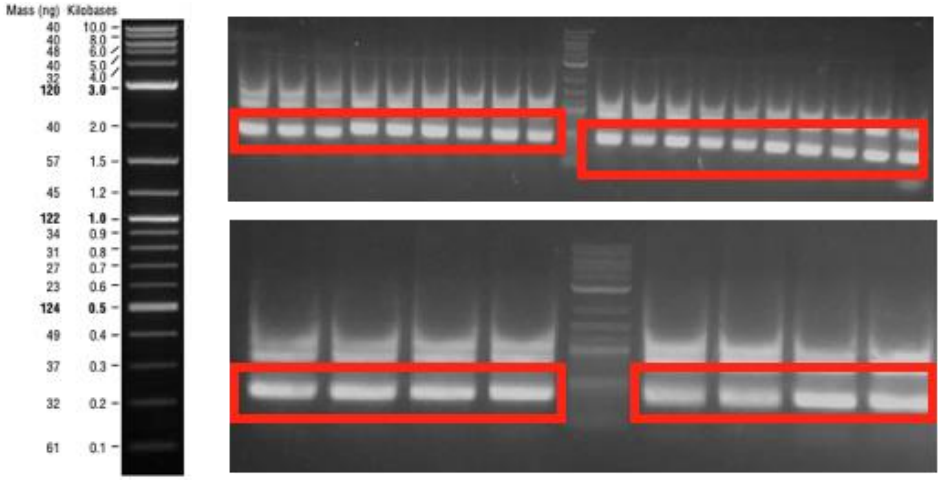

Figure 43: PCR product of M13 pIII genes that were obtained from biopanning of amyloid-β_{42} for sequencing. The expected size was 433 bp. !0 different samples were loaded and each sample gave same result. The other unexpected bands were originated from unspecific amplification of a region on M13 genome or gemone of remaining ER2738.

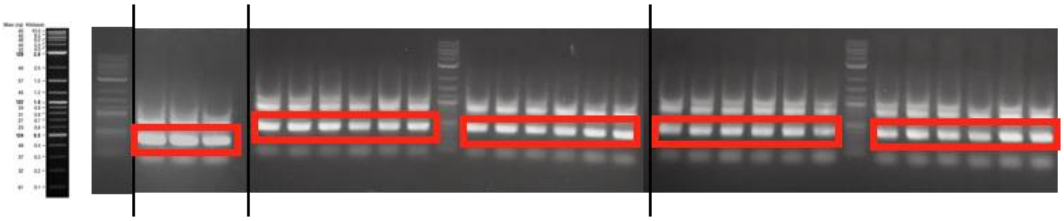

Figure 44: PCR product of M13 pIII genes that were obtained from biopanning of amyloid-β_{40X2} for sequencing. The expected size was 433 bp. 10 different samples were loaded and each sample gave same result. The other unexpected bands were originated from unspecific amplification of a region on M13 genome or gemone of remaining ER2738.

Sequencing data showed that one peptide was dominant over other peptide sequences. This might be caused from the interaction of phage with other common surface or c-myc tag expressed as a fusion of NDPs, or the peptide may interact with all NDPs studied in this project, but it is less likely.

3.6. Modelling of NDPs, Candidate Ligand Peptides and Docking Predictions

Before using the peptides for characterization experiments, it was thought that the prediction of interaction of peptides with neurodegenerative proteins, several online tools and a software, which are explained in materials and methods section, were better approach for obtaining an idea for ligand selection. In order to do that, fusion protein of NDP with Aga2p was determined to use in modeling. The reason of using fusion protein sequence for modeling is to determine the full structure of surface protein as well as determining whether the folding of NDPs were effected by fusion of Aga2p or not. Also, by using the fusion protein structure, peptide interaction is observed either with NDP or Aga2 or the linker region between them.

After 4 cycle of biopanning, phage clones, which were from biopanning of 25Q-Htt, 46Q-Htt, 103Q-Htt. amyloid-β_{40}, amyloid-β_{42} and amyloid-β_{40X2}, were send to sequencing. The sequencing data gave one type of all NDPs mentioned above, one different peptide sequence was obtained for25Q-Htt, 103Q-Htt and amyloid-β_{40}, and there was no different peptide sequence for amyloid-β_{40X2}. On the other hand, there were two different peptide sequences for 46Q-Htt and amyloid-β_{42}.

For NDPs fused with Aga2p, 5 different protein structure model predictions were obtained by I-TASSER with applying standard parameters. Then, one of the properly folded model was selected for each protein fusions. Also, for each peptide sequence, 5 different models were obtained by PEPFOLD, and one model for each peptide was selected for further use. Peptide and protein models were,

then, analyzed with HPEPDOCK server by using standard parameters. After getting 10 different prediction for interaction, the models in which peptides were seem to close to NDPs were obtained. Also, prediction of interaction of common peptide sequence that was obtained from sequencing was done for docking to α-synuclein.

For predictions of possible docking of 25Q-Htt-bound peptide and common peptide with 25Q-Htt (Figure 45), 46Q-Htt-bound peptide and common peptide with 46Q-Htt (Figure 46), 103Q-Htt-bound peptide and common peptide with 103Q-Htt (Figure 47), amyloid-β_{40}-bound peptide and common peptide with amyloid-β_{40} (Figure 48), amyloid-β_{42}-bound peptide and common peptide with amyloid-β_{42} (Figure 49), amyloid-β_{40X2}-bound peptide and common peptide with amyloid-β_{40X2} (Figure 50), common peptide with α-synuclein (Figure 51) were done.

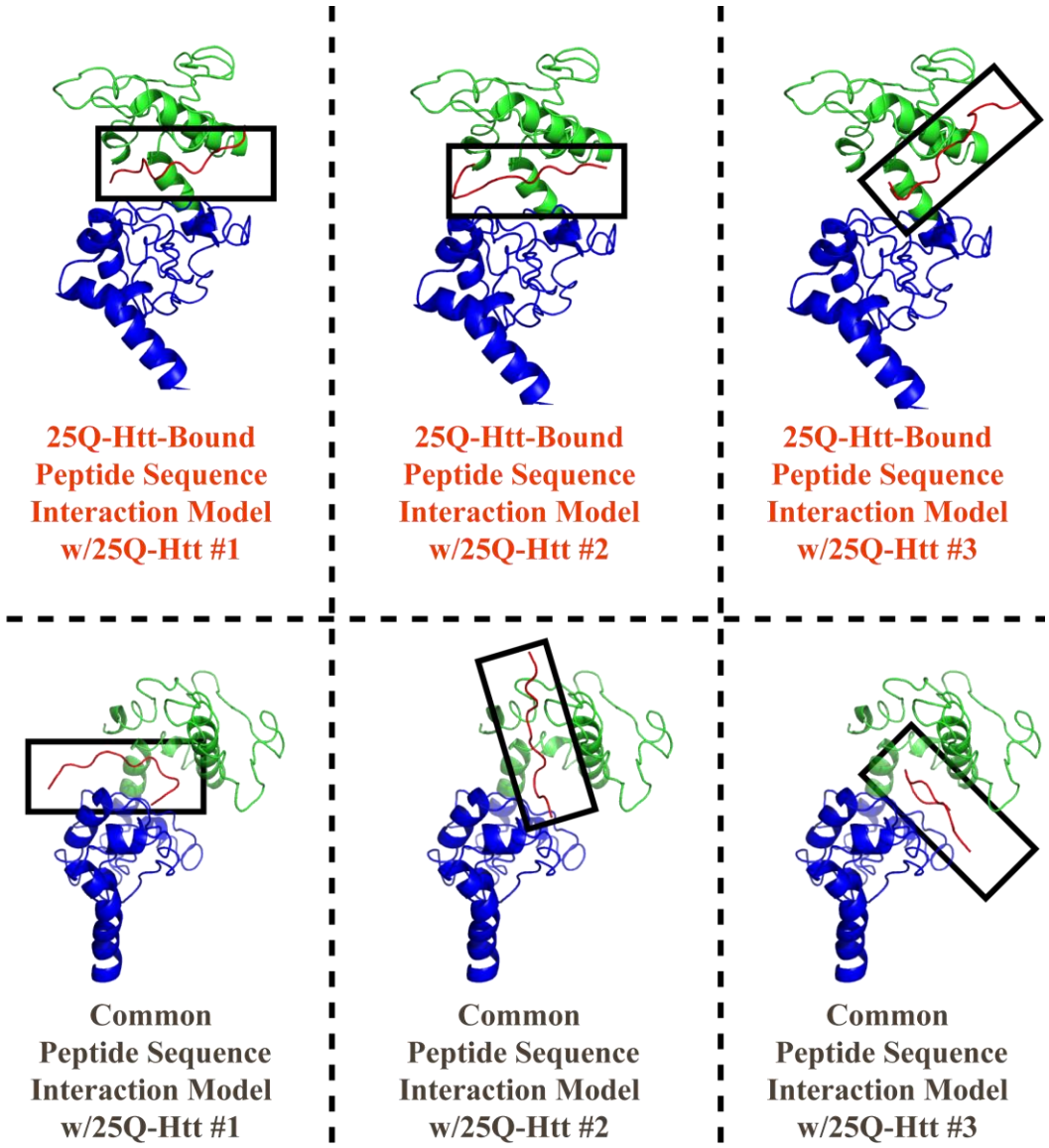

Figure 45: Prediction of docking 25Q-Htt-bound peptide and common peptide on 25Q-Htt. The blue region on the model represents Aga2, and green region on the model represents 25Q-Htt. The peptide is indicated with red color and black boxes.

For 25Q-Htt, peptides were located on a region between 25Q-Htt and Aga2p. The peptides, except model #2 of common peptide docking, might interact with both 25Q-Htt and Aga2p as well as linker region between them. Thus, these can be used for further characterization experiments.

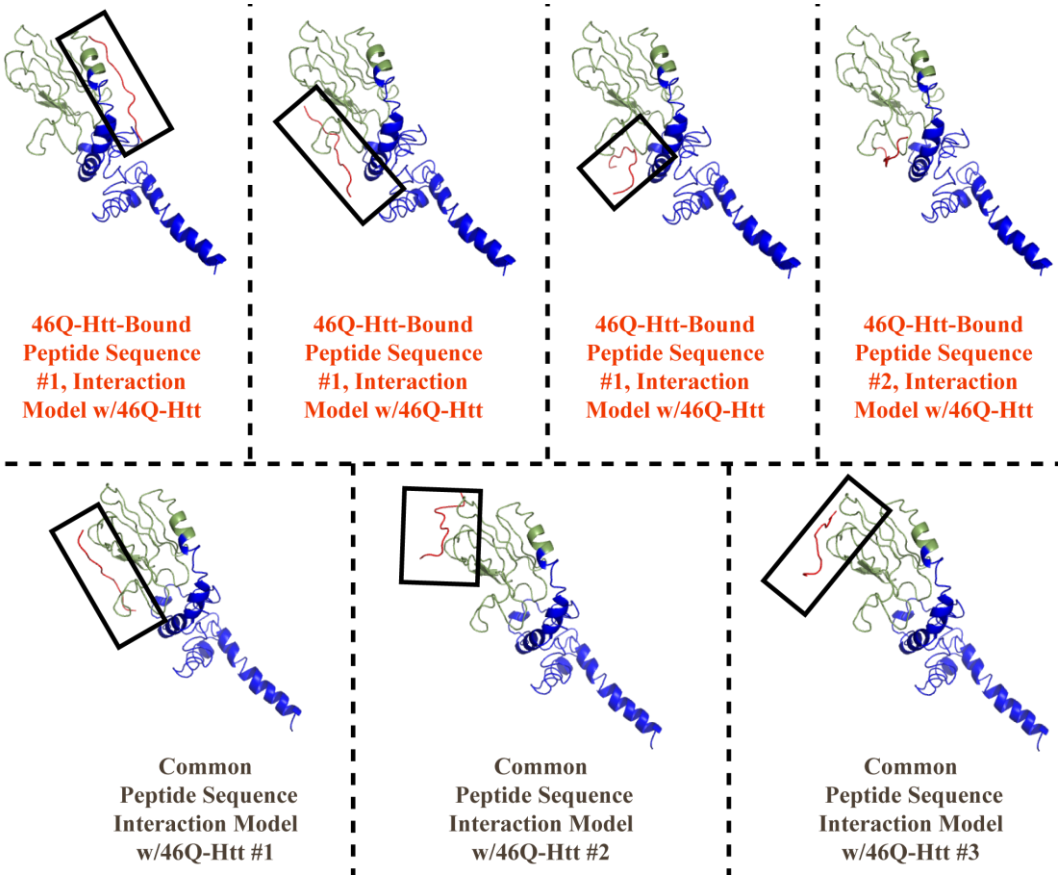

Figure 46: Prediction of docking 46Q-Htt-bound peptides and common peptide on 46Q-Htt. The blue region on the model represents Aga2, and green region on the model represents 46Q-Htt. The peptide is indicated with red color and black boxes.

The docking prediction result showed that peptides might mostly interacted with 46Q-Htt at 4 different regions.

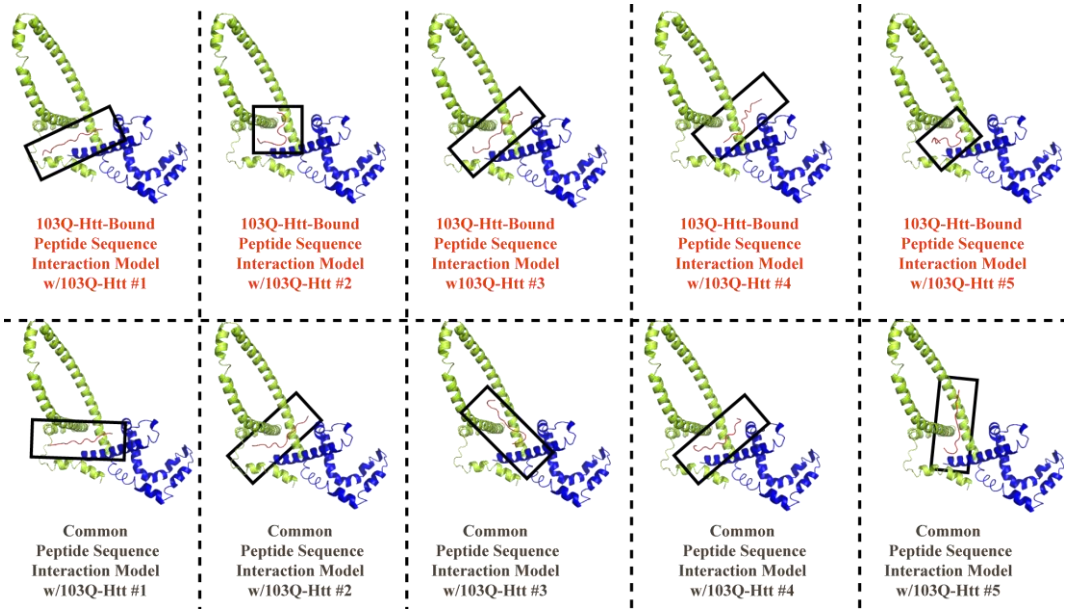

Figure 47: Prediction of docking 103Q-Htt-bound peptide and common peptide on 103Q-Htt. The blue region on the model represents Aga2, and green region on the model represents 103Q-Htt. The peptide is indicated with red color and black boxes.

According to the prediction models, peptides were shown docked about the same region on fusion protein of 103Q-Htt with Aga2p. Still, this images gave an idea that the peptides mostly interacted with 103Q-Htt.

When docking prediction model of peptides on Htt proteins compared with each other, Aga2p folding models were similar, and most of the docking profiles of peptides were similar with respect to peptide position. This might be caused from that the peptides might also be interacted with linker region between Htts and Aga2p. Thus, the clear answer obtained only from characterization experiments. These gave us just predictions.

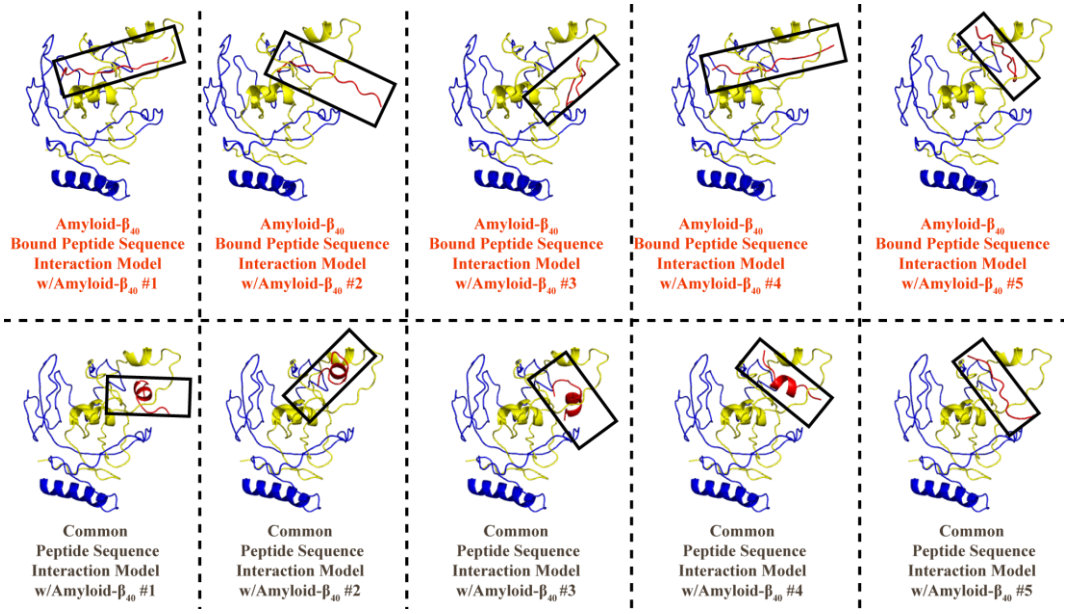

Figure 48: Prediction of docking amyloid-β_{40}-bound peptide and common peptide on amyloid-β_{40}. The blue region on the model represents Aga2, and yellow region on the model represents amyloid-β_{40}. The peptide is indicated with red color and black boxes.

According to the models, common peptides might form helix-structure. The models showed that each docking of peptides localized similar regions on amyloid-β_{40}, away from Aga2p as much as it could be. Thus, the peptides can be used in further characterization experiments.

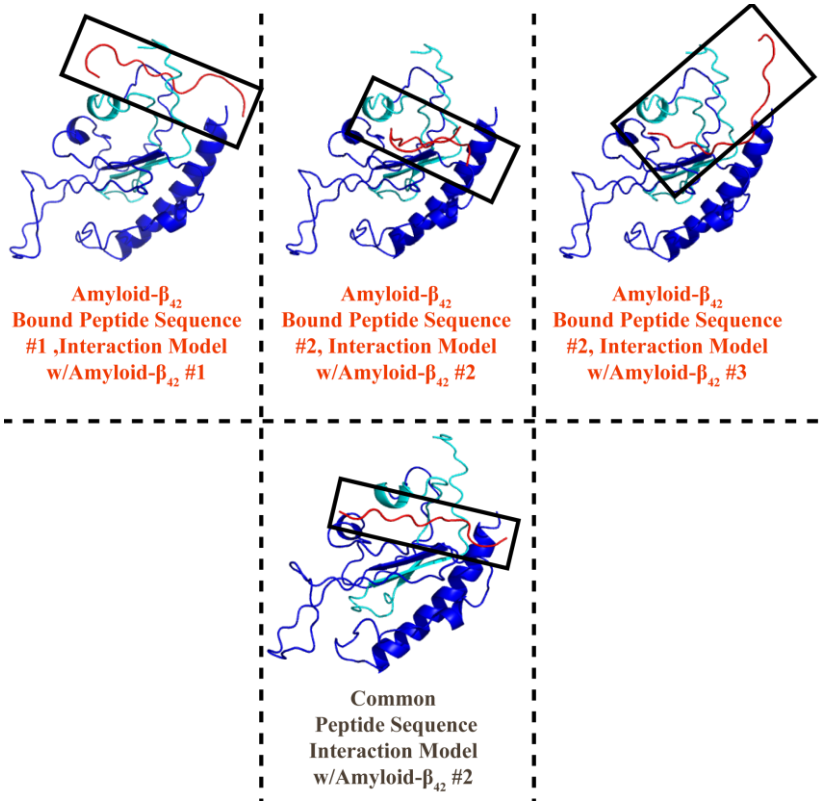

Figure 49: Prediction of docking amyloid-β_{42}-bound peptides and common peptide on amyloid-β_{42}. The blue region on the model represents Aga2, and cyan region on the model represents amyloid-β_{42}. The peptide is indicated with red color and black boxes.

The prediction of peptide docking localized at similar regions on amyloid-β_{42}. Still, it could be predicted that these peptides interact with directly amyloid-β_{42}. Thus, they can be used for further steps of characterization.

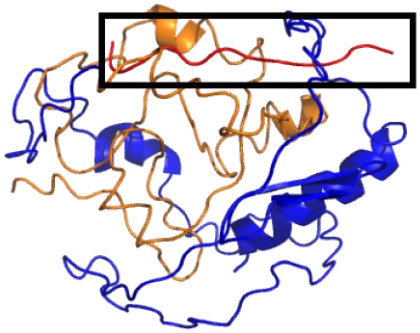

Common Peptide Sequence Interaction Model w/Amyloid-β_{40X2}

Figure 50: Prediction of docking amyloid-β_{40X2}-bound peptide and common peptide on amyloid-β_{40X2}. The blue region on the model represents Aga2, and orange region on the model represents amyloid-β_{40X2}. The peptide is indicated with red color and black boxes.

One out of ten docking prediction model, in which peptide was interacted with amyloid-β_{40X2}, was obtained for common peptide and amyloid-β_{40X2}. Thus, there should be more different peptide sequence to make a comparison. Also, this common peptide probably was not interacted directly with amyloid-β_{40X2}.

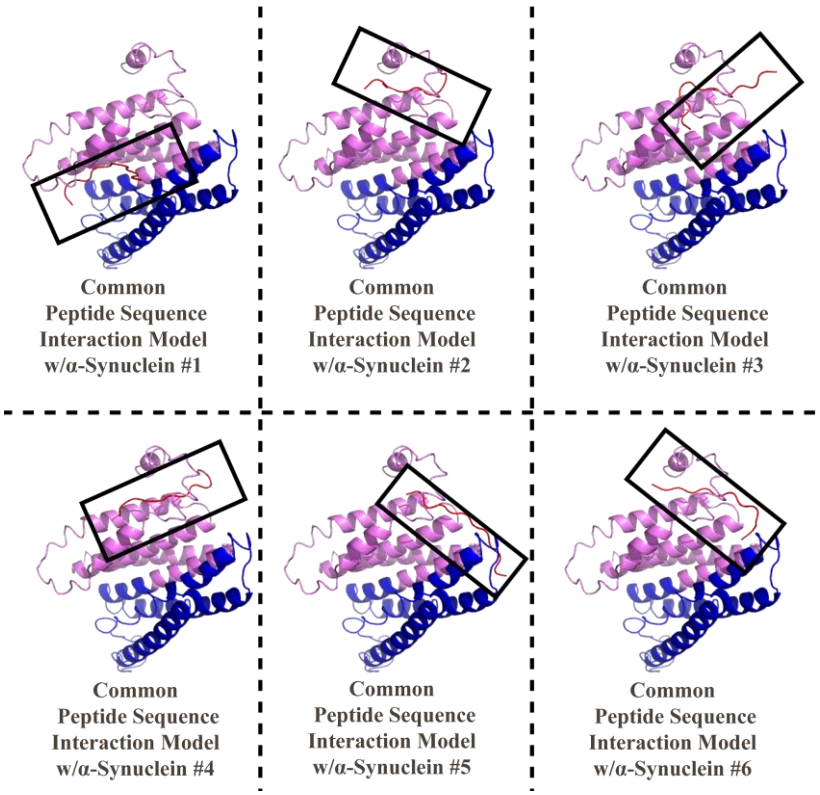

Figure 51: Prediction of docking common peptide on α-synuclein. The blue region on the model represents Aga2, and purple region on the model represents α-synuclein. The peptide is indicated with red color and black boxes.

The common peptide docked on α-synuclein showed that this common sequence might also be interacted with α-synuclein. Thus, after getting peptide sequences of phage plaques obtained from 4^{th} biopanning elution, this sequence can be compared with the sequencing results.

Except model for peptide docking on amyloid-β_{40X2}, all peptides could be using in characterization of peptides for inhibitory activity. However, some of the protein-peptide docking models were obtained different amount. Thus, less number of proper docking model might give another prediction of binding probability. In other words, less number of desired models might be caused from the less chance

of binding of peptides on NDPs. Thus, these were done for just prediction and comparision of peptide docking on NDPs.

3.7. Determination of Phage Interaction with α-Synuclein Expressed on Yeast Surface by ELISA

In order to determine whether selected phages were bound specifically to NDPs or not, ELISA was performed. In ELISA, targets such as peptides, proteins and antibodies are immobilized on a surface. Enzyme conjugated antibody then is added onto target. After several washing steps, enzyme substrate is added to detect the activity of the enzyme. If there is no interaction between immobilized target and enzyme-conjugated antibody, antibody is washed away and there is no recorded enzyme activity. In the case of interaction of antibody with target, substrate addition gives positive results for measurable product of the enzyme activity [71].

For detection of phage interaction with NDPs, couple of optimization experiments were done for determining the optimum conditions for ELISA without immobilizing yeast surface display systems as in biopanning procedure by using yeast cells only expressing Aga2p after induction (empty pETcon expressing yeast cells, or empty pETcon in short) with galactose and empty pETcon expressing yeast cell-bound phages.

The most accurate protocol was applied for α-synuclein-bound phages. First, phages obtained from 3rd biopanning elution. 10 distinct blue plaques were selected and amplified and used in ELISA. Also, NDP-bound phage library and

empty pETcon-bound phages were used against α-synuclein and empty pETcon-expressing yeast cell as controls. Besides, α-synuclein-bound phages were mixed and used in ELISA against empty pETcon-expressing yeast cells (Figure 52).

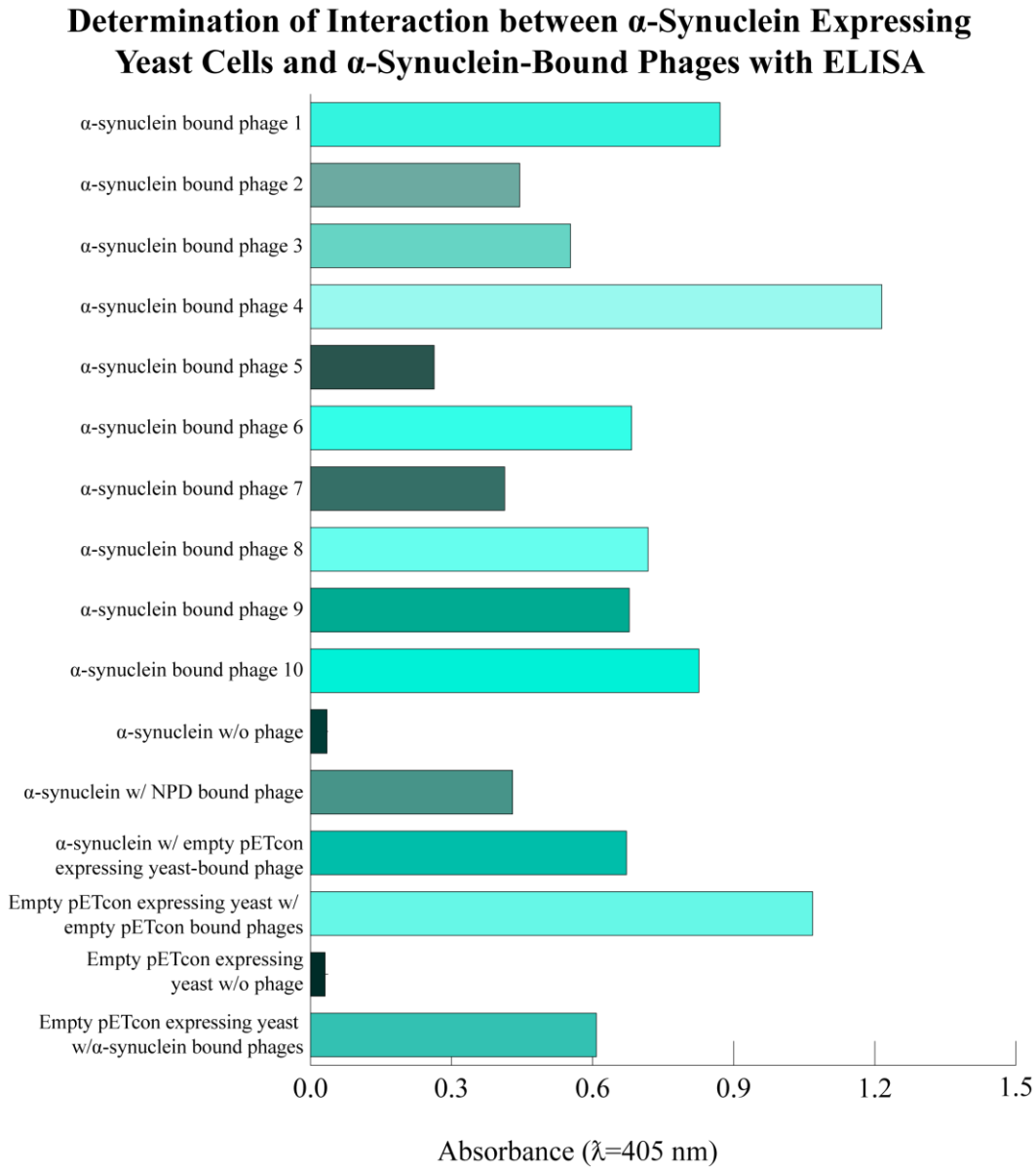

Figure 52: ELISA for detection of M13 phages eluted from α-synuclein biopanning against α-synuclein-expressing yeast cells. According to data, some of the phages were interacted with α-synuclein showinh high interaction efficiency.

According to the results, phage #1, #4, #6, #8 and #10 gave high enzyme activity with ABTS and H_2O_2 addition. However, 10-phage mixture also gave positive result with empty pETcon-expressing yeast cells during ELISA. Thus, some of the phages might interact with other surface molecules and/or c-myc tag. For controlling the nonspecific interactions of phages with empty pETcon-expressing yeast cells, phage #1, #4, #6, #8 and #10 were used in ELISA. Also, phage #5 was used since it might bind only α-synuclein (Figure 53). Hence, phage #5 gave lower absorbance for its specifically interaction with α-synuclein, and phage #1, #4, #6, #8 and #10 might also interact with other surface molecules other than α-synuclein.

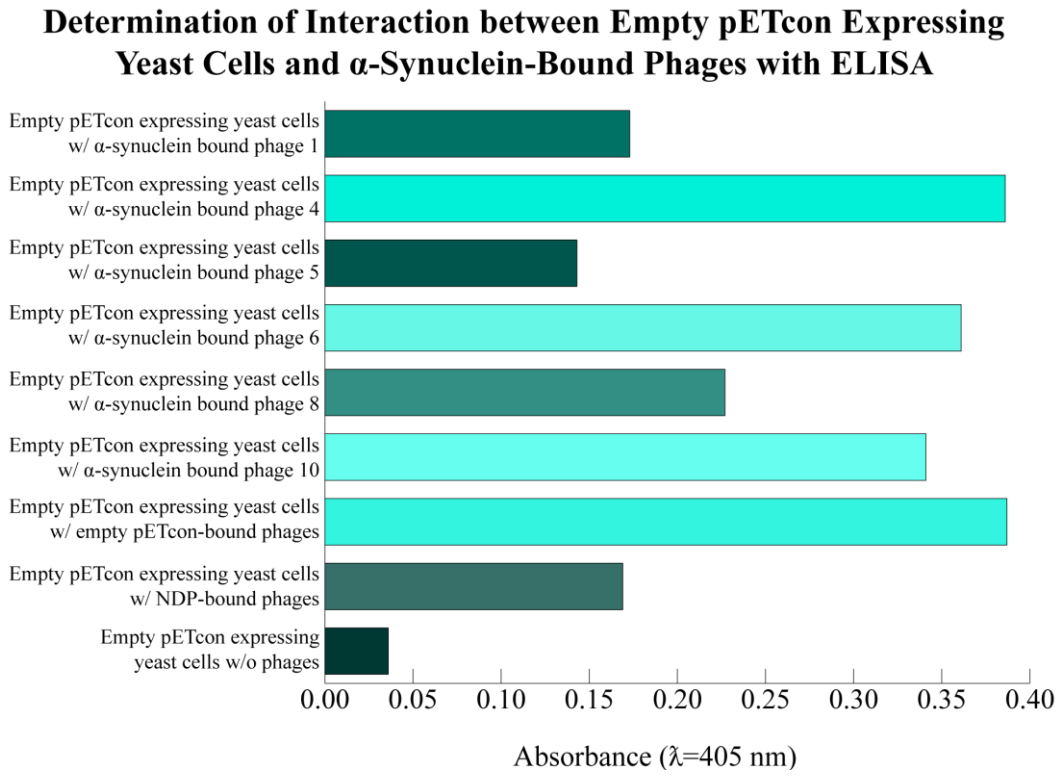

Figure 53: ELISA of empty pETcon-expressing yeast cells by using α-synuclein-bound phages.

Comparison of two different ELISA results showed us all off the phage clones interacted with α-synuclein with high efficiency than empty pETcon-expressing yeast cells.

ELISA were continued with α-synuclein with 10 different phage clones obtained from 5^{th} biopanning. The reason of continuing biopanning was to increase the specificity of phages for α-synuclein other than control yeast cells. Instead if using amplified phages from elution of 3^{rd} biopanning, 2^{nd} preselection was applied by using empty pETcon-expressing yeast cells and unbound phages were collected for further use. After selecting 10 distinct blue phage plaques from 5^{th} biopanning elution, ELISA was done for α-synuclein and empty pETcon-expressing yeast cells at the same time to get more accurate comparison data (Figure 54).

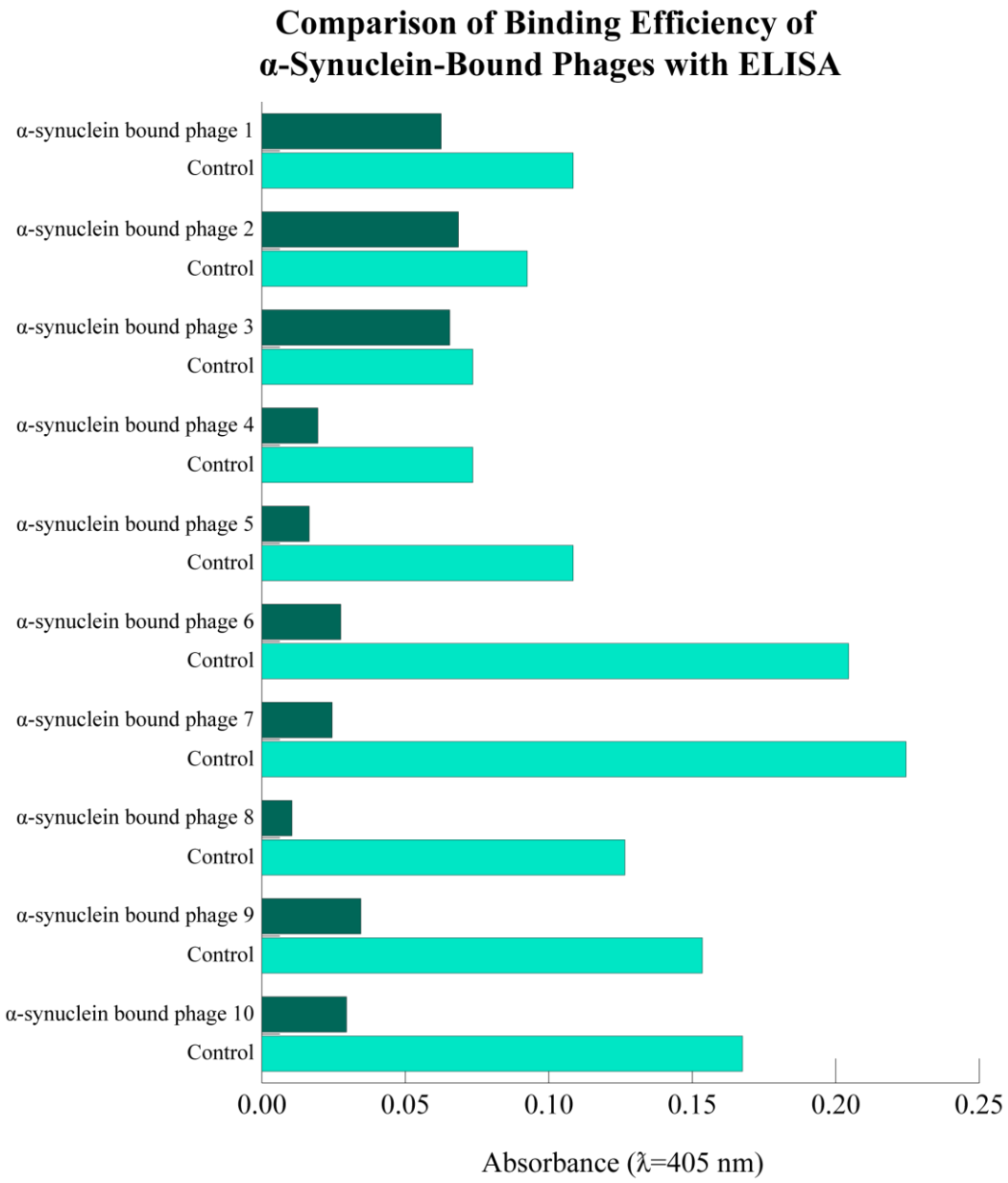

Figure 54: ELISA of α-synuclein and empty pETcon-expressing yeast cells by using α-synuclein-bound phages.

The phage clones selected for α-synuclein gave lower absorbance values than control cells. Thus, it was determined that optimization experiment was not enough. During ELISA, number of washing may be required to increase. Also, incubation time of phages and antibody should be arranged more properly. In addition, these fluctuations might be originated from increase in number of

biopanning cycle since the existence of phages interacted with other molecules displayed on yeast surface also might be enriched with α-synuclein-bound phages. During ELISA, some of α-synuclein-expressing cells might be lost. Furthermore, α-synuclein might be interacted with each other during blocking process. By, considering such probable problems, ELISA should require more optimization. Until then, phage genomes were send to sequencing to determine the peptide sequences and the peptides aimed to be used in other characterization protocols in order to determine the interaction efficiencies of phage particles.

CHAPTER 4

CONCLUSIONS

In conclusion, candidate ligand peptides were selected against neurodegenerative amyloids which are 25Q-Htt, 46Q-Htt, and 103Q-Htt α-synuclein, amyloid β_{40} and amyloid β_{42} by using yeast surface display system and M13 phage display library as well as bacterial surface display. Neurodegenerative amyloids were displayed on surfaces of both bacteria and yeast by using Ag43 autotransporter system and Aga2p-mating type protein, respectively. Selection of candidate ligand peptides were mostly done with using yeast surface display system which has some advantages such as being eukaryotic cells, more proper folding of recombinant proteins, over bacterial surface display system. During peptide selection, 4 round of biopanning were applied. For each round, bacteriophages were enriched for selection of phages highly interacted with neurodegenerative proteins expressed on yeast surfaces. After 4^{th} round of biopanning, different and distinct phage plaques were selected to determine the sequences of displayed and interacted peptides. In addition to these, determining of phage interaction with neurodegenerative proteins, ELISA was tried to be optimized but results showed that assay needed more changes in parameters. Overall, this strategy is more promising for inhibition of neurodegenerative amyloid formation with small-sized peptides since monomeric units of neurodegenerative amyloids are more easy in terms of expression, kinetics and *in vitro* studies.

BIBLIOGRAPHY

[1] Iadanza MG, Jackson MP, Hewitt EW, Ranson NA, & Radford SE. A New Era for Understanding Amyloid Structures and Disease. Nature Reviews Molecular Cell Biology, 2018; 19(12), 755–773.

[2] Maji SK, Perrin MH, Sawaya MR, Jessberger S, Vadodaria K, Rissman RA, Riek R et. al. Functional Amyloids as Natural Storage of Peptide Hormones in Pituitary Secretory Granules. Science (New York, N.Y.). 2009; 325(5938), 328–332.

[3] Chiti F & Dobson CM. Protein Misfolding, Functional Amyloid, and Human Disease: A Summary of Progress Over the Last Decade. Annu. Rev. Biochem. 2006; 86, 27–68

[4] Vassar R, Bennett BD, Babu-Khan S & Kahn S. β-Secretase Cleavage of Alzheimer's Amyloid Precursor Protein by the Transmembrane Aspartic Protease BACE. Science. 1999; 286, 735–741

[5] Warby SC et al. CAG Expansion in the Huntington Disease Gene is Associated with a Specific and Targetable Predisposing Haplogroup. Am. J. Hum. Genet. 2009; 84, 351–366

[6] Chartier-Harlin MC et al. Alpha-Synuclein Locus Duplication as a Cause of Familial Parkinson's Disease. Lancet. 2004; 364, 1167–1169

[7] Westermark P, Andersson A & Westermark GT. Islet amyloid polypeptide, Islet Amyloid, and Diabetes Mellitus. Physiol. Rev. 2011; 91, 795–826

[8] Cohen SIA. et al. Proliferation of Amyloid-β42 Aggregates Occurs Through a Secondary Nucleation Mechanism. Proc. Natl Acad. Sci. 2013; 9758–9763

[9] Xue C, Lin TY, Chang D, & Guo Z. Thioflavin T as an Amyloid Dye: Fibril Quantification, Optimal Concentration and Effect on Aggregation. Royal Society Open Science. 2017; 4(1), 160696.

[10] Yakupova EI, Bobyleva LG, Vikhlyantsev IM, & Bobylev AG. Congo Red and Amyloids: History and Relationship. Bioscience Reports. 2019; 39(1), BSR20181415

[11] Knowles TPJ et al. Role of Intermolecular Forces in Defining Material Properties of Protein Nanofibrils. Science. 2007; 318, 1900–1903

[12] Smith JF, Knowles TPJ, Dobson CM, MacPhee CE. & Welland ME. Characterization of the Nanoscale Properties of Individual Amyloid Fibrils. Proc. Natl. Acad. Sci. USA. 2006; 103, 15806–15811

[13] Riek, R., Eisenberg, D. The Activities of Amyloids from a Structural Perspective. Nature. 2016; 539, 227–235

[14] Eanes ED, Glenner GG. X-ray Diffraction Studies on Amyloid Filaments. J. Histochem. Cytochem. 1968; 16:673–77

[15] Cohen AS, Calkins E. Electron Microscopic Observations on a Fibrous Component in Amyloid of Diverse Origins. Nature. 1959; 183:1202–3

[16] Chen B, Thurber KR, Shewmaker F, Wickner RB, Tycko R. Measurement of Amyloid Fibril Mass-per-Length by Tilted-Beam Transmission Electron Microscopy. Proc. Natl. Acad. Sci. USA. 2009; 106:14339-44

[17] Gasset M, Baldwin MA, Fletterick RJ, Prusiner SB. Perturbation of the Secondary Structure of the Scrapie Prion Protein under Conditions that Alter Infectivity. Proc. Natl. Acad. Sci. USA. 1993; 90:1-5

[18] **C**hang HY, Lin JY, Lee HC, Wang HL, King CY. 2008. Strain-Specific Sequences Required for Yeast [PSI^+] Prion Propagation. Proc. Natl. Acad. Sci. USA. 2008; 105:13345-50

[19] Bai Y, Milne JS, Mayne L, Englander SW. Primary Structure Effects on Peptide Group Hydrogen Exchange. Proteins. 1993:17:75-86

[20] Miyazawa A, Fujiyoshi Y, Unwin N. Structure and Gating Mechanism of the Acetylcholine Receptor Pore. Nature. 2003; 423:949-55

[21] Zhang R, Hu X, Khant H, Ludtke SJ, Chiu W, et al. Interprotofilament Interactions between Alzheimer's Abeta1–42 Peptides in Amyloid Fibrils Revealed by cryoEM. Proc. Natl. Acad. Sci. USA. 2009; 106:4653-58

[22] Fiaux J, Bertelsen EB, Horwich AL, Wuthrich K. NMR Analysis of a 900 K GroEL GroES Complex. Nature. 2002; 418:207-11

[23] Nelson R, Sawaya MR, Balbirnie M, Madsen AO, Riekel C, et al. Structure of the Cross-Beta Spine of Amyloid-Like Fibrils. Nature. 2005; 435:773-78

[24] Gremer L. et al. Fibril Structure of Amyloid-β(1–42) by cryo-Electron Microscopy. Science. 2017; 358, 116–119

[25] Linse S. Mechanism of Amyloid Protein Aggregation and the Role of Inhibitors. Pure and Applied Chemistry. 2019; 91(2), 211–229.

[26] Linse S. Monomer-Dependent Secondary Nucleation in Amyloid Formation. Biophys Rev. 2017; 9: 329-338

[27] Ren B, Zhang Y, Zhang M, Liu Y, Zhang D, Gong X, Feng Z, Tang J, Chang Y and Zheng J. Fundamentals of Cross-Seeding of Amyloid Proteins: An Introduction. Journal of Materials Chemistry B. 2019; 7(46), pp.7267-7282.

[28] Pellarin, R. Pathways of Amyloid Fibril Formation Using a Simplified Peptide Model. J Mol Biol. 2007; 374:917–924.

[29] Cohen AS, Shirahama T, Skinner M. Electron Microscopy of Amyloid. Academic Press, London. 1982; vol3, pp. 165-205

[30] Serpell LC, Sunde M, Benson MD, Tennent GA, Pepys MB and Fraser PE. The Protofilament Substructure of Amyloid Fibrils. Journal of Molecular Biology. 2000; 330 (5). pp. 1033-1039

[31] Pellarin R, Caflisch A. Interpreting the Aggregation Kinetics of Amyloid Peptides.

J. Mol. Biol. 2006; 360, pp. 882-892

[32] Schleeger M, Vandenakker CC, Deckert-Gaudig T, Deckert V, Velikov KP, Koenderink G, & Bonn M. Amyloids: From Molecular Structure to Mechanical Properties. Polymer. 2013; 54(10), 2473–2488.

[33] Arosio P, Knowles TPJ, & Linse S. On the Lag Phase in Amyloid Fibril Formation. Physical Chemistry Chemical Physics.2015; 17(12), 7606–7618

[34] Knowles TPJ, Vendruscolo M, & Dobson CM. The Amyloid State and Its Association with Protein Misfolding Diseases. Nature Reviews Molecular Cell Biology. 2014; 15(6), 384–396

[35] Riboldi GM, & Fonzo ABD. GBA, Gaucher Disease, and Parkinson's Disease: From Genetic to Clinic to New Therapeutic Approaches. Cells. 2019; 8(4), 364

[36] Masters C, Bateman R, Blennow K et al. Alzheimer's Disease. Nat Rev Dis Primers. 2015; 1, 15056

[37] Kim K, Kim MJ, Kim DW, Kim SY, Park S, & Park CB. Clinically Accurate Diagnosis of Alzheimer's Disease via Multiplexed Sensing of Core Biomarkers in Human Plasma. Nature Communications. 2020; 11(1).

[38] Warmack RA, Boyer DR, Zee CT, Richards LS, Sawaya MR, Cascio D, Clarke SG. et al. Structure of amyloid-β (20-34) with Alzheimer's-Associated Isomerization at Asp23 Reveals a Distinct Protofilament Interface. Nature Communications. 2019; 10(1).

[39] Ma X, He Y, & Zhou Y. Amyloid β Oligomers Suppress Excitatory Transmitter Release via Presynaptic Depletion of Phosphatidylinositol-4,5-Bisphosphate. IBRO Reports. 2019; 6.

[40] Wang J, Gu BJ, Masters CL, & Wang YJ. Erratum: A Systemic View of Alzheimer Disease — Insights from Amyloid-B Metabolism Beyond the Brain. Nature Reviews Neurology. 2017; 13(11), 703–703.

[41] Zhang YW, Thompson R, Zhang H & Xu H. APP Processing in Alzheimer's Disease. Molecular brain. 2011: 4, 3

[42] Chen M. The Maze of APP Processing in Alzheimer's Disease: Where Did We Go Wrong in Reasoning? Frontiers in Cellular Neuroscience. 2015; 9.

[43] Strooper BD, Vassar R & Golde T. The Secretases: Enzymes with Therapeutic Potential in Alzheimer Disease. Nature Reviews Neurology. 2010; 6(2), 99–107.

[44] Meade RM, Fairlie DP, & Mason JM. Alpha-Synuclein Structure and Parkinson's Disease – Lessons and Emerging Principles. Molecular Neurodegeneration. 2019; 14(1).

[45] Dauer W, Przedborski S. Parkinson's Disease: Mechanisms and Models

Neuron. 2003; 39(6), pp. 889-909

[46] Xu L, & Pu J. Alpha-Synuclein in Parkinson's Disease: From Pathogenetic Dysfunction to Potential Clinical Application. Parkinsons Disease. 2016; 1–10.

[47] Leitao, A., Bhumkar, A., Hunter, D., Gambin, Y., & Sierecki, E. (2018). Unveiling a Selective Mechanism for the Inhibition of α-Synuclein Aggregation by β-Synuclein. International Journal of Molecular Sciences, 19(2), 334.

[48] Bridi JC, & Hirth F. Mechanisms of α-Synuclein Induced Synaptopathy in Parkinson's Disease. Frontiers in Neuroscience. 2018; 12, 80.

[49] Bozza A, Malagù S, Calzolari E, Novelletto A, Pavoni M, & Senno L. Expansion of a (CAG)n repeat region in a sporadic case of HD. Acta Neurologica Scandinavica. 2009; 92(2), 132–134.

[50] Bates G, Dorsey R, Gusella J et al. Huntington Disease. Nat Rev Dis Primers. 2015; 1, 15005

[51] Bachoud-Lévi AC, Ferreira J, Massart R, Youssov K, Rosser A, Busse M, Burgunder JM. International Guidelines for the Treatment of Huntington's Disease. Frontiers in Neurology. 2019; 10, 710

[52] Finkbeiner S. Huntington's Disease. Cold Spring Harbor Perspectives in Biology. 2011: 3(6), a007476

[53] Hatters DM. Protein misfolding inside cells: The Case of Huntingtin and Huntingtons Disease. IUBMB Life. 2008; 60(11), 724–728.

[54] Genetic Modifiers of Huntington's Disease Consortium, Lee JM, Correia K et al.CAG Rpeat not Polyglutamine Length Determines Timing of Huntington's Disease Onset. Cell. 2019; 178, pp. 887-900

[55] Eisele YS, Monteiro C, Fearns C, Encalada SE, Wiseman RL, Powers ET, & Kelly JW. Targeting Protein Aggregation for the Treatment of Degenerative Diseases. Nature Reviews Drug Discovery. 2015; 14(11), 759–780.

[56] Mimmi S, Maisano D, Quinto I, Iaccino E. Phage Display: An Overview in Context to Drug Discovery. Trends Pharmacol. Sci. 2018

[57] Galán A, Comor L , Horvatić A , Kuleš J , Guillemin N , Mrljak V & Bhide M. Library-Based Display Technologies: Where Do We Stand? Mol. BioSyst. 2016; 12 , 2342 —2358

[58] Omidfar K & Daneshpour M. Advances in Phage Display Technology for Drug Discovery. Expert Opinion on Drug Discovery. 2015; 10:6, 651-669

[59] Yang J, & Zhang Y. Protein Structure and Function Prediction Using I-TASSER. Current Protocols in Bioinformatics. 2015; 2, 5.8.1–5.8.15.

[60] Thévenet P, Shen Y, Maupetit J, Guyon F, Derreumaux P, & Tufféry P. PEP-FOLD: An Updated de novo Structure Prediction Server for Both Linear and Disulfide Bonded Cyclic Peptides. Nucleic acids research. 2012; 40, W288–W293.

[61] Zhou P, Jin B, Li H, & Huang SY. HPEPDOCK: A Web Server for Blind Peptide-Protein Docking Based on a Hierarchical Algorithm. Nucleic acids research. 2018; 46(W1), W443–W450.

[62] Yuan S, Chan HCS, Hu Z. Using PyMOL as a Platform for Computational Drug Design. Wiley Interdisciplinary Reviews: Computational Molecular Science. 2017, 7, e1298

[63] Woude MWVD, & Henderson IR. Regulation and Function of Ag43 (Flu). Annual Review of Microbiology. 2008; 62(1), 153–169.

[64] Ahan RE, Kırpat BM, Saltepe B, & Şeker UÖŞ. A Self-Actuated Cellular Protein Delivery Machine. ACS Synthetic Biology. 2019; 8(4), 686–696.

[65] Kjaergaard K, Hasman H, Schembri MA, & Klemm P. Antigen 43-Mediated Autotransporter Display, a Versatile Bacterial Cell Surface Presentation System. Journal of Bacteriology. 2002; 184(15), 4197–4204.

[66] Ledsgaard L, Kilstrup M, Karatt-Vellatt A, Mccafferty J, & Laustsen A. Basics of Antibody Phage Display Technology. Toxins. 2018; 10(6), 236.

[67] Hess GT, Cragnolini JJ, Popp MW, Allen MA, Dougan SK, Spooner E, Guimaraes CP et. al. M13 Bacteriophage Display Framework that Allows Sortase-Mediated Modification of Surface-Accessible Phage Proteins. Bioconjugate Chemistry. 2012; 23(7), 1478–1487.

[68] Sun Y, Yang C, Wu B, Wang J, Qu S, Weng J, & Feng B. Fabrication of Nanostructured M13 Bacteriophage Films on Titanium Surfaces. Materials Letters. 2016; 182, 39–42.

[69] Shin Y, Lee J, Jin L, Kim M, Oh JW, Kim T, & Han DW. Cell-Adhesive RGD Peptide-Displaying M13 Bacteriophage/PLGA Nanofiber Matrices for Growth of Fibroblasts. Biomaterials Research. 2014; 18(1), 14.

[70] Ngo-Duc TT, Zaman MS, Moon CH, & Haberer ED. Morphology Manipulation of M13 Bacteriophage Template for Nanostructure Assembly. Nanobiosystems: Processing, Characterization, and Applications. 2014; VII

[71] Adhu A. The Enzyme-Linked Immunosorbent Assay (ELISA). Bull World Health Organ. 1976; 54:129–39

APPENDIX A

DNA and selected peptide sequences mentioned in this study

Table A.1: DNA sequences of genes and fragments used in this study

Gene / Fragment	Sequence (5’ to 3’)
25Q-Htt	ATGGCGACCCTGGAAAAGCTGATGAAGGCCTTCGAG TCCCTCAAAAGCTTCCAACAGCAGCAACAGCAACAA CAGCAGCAACAGCAACAACAGCAGCAACAGCAACA ACAGCAGCAACAGCAACAACCGCCACCACCTCCCCC TCCACCCCCACCTCCTCAACTTCCTCAACCTCCTCCA CAGGCACAGCCTCTGCTGCCTCAGCCACAACCTCCT CCACCTCCACCTCCACCTCCTCCAGGCCCAGCTGTGG CTGAGGAGCCTCTGCACCGACCT
46Q-Htt	ATGGCGACCCTGGAAAAGCTGATGAAGGCCTTCGAG TCCCTCAAAAGCTTCCAACAGCAGCAACAGCAACAA CAGCAGCAACAGCAACAACAGCAGCAACAGCAACA ACAGCAGCAACAGCAGCAACAGCAACAACAGCAGC AACAGCAACAACAGCAGCAACAGCAACAACAGCAG CAACAGCAACAACCGCCACCACCTCCCCCTCCACCC

	CCACCTCCTCAACTTCCTCAACCTCCTCCACAGGCAC AGCCTCTGCTGCCTCAGCCACAACCTCCTCCACCTCC ACCTCCACCTCCTCCAGGCCCAGCTGTGGCTGAGGA GCCTCTGCACCGACCT
103Q-Htt	ATGGCGACCCTGGAAAAGCTGATGAAGGCCTTCGAG TCCCTCAAAAGCTTCCAGCAACAGCAACAACAACAA CAGCAGCAACAGCAACAGCAGCAACAGCAACAACA GCAGCAACAGCAACAACAGCAGCAACAGCAACAAC AGCAGCAACAGCAACAACAACAACAGCAGCAACAG CAACAACAGCAGCAACAGCAACAACAGCAGCAACA GCAACAACAACAACAGCAGCAACAGCAACAACAGC AGCAACAGCAACAACAGCAGCAACAGCAACAACAG CAGCAACAGCAACAACAACAACAGCAGCAACAGCA ACAACAGCAGCAACAGCAACAACAGCAGCAACAGC AACAACAACCGCCACCACCTCCCCCTCCACCCCCAC CTCCTCAACTTCCTCAACCTCCTCCACAGGCACAGCC TCTGCTGCCTCAGCCACAACCTCCTCCACCTCCACCT CCACCTCCTCCAGGCCCAGCTGTGGCTGAGGAGCCT CTGCACCGACCT
Amyloid β_{40}	ATGGACGCGGAGTTTCGTCACGATAGTGGATATGAG GTTCATCATCAAAAGCTAGTCTTCTTTGCGGAGGAT GTAGGTTCTAATAAAGGTGCCATAATCGGACTAATG

	GTCGGCGGAGTTGTG
Amyloid β_{42}	ATGGACGCGGAGTTTCGTCACGATAGTGGATATGAG GTTCATCATCAAAAGCTAGTCTTCTTTGCGGAGGAT GTAGGTTCTAATAAAGGTGCCATAATCGGACTAATG GTCGGCGGAGTTGTGATAGCT
Amyloid β_{40X2}	ATGGACGCGGAGTTTCGTCACGATAGTGGATATGAG GTTCATCATCAAAAGCTAGTCTTCTTTGCGGAGGAT GTAGGTTCTAATAAAGGTGCCATAATCGGACTAATG GTCGGCGGAGTTGTGACGCGTGGGGGCGGATCCGGT ACCGGGGGCGGATCCACGCGTATGGACGCGGAGTTT CGTCACGATAGTGGATATGAGGTTCATCATCAAAAG CTAGTCTTCTTTGCGGAGGATGTAGGTTCTAATAAA GGTGCCATAATCGGACTAATGGTCGGCGGAGTTGTG
α-synuclein	ATGGACGTTTTCATGAAGGGTCTTTCTAAAGCGAAA GAGGGCGTGGTAGCTGCGGCCGAAAAAACTAAACA AGGGGTGGCCGAGGCTGCTGGGAAAACGAAGGAAG GTGTATTGTACGTTGGTTCAAAGACCAAAGAGGGAG TAGTTCACGGAGTCGCCACAGTTGCCGAGAAGACCA AGGAACAGGTAACGAATGTGGGAGGTGCAGTGGTG ACTGGTGTCACTGCGGTCGCCCAAAAAACAGTTGAA GGAGCGGGATCAATAGCCGCAGCAACGGGATTTGTT

	AAGAAGGACCAATTAGGAAAAAATGAAGAGGGAGC ACCTCAAGAAGGTATTCTAGAGGATATGCCAGTCGA CCCCGATAACGAGGCTTATGAGATGCCGTCAGAGGA AGGGTATCAGGACTATGAGCCAGAAGCC
sfGFP	ATGCGTAAAGGCGAAGAGCTGTTCACTGGTGTCGTC CCTATTCTGGTGGAACTGGATGGTGATGTCAACGGT CATAAGTTTTCCGTGCGTGGCGAGGGTGAAGGTGAC GCAACTAATGGTAAACTGACGCTGAAGTTCATCTGT ACTACTGGTAAACTGCCGGTACCTTGGCCGACTCTG GTAACGACGCTGACTTATGGTGTTCAGTGCTTTGCTC GTTATCCGGACCATATGAAGCAGCATGACTTCTTCA AGTCCGCCATGCCGGAAGGCTATGTGCAGGAACGCA CGATTTCCTTTAAGGATGACGGCACGTACAAAACGC GTGCGGAAGTGAAATTTGAAGGCGATACCCTGGTAA ACCGCATTGAGCTGAAAGGCATTGACTTTAAAGAAG ACGGCAATATCCTGGGCCATAAGCTGGAATACAATT TTAACAGCCACAATGTTTACATCACCGCCGATAAAC AAAAAAATGGCATTAAAGCGAATTTTAAAATTCGCC ACAACGTGGAGGATGGCAGCGTGCAGCTGGCTGATC ACTACCAGCAAAACACTCCAATCGGTGATGGTCCTG TTCTGCTGCCAGACAATCACTATCTGAGCACGCAAA GCGTTCTGTCTAAAGATCCGAACGAGAAACGCGATC ATATGGTTCTGCTGGAGTTCGTAACCGCAGCGGGCA

	TCACGCATGGTATGGATGAACTGTACAAA
Ag43 β-Translocation Domain	GAAGGTCACATTCAGTGTGGCCTGACCGTTATACCC TTCAGCGCTGCTGCCGCTGACGCTGTGGGCATAACC GGCCTGAACGCCCAGGGTGATATTTTCCCGGACACG GGCTTCCAGTCCGGCCTGCAGGTCCAGTGATGTGCC ATTCTGTGAGGGAGAGAACGTCATCCCGCTGCCTGC AGTGGAAGTCCCCACACGCATATCTCCCCGGGAGCT GAAGGTGCGGATAACAGAAGGCTGTACCCACCAGTT CACCGGTAATTCACTCACACTGTGTTTTGCACTGTCA CGCAGGGGGGCACGGGATGAGGTGCCTTCGCCAAA GGTCATATCGTTGTGGCTGCCCAGACGGAAACCGGC ACGCACATGTTGTGCACTGCCATGCCCGAACTTCAC ATAACCGGCGTTGTCCTTACCGTCATCCAGGGAAAG TCCCTGCCAGGTATACTGCAGTTGTGGCTCCAGCATC AGGTTGTCAGTGATACTGAAGGGCAGACCGGTTTCC AGTGAGCCCAGCCAGCCCCAGCCCCGGGCGCGGAA GTCGTTATTGTCCGATGACGCTTTCATGCTGTGGCGG GTTCCCTGTGCCACAATGTCAGCCCACAGGCCGGAG GACGTGTGTACCAGATTCAGGTATCCGCCCAGGCTG CCGGCATCATCCCGGACCGTGCCGGCACGGGAGCCG TCATCATCCTTAACATCAACGGAAGAATGGCCAGCA GCACCATATACCCCCGCGGTCACAGACATACCGGCA ACCTCTGTTCTCATCAGGTCACCCTCCAGACGGACG

	AATCCATAGCTGCCGCTGCTTTCCGGCGTGGCCCCA CGGGCAATACCGCCATTGTTATCGTGACCGAGATGA CCGCCCTGAATGCTGAGACGGACGCTGTTGTTTTCA CCATTTACACCGGTCTGATGGCTGCGGGAGCCTGCC ACAATCCGGTCATAGTCCATTGCCTGTGTCAGCATG GAGGCATACAGGGGGACTTCTGCACGATAAGCATTT TCACTGCGCAGATACCAGCTCTCATCACTGTCCCGGT TGAGGGAGTAGTTAAAGGCACCGGCCTGCAGCCTGT TCCCCTGGACAAAGGCCCCTTCCTCCGTGGTGGCAC CGTTAATGGCTTCCACCACCTGAATACCCTTACCGCT GGTCGCCAGCCCCGACGCACTGTTGCCGGCGTTCAC CAGGTTCAGGATGGTTTTTCCGGTTGCCCTGCCGCCG TCAATGACCAGTCTGTCAGCATTGTTCTGTGCCATAT CCGGGCGTACACGCAGGCTGATGGTGCCATTCTGTC CGTTCAGGTTTTTCACTTTCAGGGTTGCCGGTACGAA CTTCCCTGTGCGGGTGGAGGTGAAATGAATCTGTCC GGCATGGCTGAGGTCATCCACCACCGACTGCACCGT GGCGTTATCGGGGATATTCCAGGTGGCACCGGAGGC GAGAGTGACATTCGTGGG
Ag43 α-Subunit	CGCACAACCATCAATAAAAACGGTCGCCAGATTGTG AGAGCTGAAGGAACGGCAAATACCACTGTGGTTTAT GCCGGCGGCGACCAGACTGTACATGGTCACGCACTG GATACCACGCTGAATGGGGGATACCAGTATGTGCAC

	AACGGCGGTACAGCGTCTGACACTGTTGTGAACAGT GACGGCTGGCAGATTGTCAAAAACGGGGGTGTGGCC GGGAATACCACCGTTAATCAGAAGGGCAGACTGCA GGTGGACGCCGGTGGTACAGCCACGAATGTCACCCT GAAGCAGGGCGGCGCACTGGTTACCAGTACGGCTGC AACCGTTACCGGCATAAACCGCCTGGGAGCATTCTC TGTTGTGGAGGGTAAAGCTGATAATGTCGTACTGGA AAATGGCGGACGCCTGGATGTGCTGACCGGACACAC AGCCACTAATACCCGCGTGGATGATGGCGGAACGCT GGATGTCCGCAACGGTGGCACCGCCACCACCGTATC CATGGGAAATGGCGGTGTACTGCTGGCCGATTCCGG TGCCGCTGTCAGTGGTACCCGGAGCGACGGAAAGGC ATTCAGTATCGGAGGCGGTCAGGCGGATGCCCTGAT GCTGGAAAAAGGCAGTTCATTCACGCTGAACGCCGG TGATACGGCCACGGATACCACGGTAAATGGCGGACT GTTCACCGCCAGGGGCGGCACACTGGCGGGCACCAC CACGCTGAATAACGGCGCCATACTTACCCTTTCCGG GAAGACGGTGAACAACGATACCCTGACCATCCGTGA AGGCGATGCACTCCTGCAGGGAGGCTCTCTCACCGG TAACGGCAGCGTGGAAAAATCAGGAAGTGGCACAC TCACTGTCAGCAACACCACACTCACCCAGAAAGCCG TCAACCTGAATGAAGGCACGCTGACGCTGAACGACA GTACCGTCACCACGGATGTCATTGCTCAGCGCGGTA

	CAGCCCTGAAGCTGACCGGCAGCACTGTGCTGAACG GTGCCATTGAC
M13 pIII	GTGAAAAAATTATTATTCGCAATTCCTTTAGTGGTAC CTTTCTATTCTCACTCTTCGGCCGAAACTGTTGAAAG TTGTTTAGCAAAATCCCATACAGAAAATTCATTTACT AACGTCTGGAAAGACGACAAAACTTTAGATCGTTAC GCTAACTATGAGGGCTGTCTGTGGAATGCTACAGGC GTTGTAGTTTGTACTGGTGACGAAACTCAGTGTTAC GGTACATGGGTTCCTATTGGGCTTGCTATCCCTGAAA ATGAGGGTGGTGGCTCTGAGGGTGGCGGTTCTGAGG GTGGCGGTTCTGAGGGTGGCGGTACTAAACCTCCTG AGTACGGTGATACACCTATTCCGGGCTATACTTATAT CAACCCTCTCGACGGCACTTATCCGCCTGGTACTGA GCAAAACCCCGCTAATCCTAATCCTTCTCTTGAGGA GTCTCAGCCTCTTAATACTTTCATGTTTCAGAATAAT AGGTTCCGAAATAGGCAGGGGGCATTAACTGTTTAT ACGGGCACTGTTACTCAAGGCACTGACCCCGTTAAA ACTTATTACCAGTACACTCCTGTATCATCAAAAGCC ATGTATGACGCTTACTGGAACGGTAAATTCAGAGAC TGCGCTTTCCATTCTGGCTTTAATGAGGATTTATTTG TTTGTGAATATCAAGGCCAATCGTCTGACCTGCCTCA ACCTCCTGTCAATGCTGGCGGCGGCTCTGGTGGTGG TTCTGGTGGCGGCTCTGAGGGTGGTGGCTCTGAGGG

	TGGCGGTTCTGAGGGTGGCGGCTCTGAGGGAGGCGG TTCCGGTGGTGGCTCTGGTTCCGGTGATTTTGATTAT GAAAAGATGGCAAACGCTAATAAGGGGGCTATGAC CGAAAATGCCGATGAAAACGCGCTACAGTCTGACGC TAAAGGCAAACTTGATTCTGTCGCTACTGATTACGG TGCTGCTATCGATGGTTTCATTGGTGACGTTTCCGGC CTTGCTAATGGTAATGGTGCTACTGGTGATTTTGCTG GCTCTAATTCCCAAATGGCTCAAGTCGGTGACGGTG ATAATTCACCTTTAATGAATAATTTCCGTCAATATTT ACCTTCCCTCCCTCAATCGGTTGAATGTCGCCCTTTT GTCTTTGGCGCTGGTAAACCATATGAATTTTCTATTG ATTGTGACAAAATAAACTTATTCCGTGGTGTCTTTGC GTTTCTTTTATATGTTGCCACCTTTATGTATGTATTTT CTACGTTTGCTAACATACTGCGTAATAAGGAGTCTT AA
M13 Degenerate Oligonucleotide	CCATTCATGTTTCGGCCGANNNNNNNNNNNNNNN NNNNNNNNNNNNNNNNNNNNAGAGTGAG AATAGAAAGGTACCCGGG

Table A.2: Selected peptide sequences and their translations

Peptides	**DNA Sequence (5' to 3')**	**Amino Acid Sequence**
Common Peptide Sequence	ACCTCCACCATGCTTCTG CGTAATATAAATATTCAA	HLNLNIYITQKH
25Q-Htt-Bound Peptide	CATTCTTGGCTTGGTGAG GTGTTGGTTCAGAATACT	HSWLGEVLVQNT
46Q-Htt-Bound Peptide #1	GATATGCATGGGCGGTAT ATGATGACTACTAGGGAG	DMHGRYMMTTRE
46Q-Htt-Bound Peptide #2	ACCTCCACCACCCACCGT ATACTGATGATACGTAT	NHHYTYHQYTVG
103Q-Htt-Bound Peptide	ACCTCCACCCTCCGCCTT CCAATCCATAGACGGCCA	WDMWPSMDWKAE
Amyloid β_{40}-Bound Peptide	ACCTCCACCACTAAAACC ACGCATCCGATTAAGCA	DGSMLNRMRGFS
Amyloid β_{42}-Bound Peptide #1	ACCTCCACCCTGAGCAGC CCCAGGATACGTAGCAAA	KCCFATYPGAAQ
Amyloid β_{42}-Bound Peptide #2	ACCTCCACCCGGAGAACT CCACGAAATAGTAACATT	SYPNVTISWSSP

APPENDIX B

List of primers used in this study

Table B.1: PCR primers mentioned in materials and methods section

#	Primer Name	Sequence (5'-3')
1	pCEO3	CTGCACCGACCTCTCGAGGGGGGCGGATCCA TGCGTAAAGGCGAAGAGC
2	pCEO7	CTGCACCGACCTCTCGAGGGGGGCGGATCCA TGCGTAAAGGCGAAGAGC
3	pCEO9	ATGGTCGGCGGAGTTGTGATAGCTCTCGAGG GGGGCGGATCCATGCGTAAAGGCGAAGAGC
4	pCEO11	GGACTAATGGTCGGCGGAGTTGTGCTCGAGG GGGGCGGATCCATGCGTAAAGGCGAAGAGC
5	pCEO13	CAAGTCCTCTTCAGAAATAAGCTTTTGTTCTT TGTACAGTTCATCCATACCATGCG
6	pCEO14	GAGCCAGAAGCCCTCGAGGGGGGCGGATCC ATGCGTAAAGGCGAAGAGCT

7	pCEO35	GTACCTTTCTATTCTCACTCTNNNNNNNNNNNNNNNNNNNNNNNNNNNNNNNNNNNNNNNNNNNTCGGCCGAAACTGTTGAAAG
8	pCEO36	AGAGTGAGAATAGAAAGGTAC
9	pCEO49	TTCGCAATTCCTTTAGTGGTACCTTTCTATTCTCACTCTTCGGCCGAAACTGTTGAAAG
10	pCEO52	GGCGACCGTTTTTATTGATGGTTGTGCGCTTAAGGGATCCGCCCCCCTCGAGAG
11	pCEO53	CTCCTCGCTGCCCAGCCGGCGATGGCCATGGGCACTAGTATGGCGACCCTGGAAAAG
12	pCEO54	GGCGACCGTTTTTATTGATGGTTGTGCGCTTAAGGGATCCGCCCCCCTCGAGGG
13	pCEO55	GCTCCTCGCTGCCCAGCCGGCGATGGCCATGGGCACTAGTATGGACGTTTTCATGAAGGGTCTTTC
14	pCEO65	GTTTTTATTGATGGTTGTGCGCTTAAGGGATCCGCCCCCCTCGAGCACAACTCCGCCGACC
15	pCEO66	CTCCTCGCTGCCCAGCCGGCGATGGCCATGG

		GCACTAGTATGGAC
16	pCEO71	GCACCGACCTCTCGAGGGGGGCGGATCCCTTAAGCGCACAACCATCAATAAAAACG
17	pCEO83	CCCTCATAGTTAGCGTAACG
18	pCEO85	CATGCCCGGGTACCTTTCTATTCTC
19	pCEO86 (for PCR of M13 Sequencing)	CACCTCGAAAGCAAGCTGA
20	pCEO87 (for PCR of M13 Sequencing)	GGTTTAGTACCGCCACCCTC
21	pREA17	TCAGTGGTGGTGGTGGTGGTGCTCGAGTCATCAGAAGGTCACATTCAGTG

APPENDIX C

Plasmid maps used in this study

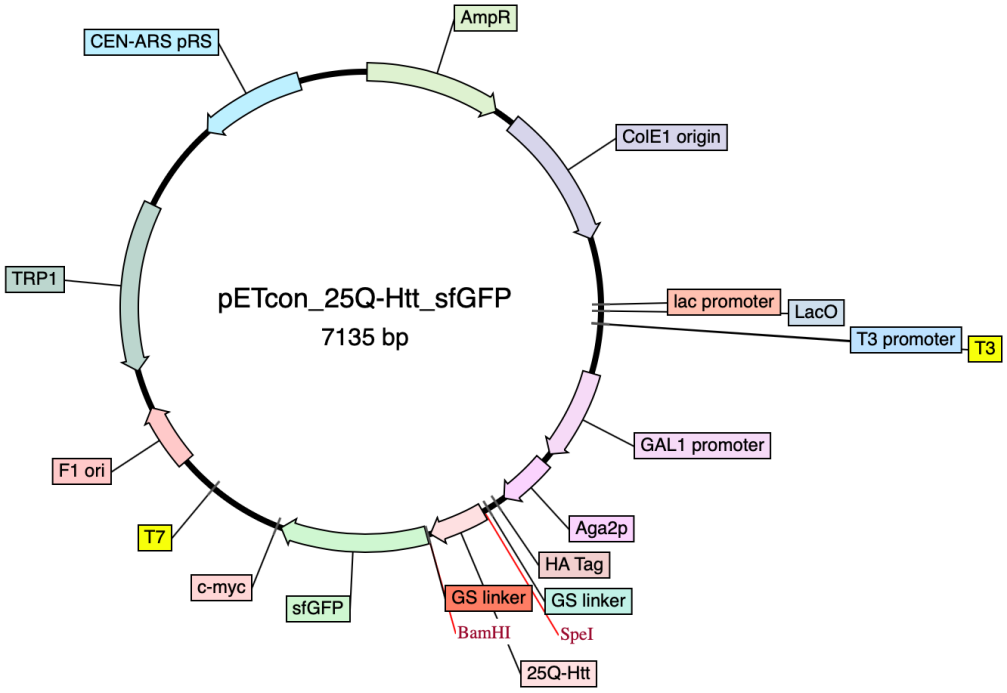

Figure C1: Plasmid map representation of pETcon_Aga2_25Q-Htt_sfGFP vector

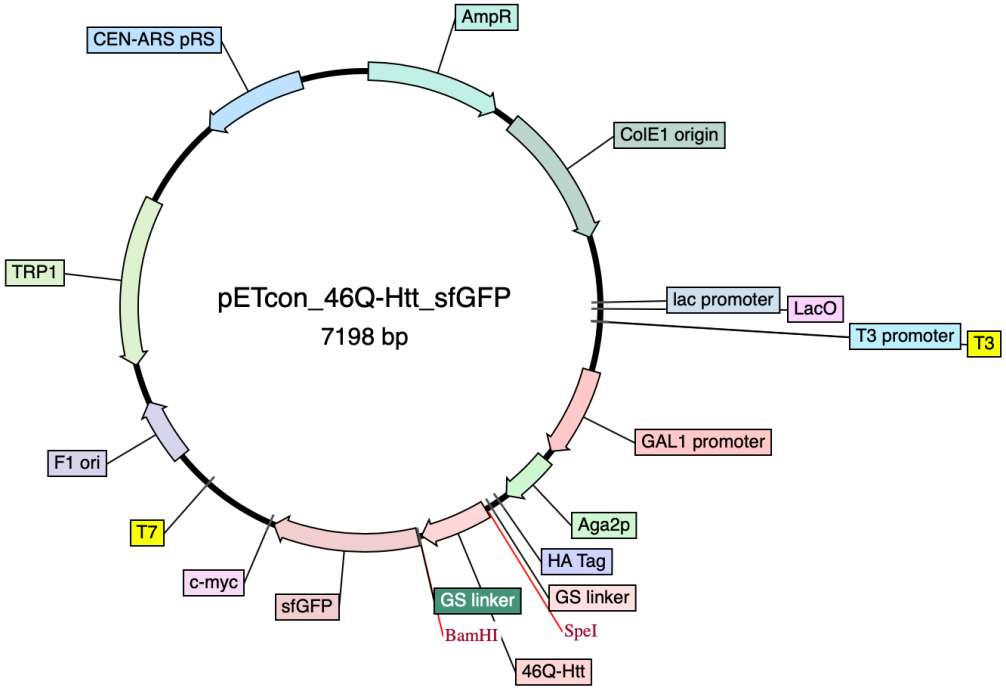

Figure C2: Plasmid map representation of pETcon_Aga2_46Q-Htt_sfGFP vector

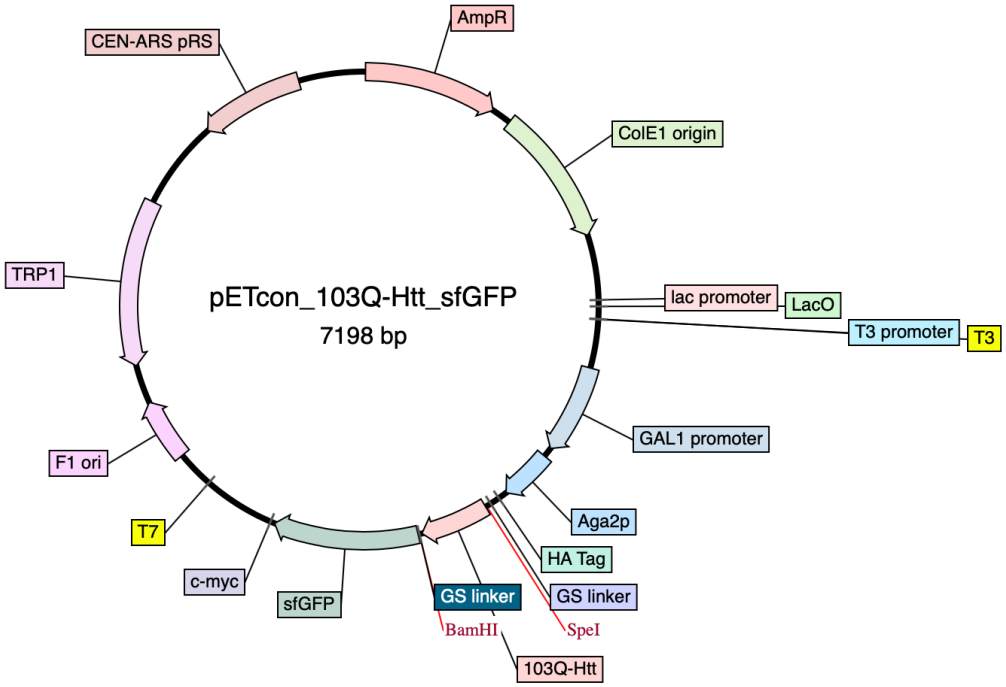

Figure C3: Plasmid map representation of pETcon_Aga2_103Q-Htt_sfGFP vector

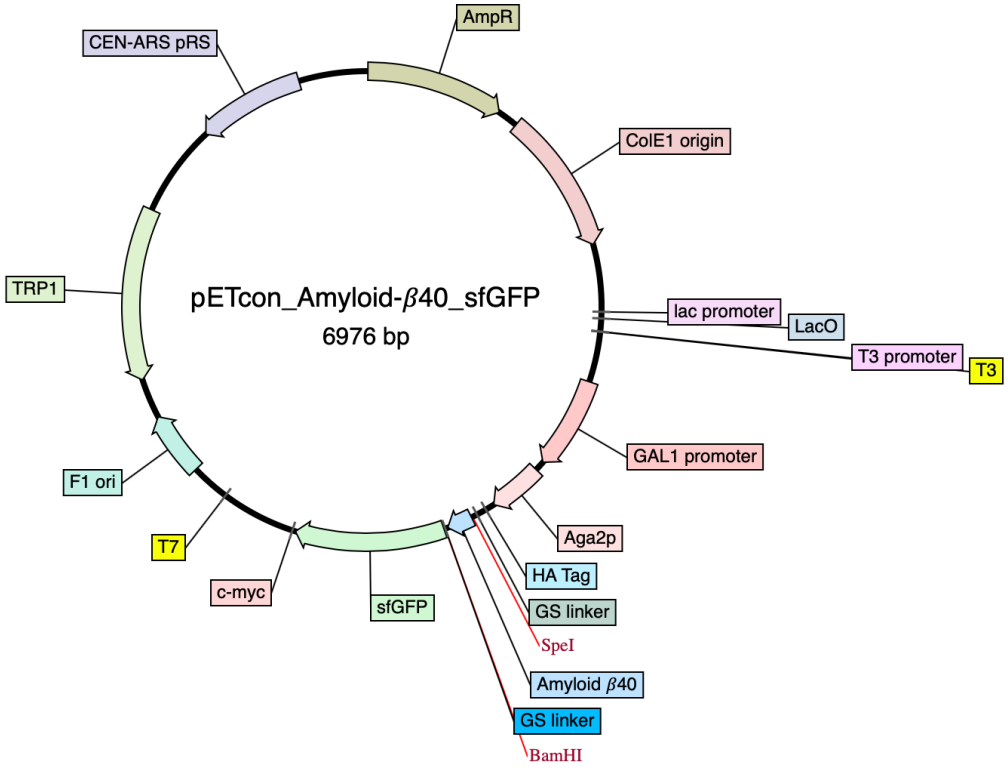

Figure C4: Plasmid map representation of pETcon_Aga2_ Amyloid-β_{40}_sfGFP vector

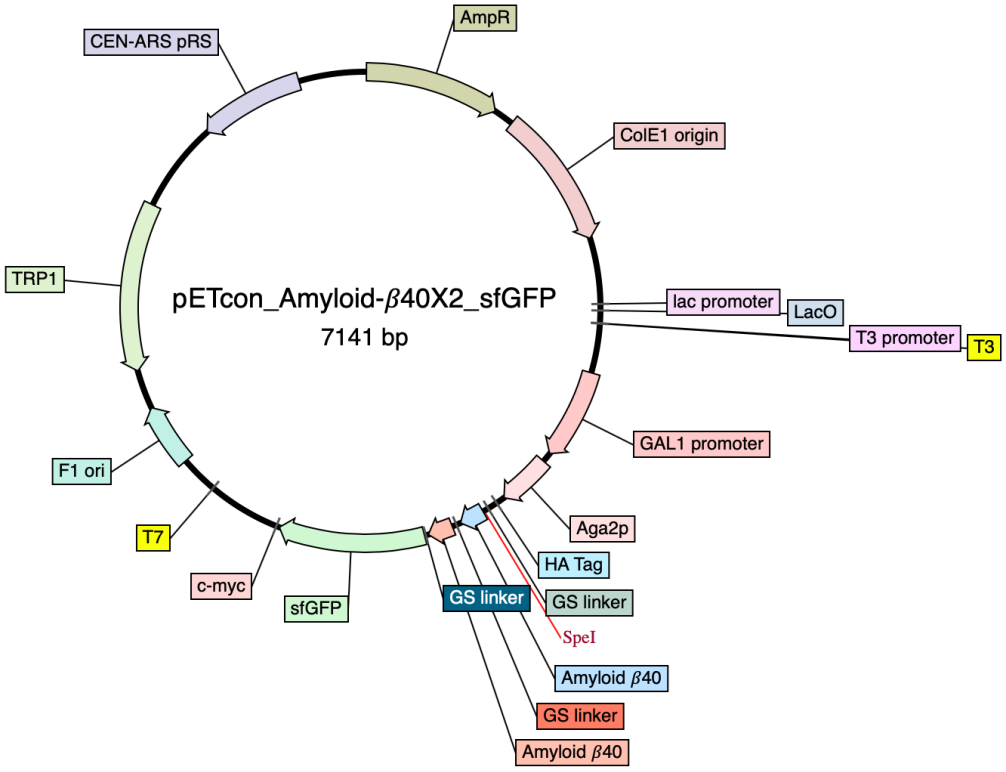

Figure C5: Plasmid map representation of pETcon_Aga2_ Amyloid-β_{40X2}_sfGFP vector

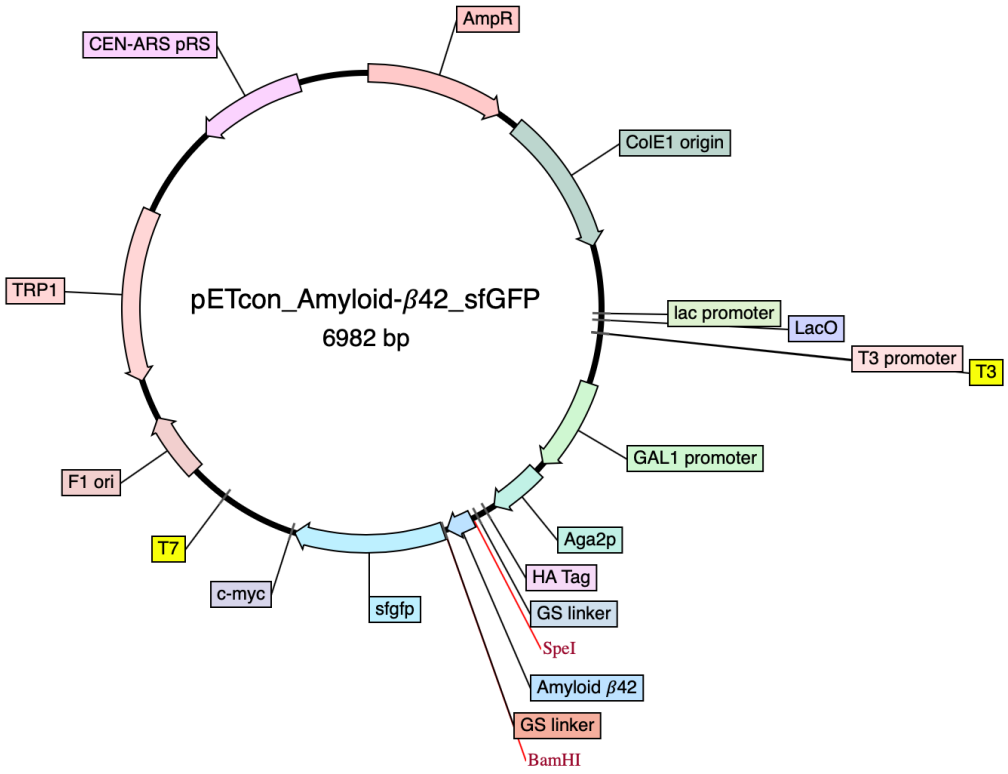

Figure C6: Plasmid map representation of pETcon_Aga2_ Amyloid-β_{42}_sfGFP vector

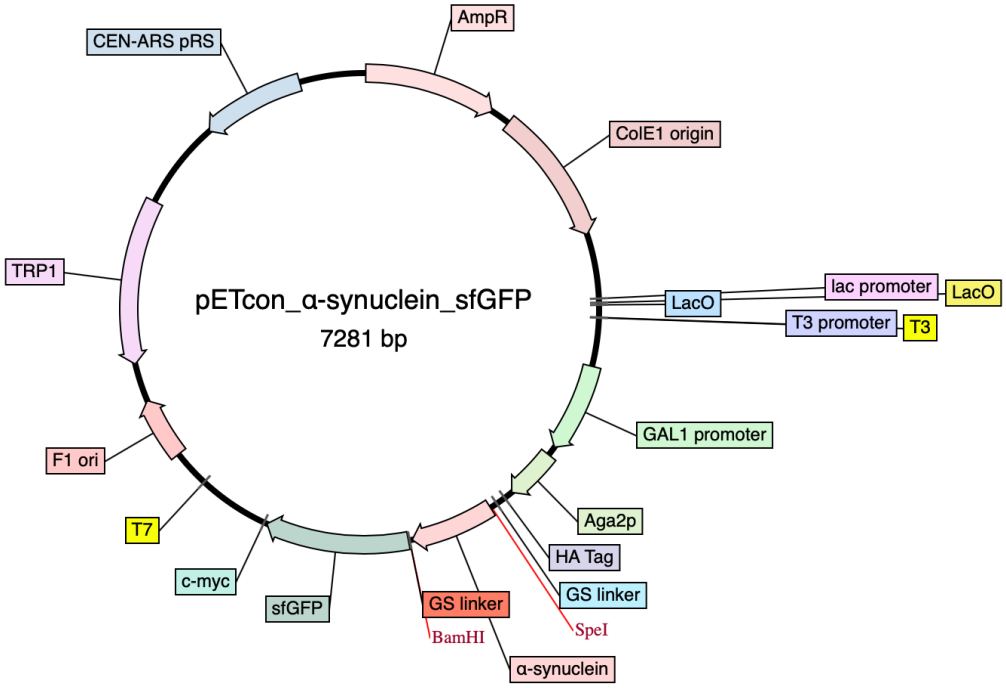

Figure C7: Plasmid map representation of pETcon_Aga2_ α-Synuclein_sfGFP vector

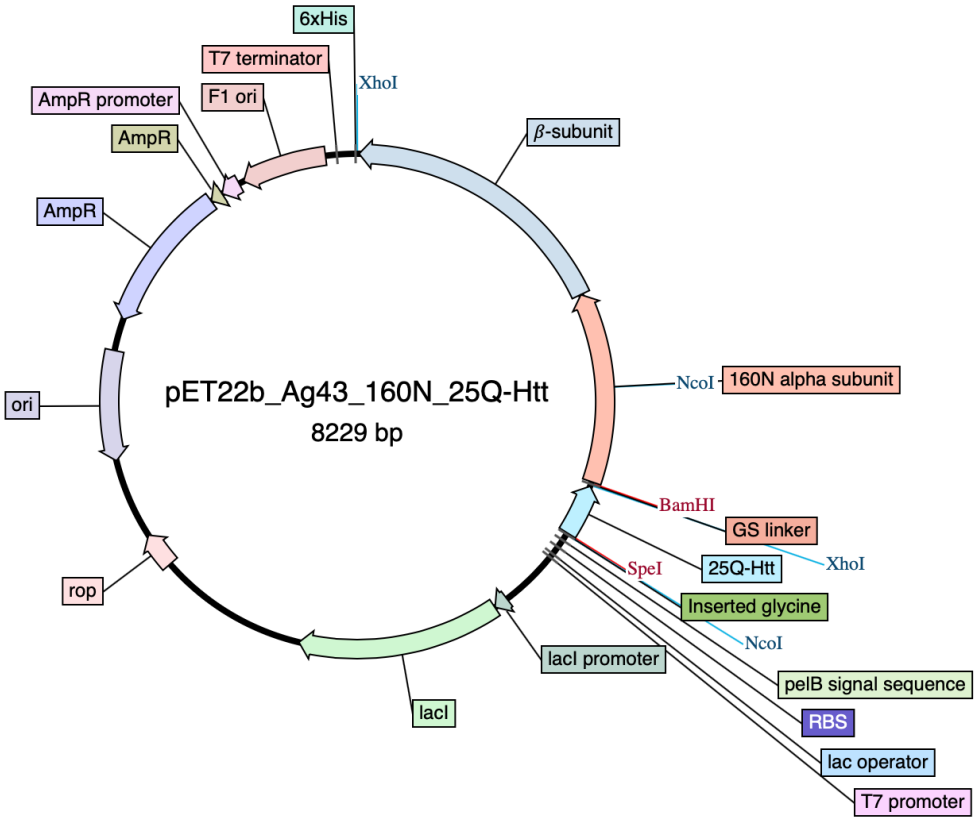

Figure C8: Plasmid map representation of pET22b_Ag45_160N_25Q-Htt vector

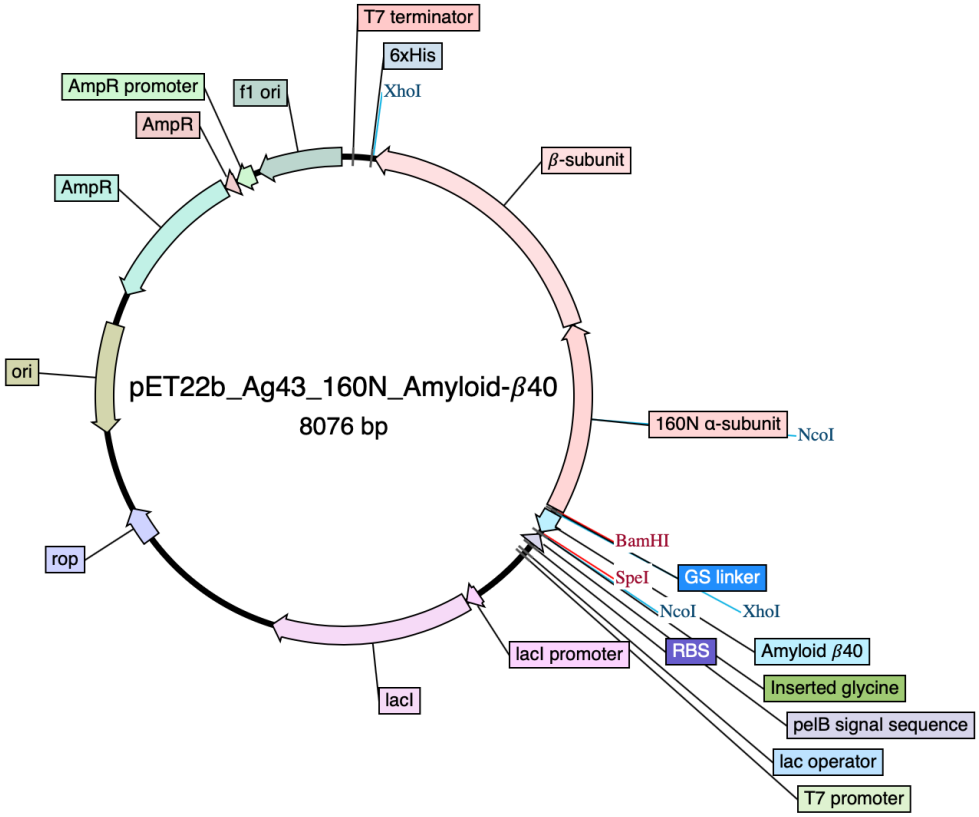

Figure C9: Plasmid map representation of pET22b_Ag45_160N_ Amyloid-β_{40} vector

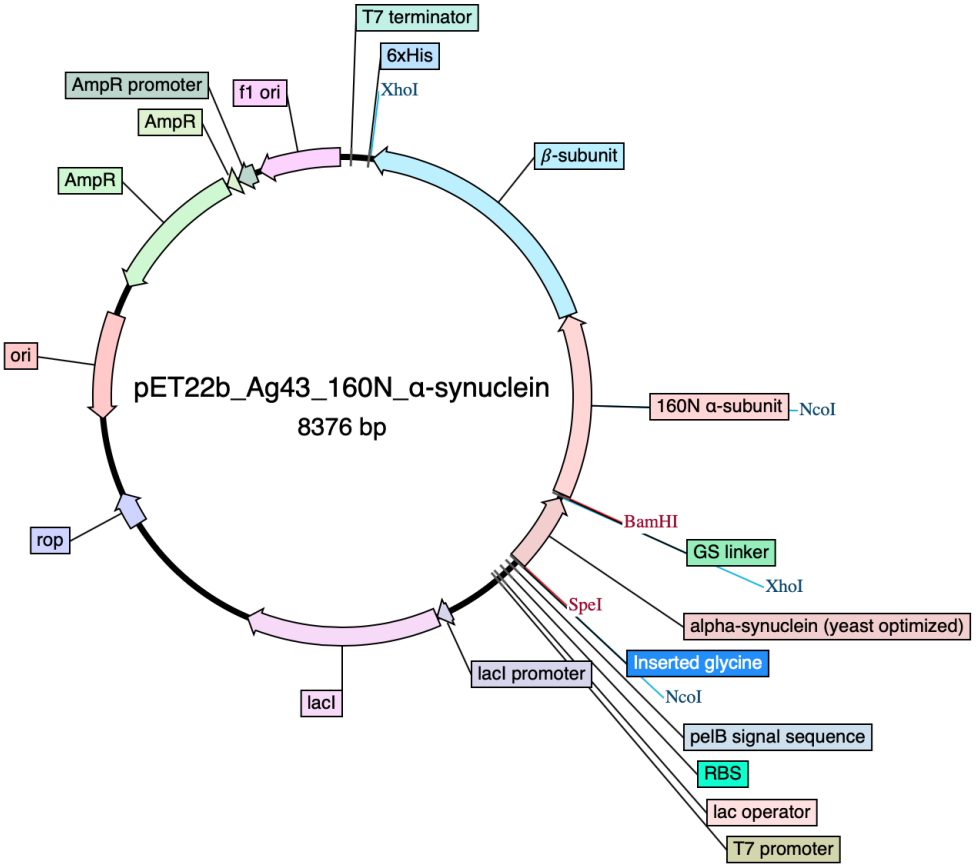

Figure C.10: Plasmid map representation of pET22b_Ag45_160N_ α-Synuclein vector

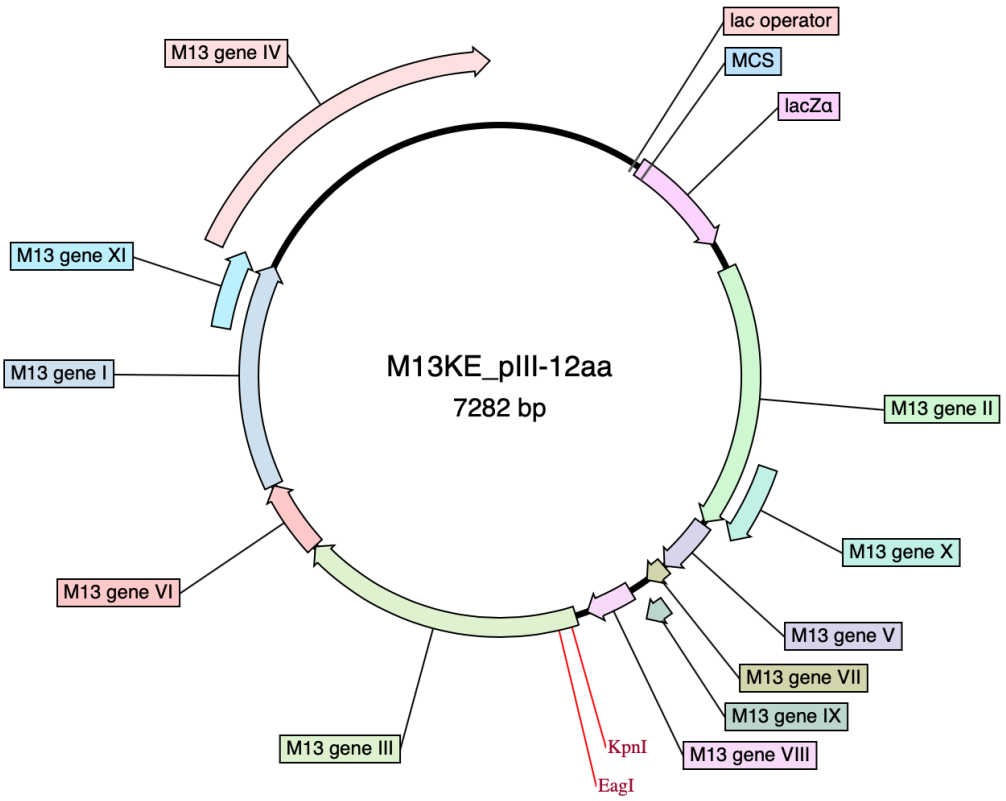

Figure C.11: Plasmid map representation of ss-M13 genome Displaying Peptides on *gIII*

APPENDIX D

Sanger sequencing results for clonings done in this study

For all sequencing results, red rectangle indicates the sequencing data and blue rectangle indicates the original sequence. Note that, all unreaded nucleotides were actually correctly inserted since other characterizations were gave positive results. Also, close to or far away from the sequencing primer annealing site may not be read properly generally.

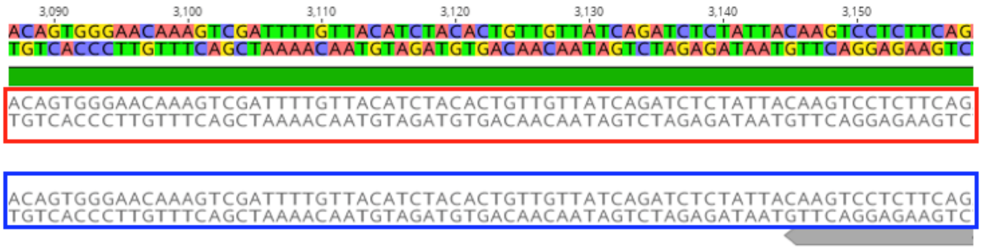

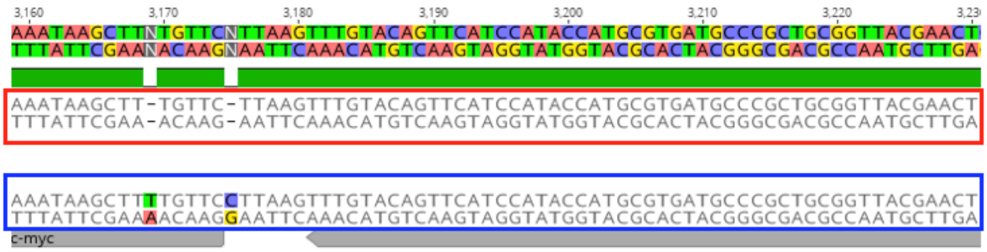

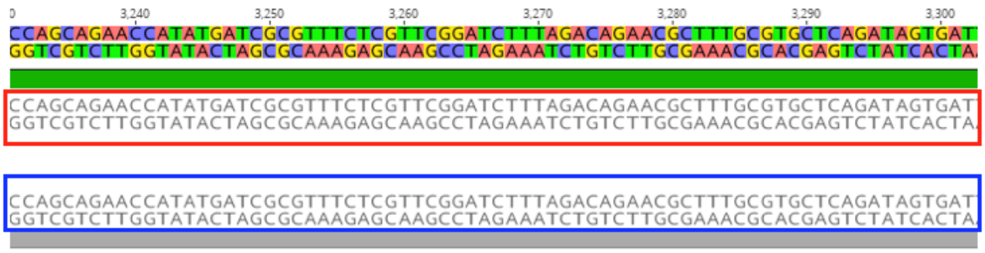

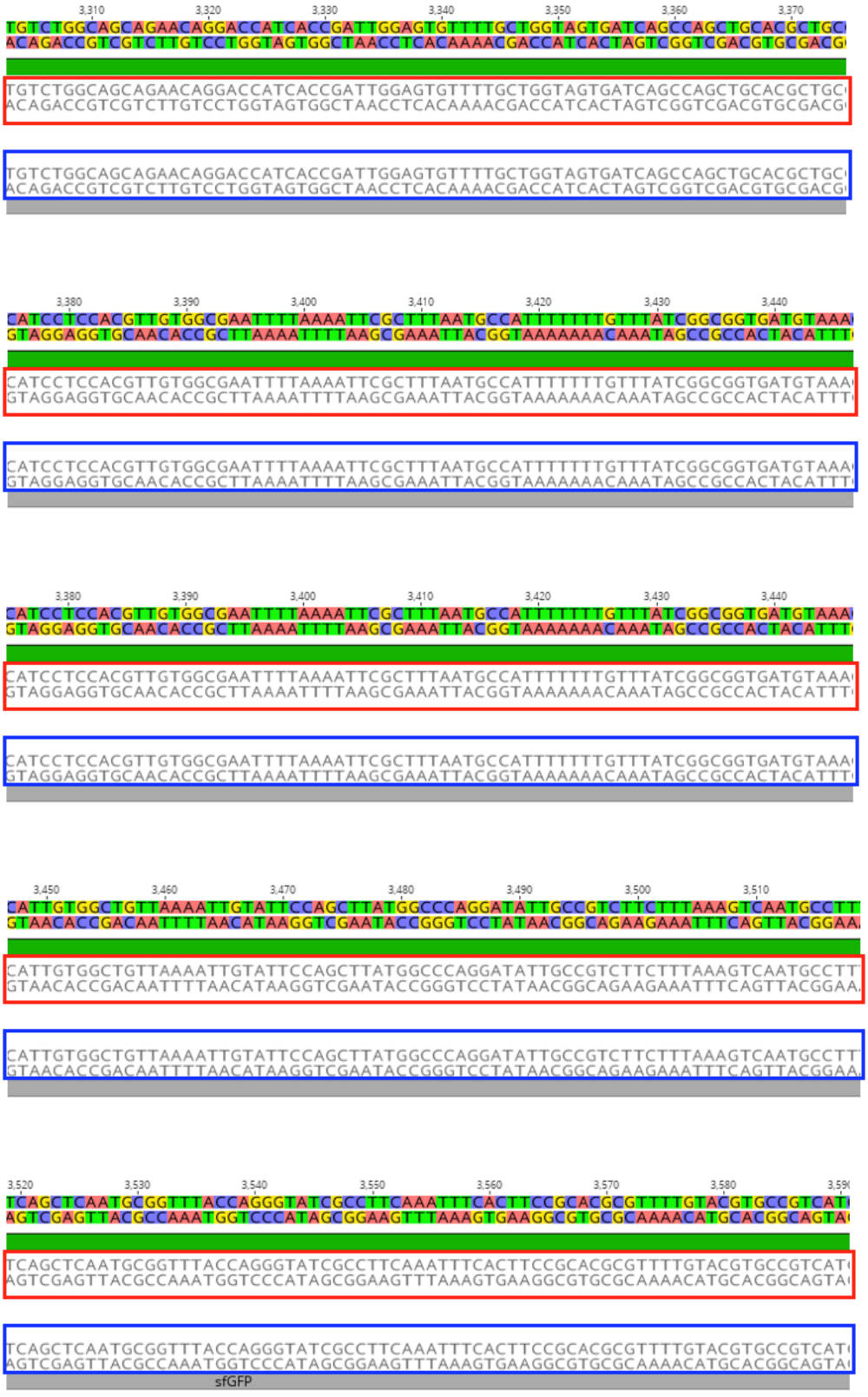
3,310
3,320
3,330
3,340
3,350
3,360
3,370
3,380
3,390
3,400
3,410
3,420
3,430
3,440
3,450
3,460
3,470
3,480
3,490
3,500
3,510
3,520
3,530
3,540
3,550
3,560
3,570
3,580
sfGFP

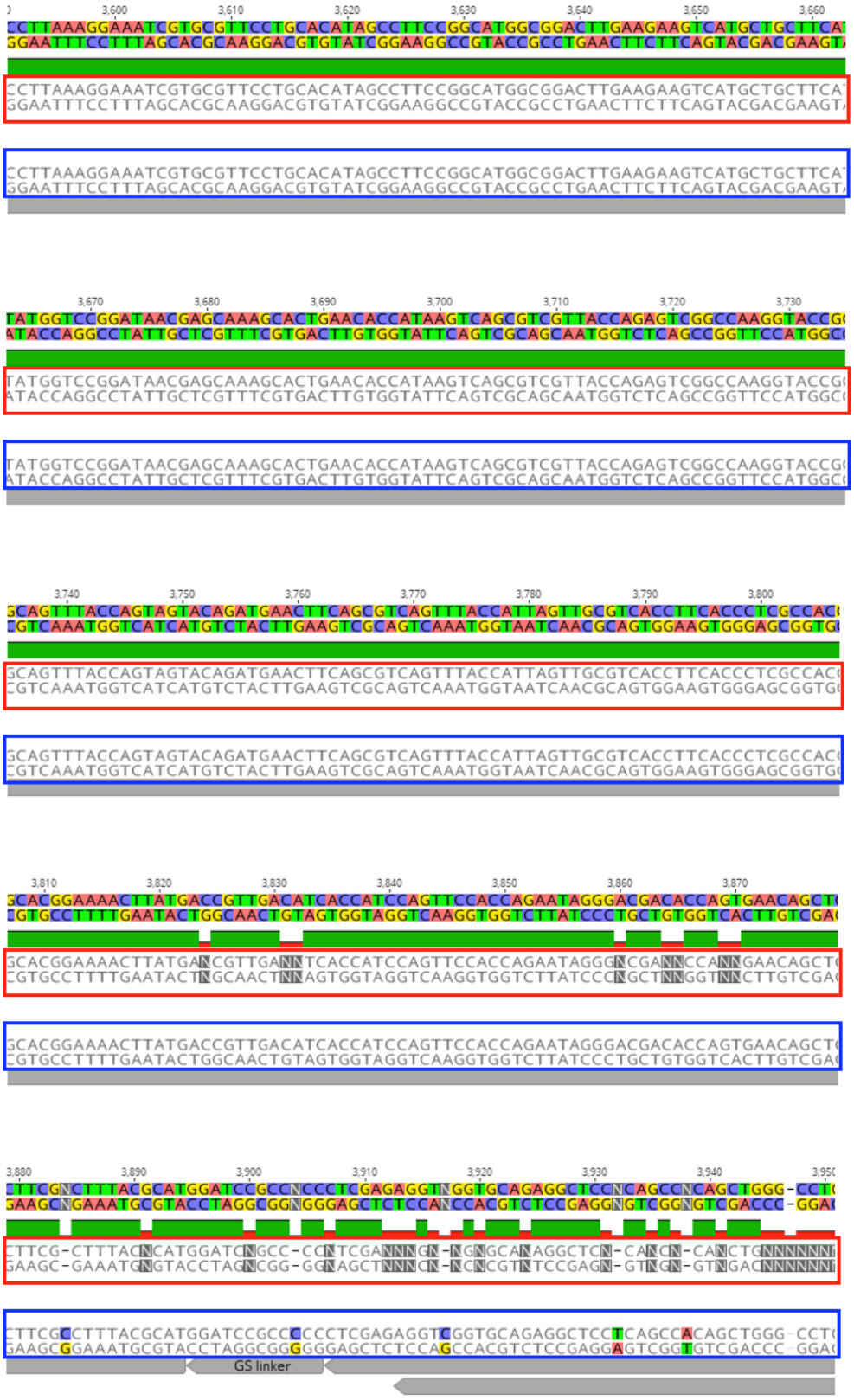

Figure D.1: Sequencing result of sfGFP from pETcon_25Q-Htt_sfGFP

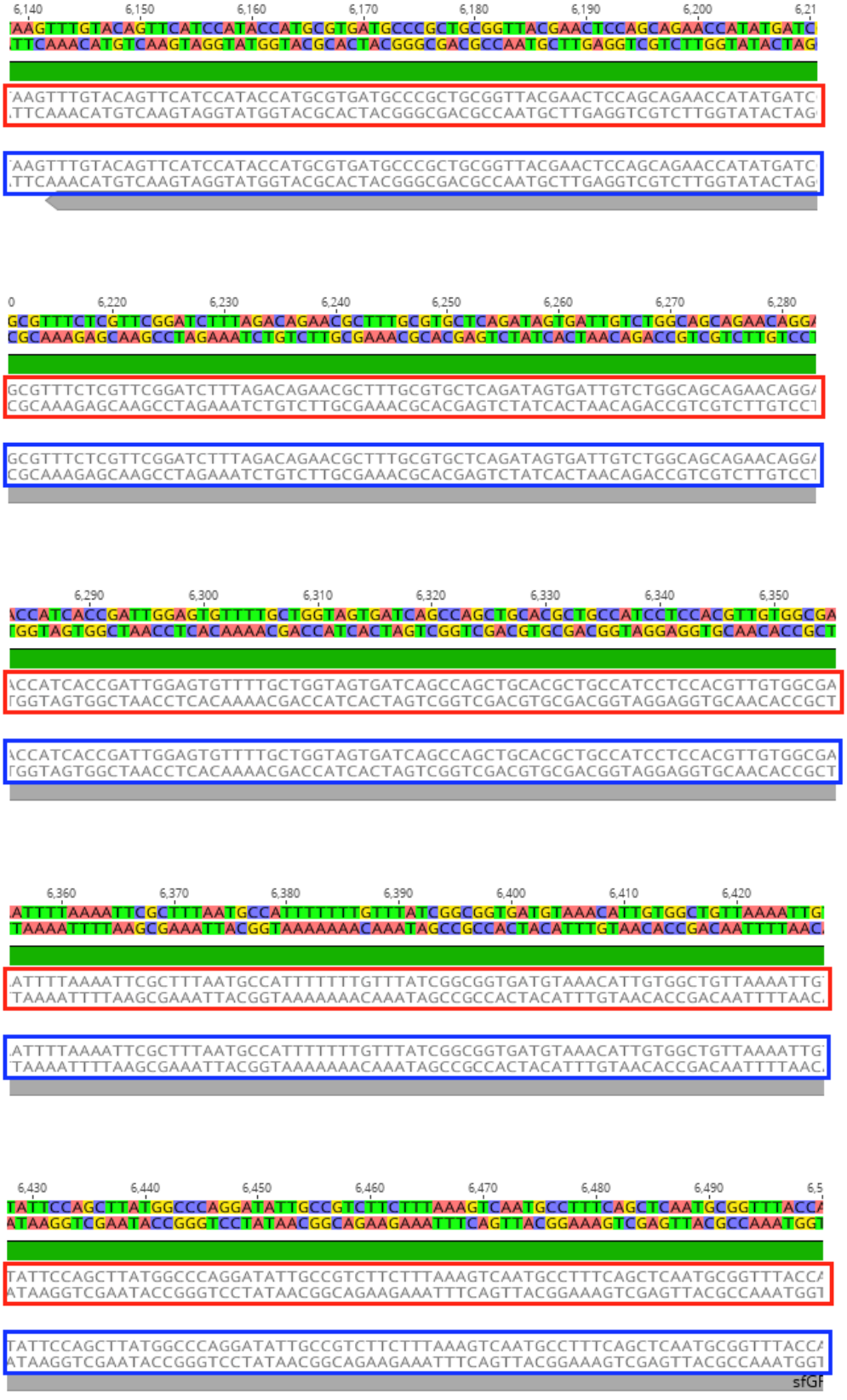
6,140 6,150 6,160 6,170 6,180 6,190 6,200 6,21
AAGTTTGTACAGTTCATCCATACCATGCGTGATGCCCGCTGCGGTTACGAACTCCAGCAGAACCATATGATC
TTCAAACATGTCAAGTAGGTATGGTACGCACTACGGGCGACGCCAATGCTTGAGGTCGTCTTGGTATACTAG
0 6,220 6,230 6,240 6,250 6,260 6,270 6,280
GCGTTTCTCGTTCGGATCTTTAGACAGAACGCTTTGCGTGCTCAGATAGTGATTGTCTGGCAGCAGAACAGGA
CGCAAAGAGCAAGCCTAGAAATCTGTCTTGCGAAACGCACGAGTCTATCACTAACAGACCGTCGTCTTGTCCT
6,290 6,300 6,310 6,320 6,330 6,340 6,350
ACCATCACCGATTGGAGTGTTTTGCTGGTAGTGATCAGCCAGCTGCACGCTGCCATCCTCCACGTTGTGGCGA
TGGTAGTGGCTAACCTCACAAAACGACCATCACTAGTCGGTCGACGTGCGACGGTAGGAGGTGCAACACCGCT
6,360 6,370 6,380 6,390 6,400 6,410 6,420
ATTTTAAAATTCGCTTTAATGCCATTTTTTTGTTTATCGGCGGTGATGTAAACATTGTGGCTGTTAAAATTG
TAAAATTTTAAGCGAAATTACGGTAAAAAAACAAATAGCCGCCACTACATTTGTAACACCGACAATTTTAAC
6,430 6,440 6,450 6,460 6,470 6,480 6,490 6,5
TATTCCAGCTTATGGCCCAGGATATTGCCGTCTTCTTTAAAGTCAATGCCTTTCAGCTCAATGCGGTTTACCA
ATAAGGTCGAATACCGGGTCCTATAACGGCAGAAGAAATTTCAGTTACGGAAAGTCGAGTTACGCCAAATGGT

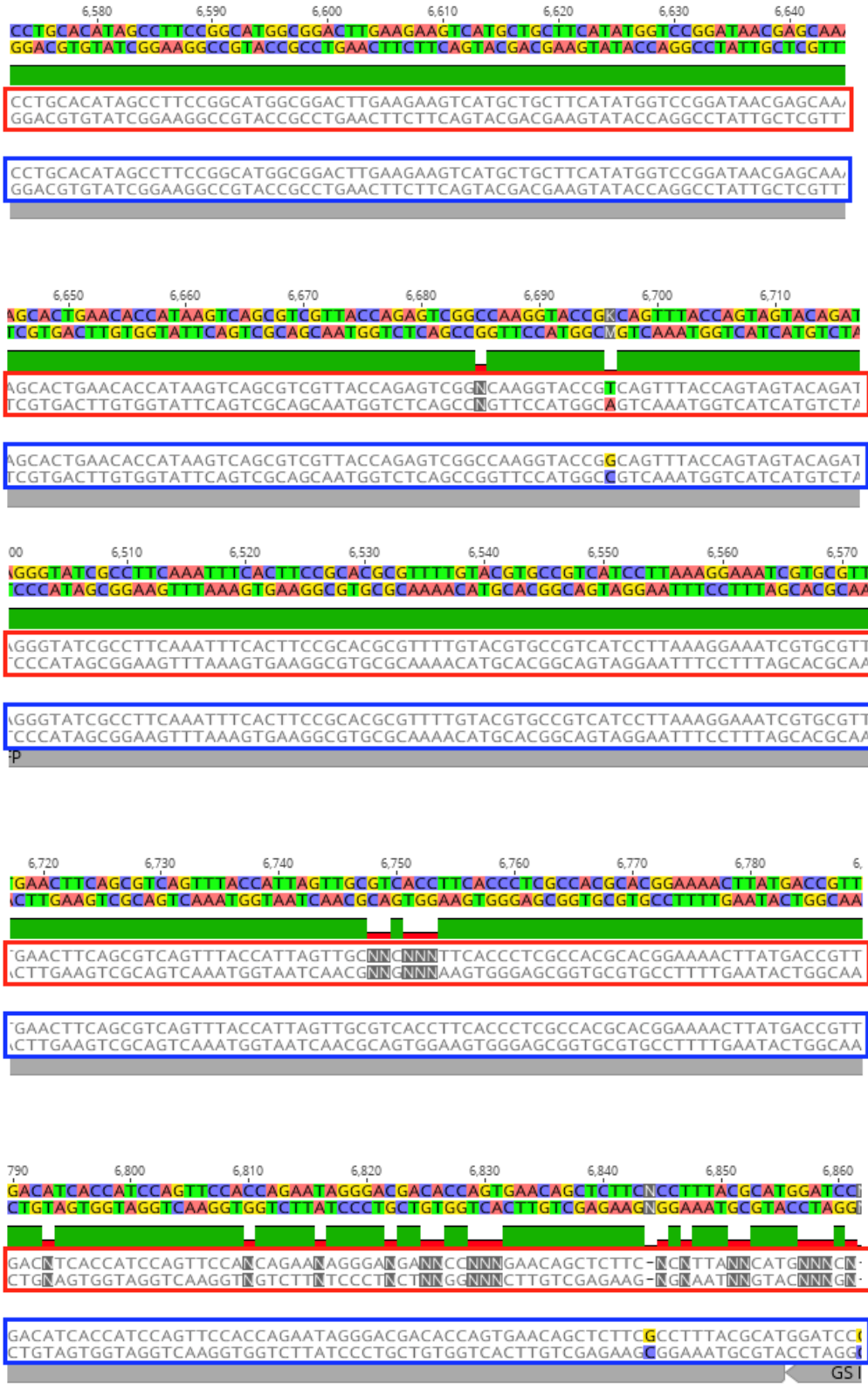

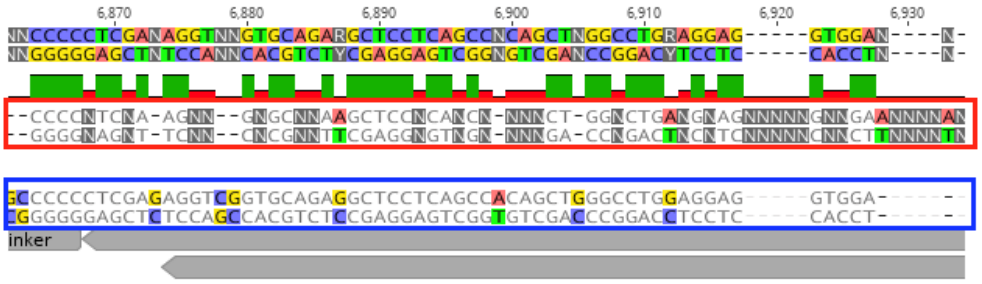

Figure D.2: Sequencing result of sfGFP from pETcon_46Q-Htt_sfGFP

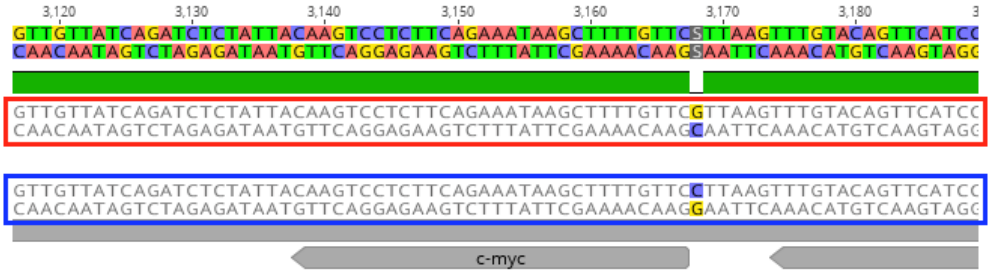

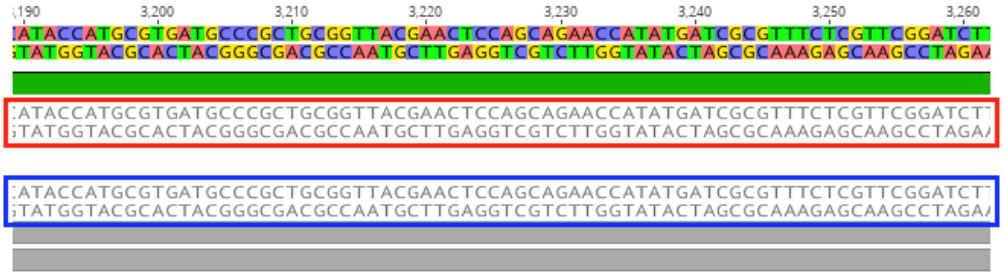

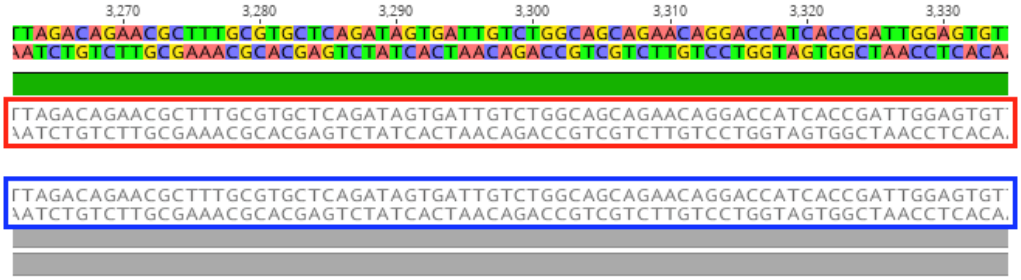

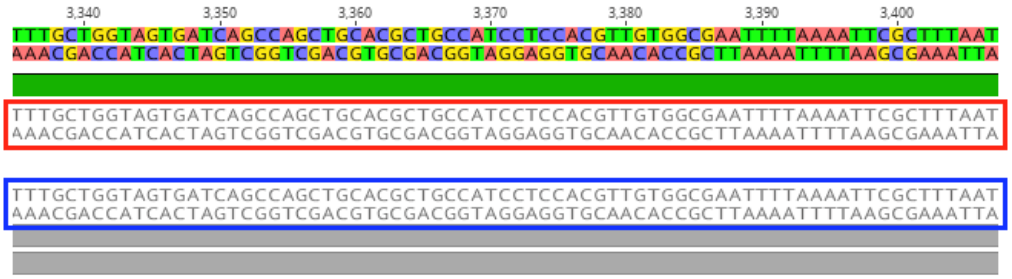
3,340
3,350
3,360
3,370
3,380
3,390
3,400

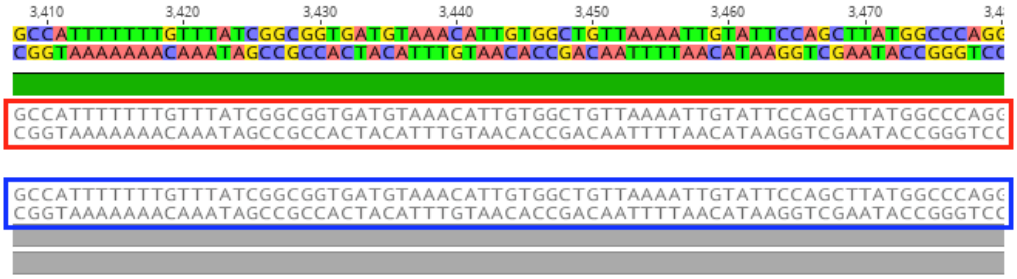
3,410
3,420
3,430
3,440
3,450
3,460
3,470

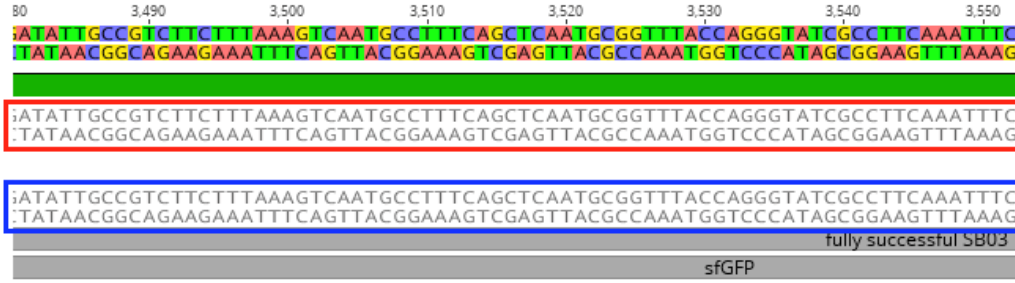
3,490
3,500
3,510
3,520
3,530
3,540
3,550
fully successful SB03
sfGFP

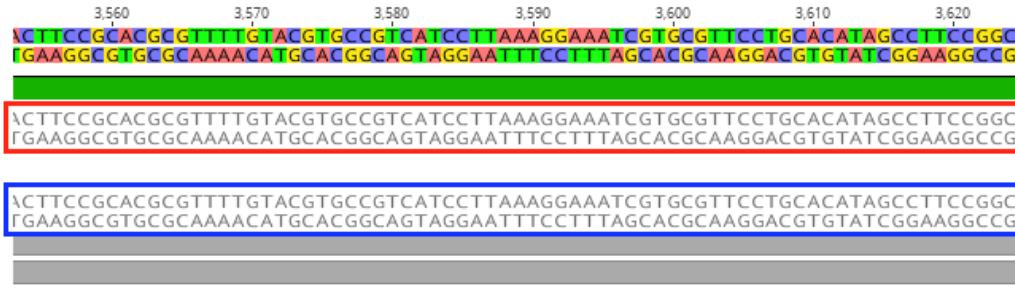
3,560
3,570
3,580
3,590
3,600
3,610
3,620

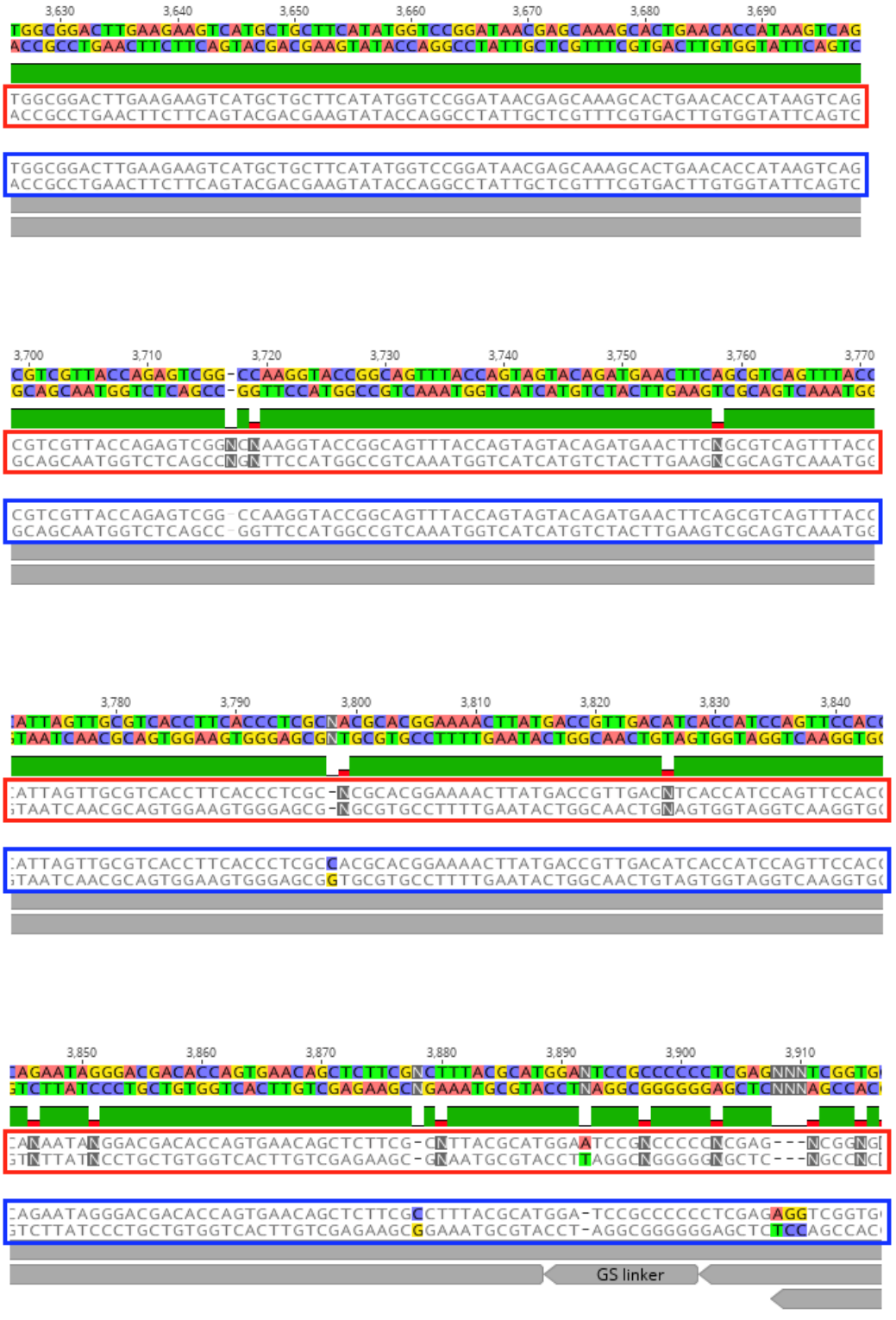

Figure D.3: Sequencing result of sfGFP from pETcon_103Q-Htt_sfGFP

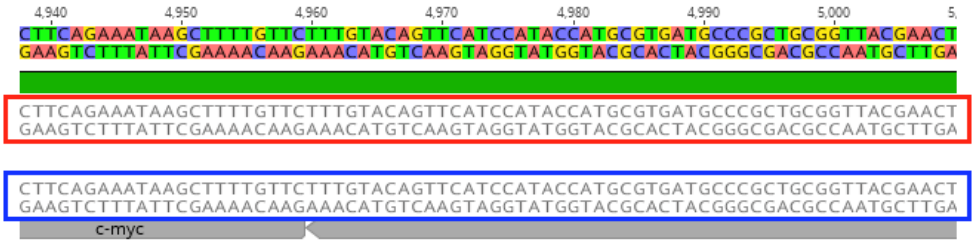
4,940
4,950
4,960
4,970
4,980
4,990
5,000
c-myc

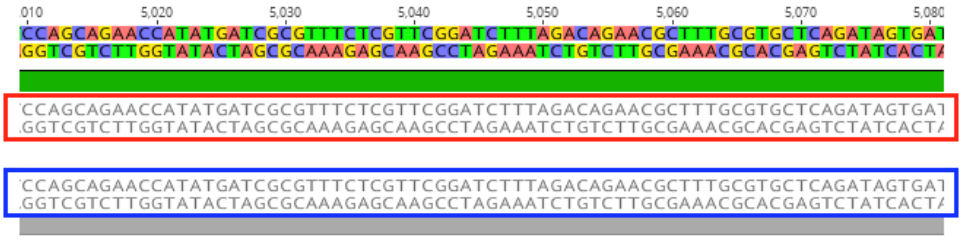
5,010
5,020
5,030
5,040
5,050
5,060
5,070
5,080

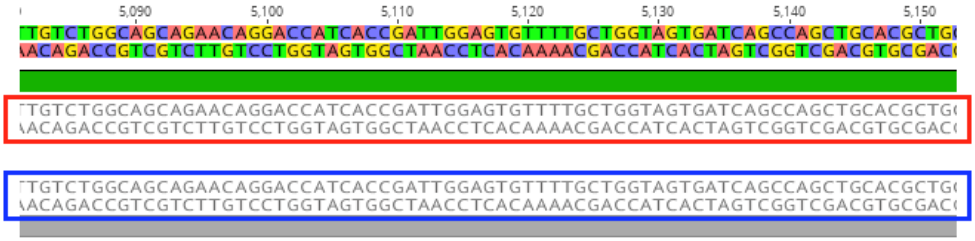
5,090
5,100
5,110
5,120
5,130
5,140
5,150

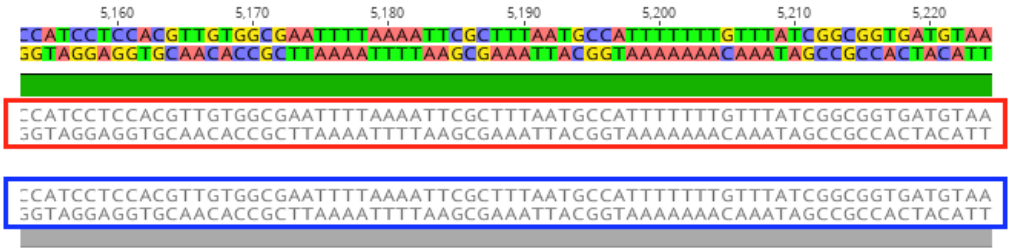
5,160
5,170
5,180
5,190
5,200
5,210
5,220

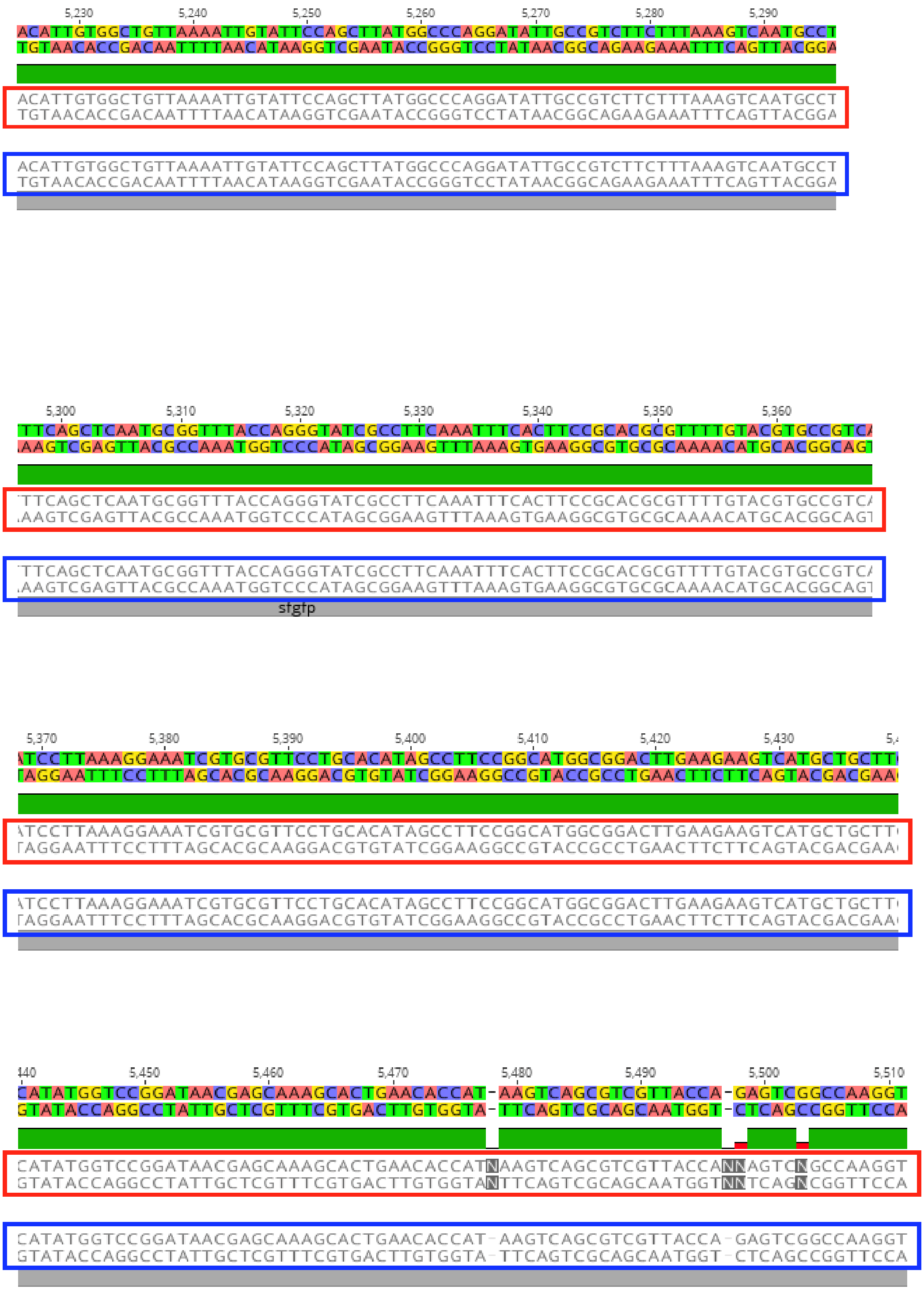
5,230 5,240 5,250 5,260 5,270 5,280 5,290
ACATTGTGGCTGTTAAAATTGTATTCCAGCTTATGGCCCAGGATATTGCCGTCTTCTTTAAAGTCAATGCCT
TGTAACACCGACAATTTTAACATAAGGTCGAATACCGGGTCCTATAACGGCAGAAGAAATTTCAGTTACGGA
5,300 5,310 5,320 5,330 5,340 5,350 5,360
TTCAGCTCAATGCGGTTTACCAGGGTATCGCCTTCAAATTTCACTTCCGCACGCGTTTTGTACGTGCCGTCA
AAGTCGAGTTACGCCAAATGGTCCCATAGCGGAAGTTTAAAGTGAAGGCGTGCGCAAAACATGCACGGCAGT
sfgfp
5,370 5,380 5,390 5,400 5,410 5,420 5,430
ATCCTTAAAGGAAATCGTGCGTTCCTGCACATAGCCTTCCGGCATGGCGGACTTGAAGAAGTCATGCTGCTT
TAGGAATTTCCTTTAGCACGCAAGGACGTGTATCGGAAGGCCGTACCGCCTGAACTTCTTCAGTACGACGAA
5,450 5,460 5,470 5,480 5,490 5,500 5,510
CATATGGTCCGGATAACGAGCAAAGCACTGAACACCAT-AAGTCAGCGTCGTTACCA-GAGTCGGCCAAGGT
GTATACCAGGCCTATTGCTCGTTTCGTGACTTGTGGTA-TTCAGTCGCAGCAATGGT-CTCAGCCGGTTCCA

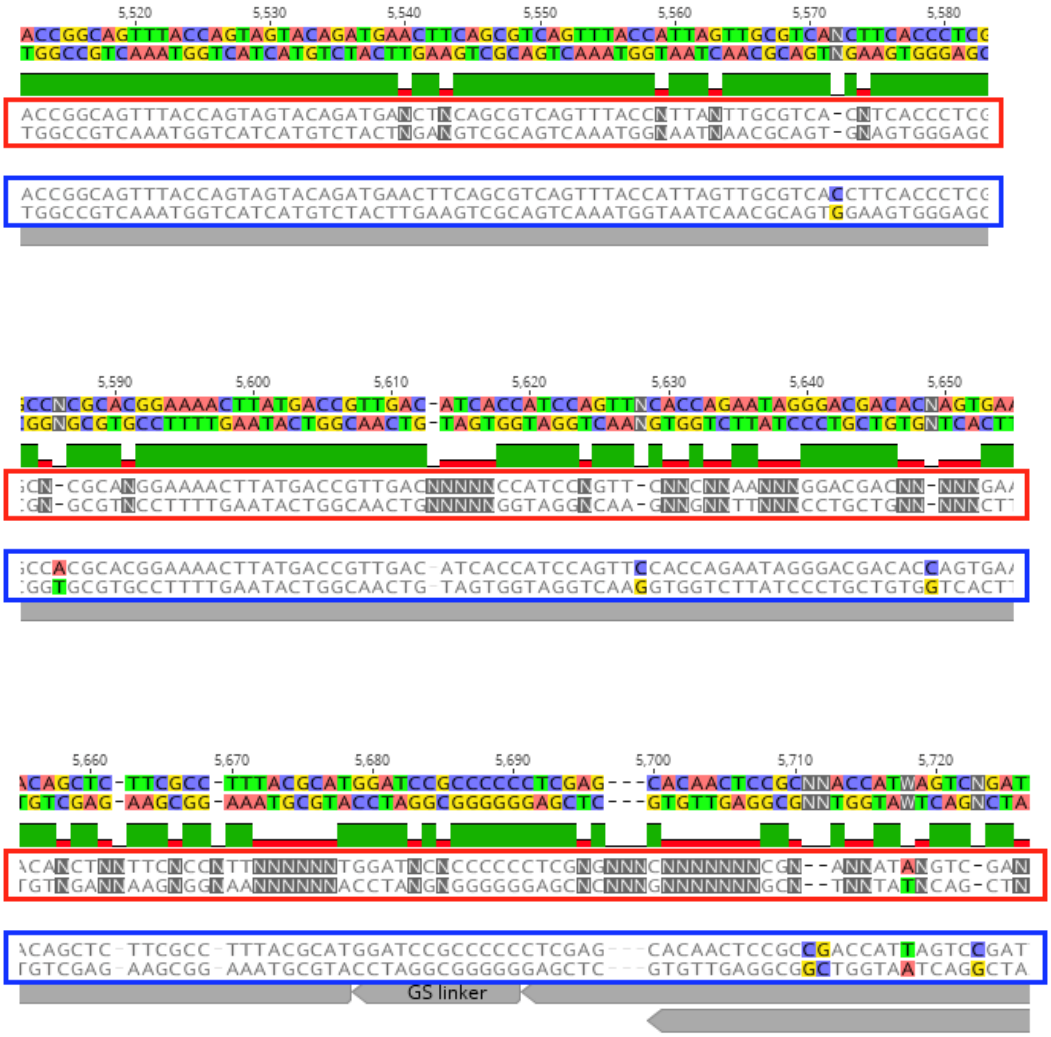

Figure D.4: Sequencing result of sfGFP from pETcon_Amyloid-β_{40}_sfGFP

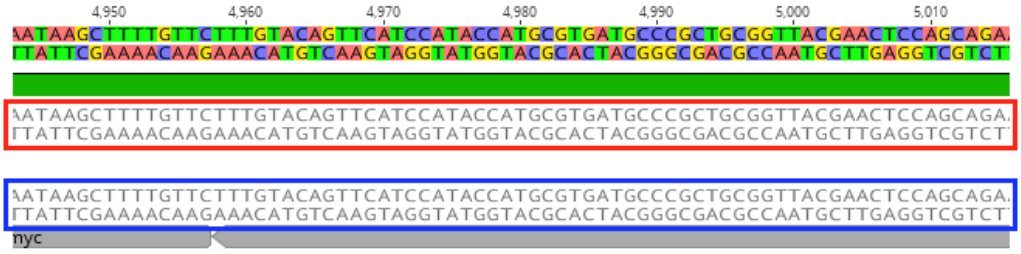

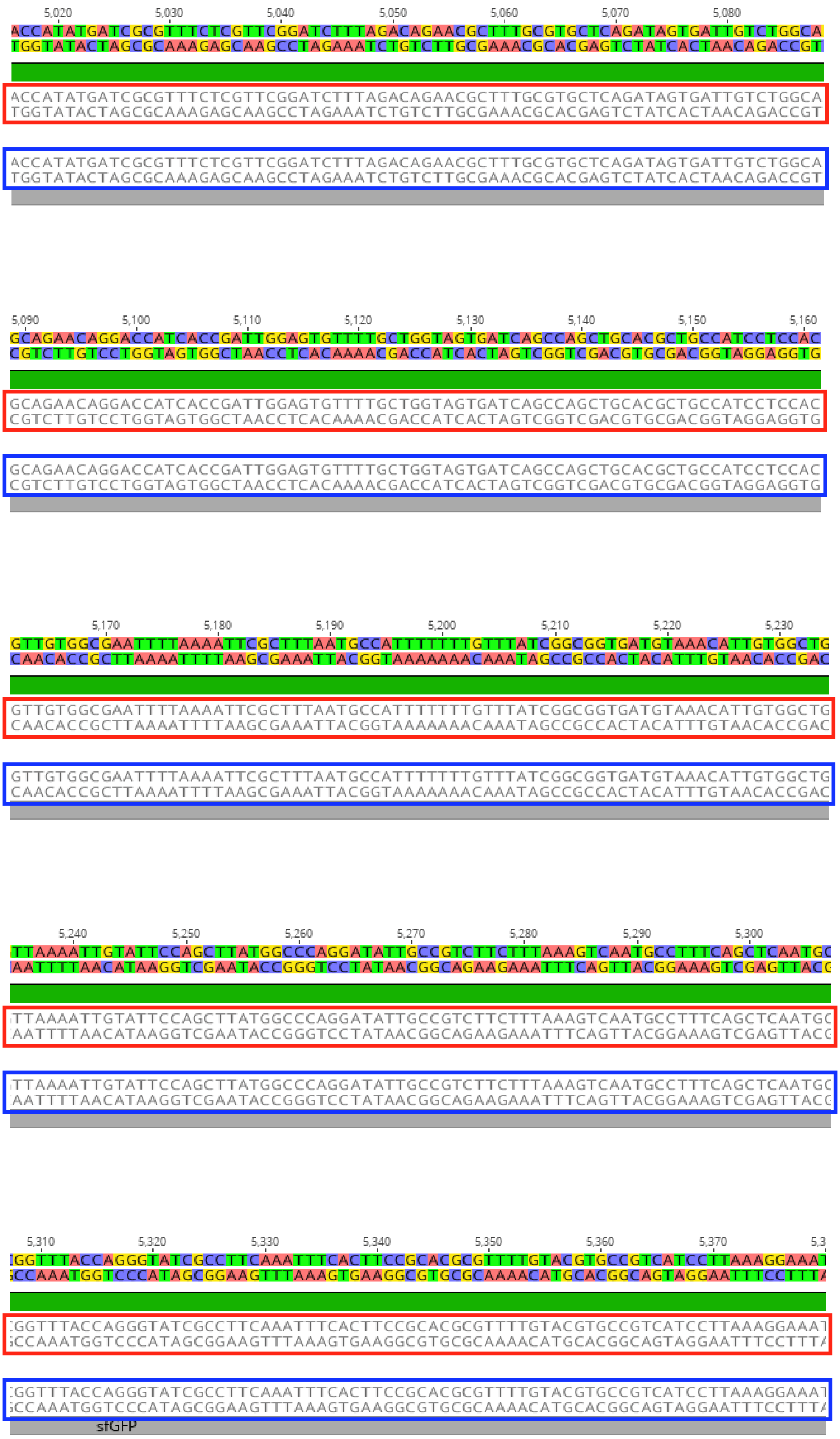
sfGFP

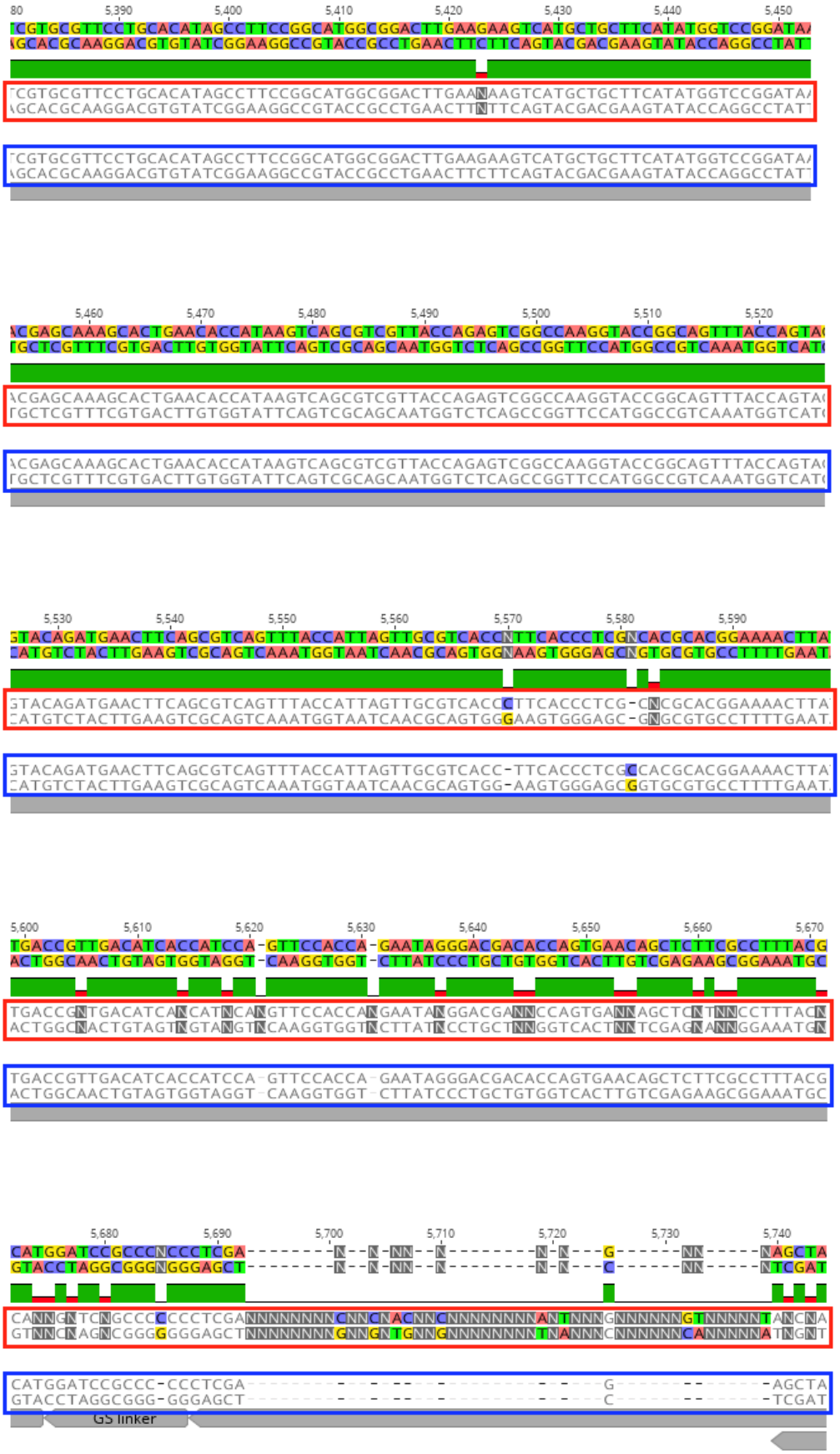
GS linker

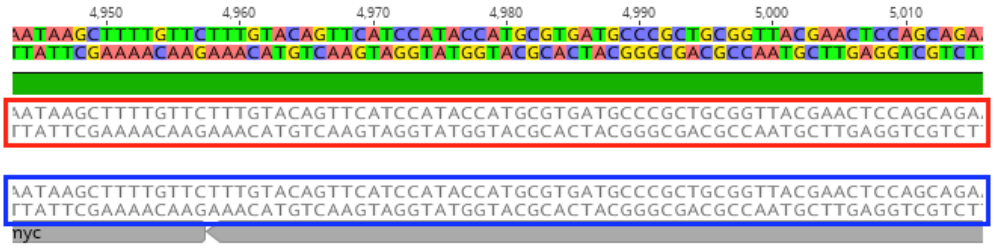
4,950
4,960
4,970
4,980
4,990
5,000
5,010
nyc

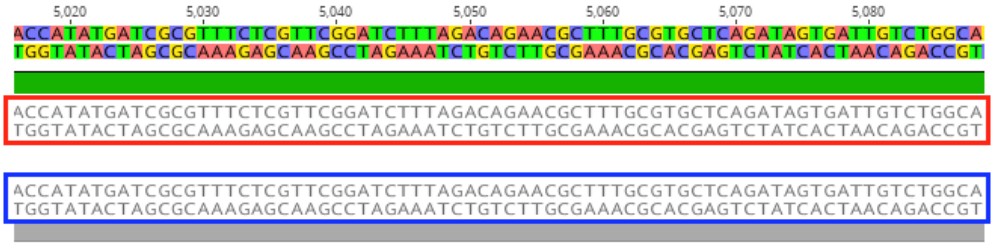
5,020
5,030
5,040
5,050
5,060
5,070
5,080

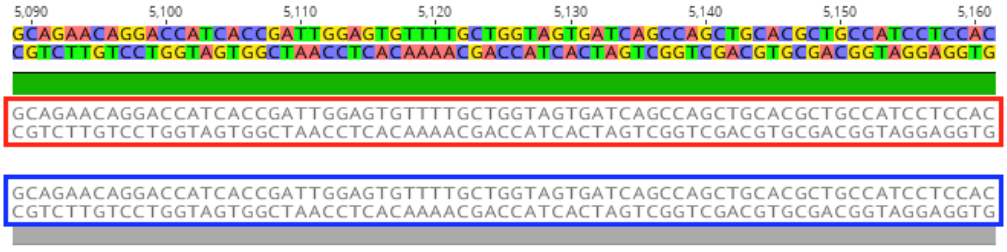
5,090
5,100
5,110
5,120
5,130
5,140
5,150
5,160

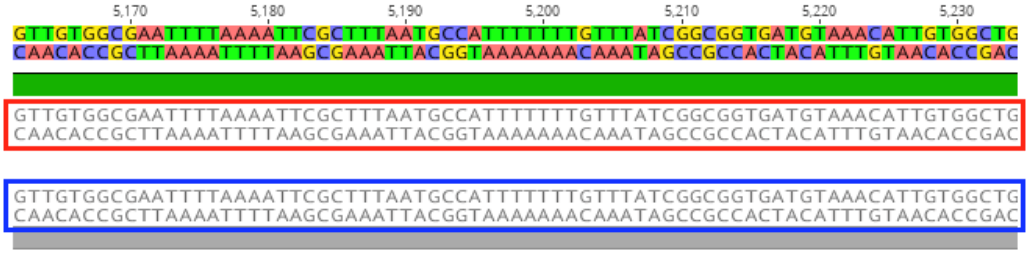
5,170
5,180
5,190
5,200
5,210
5,220
5,230

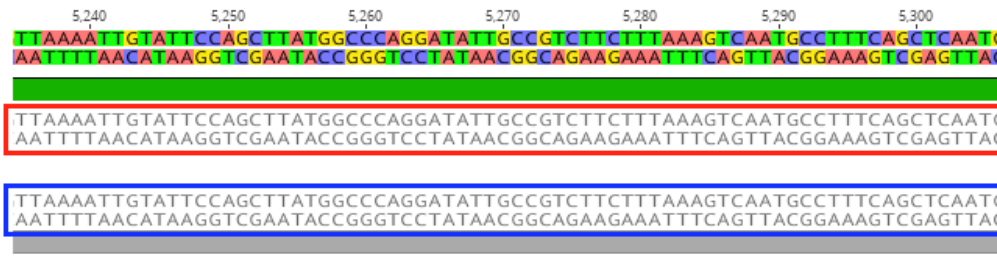
5,240
5,250
5,260
5,270
5,280
5,290
5,300

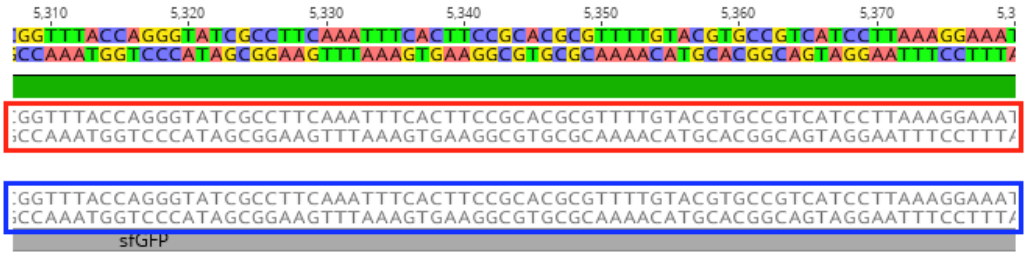
5,310
5,320
5,330
5,340
5,350
5,360
5,370
sfGFP

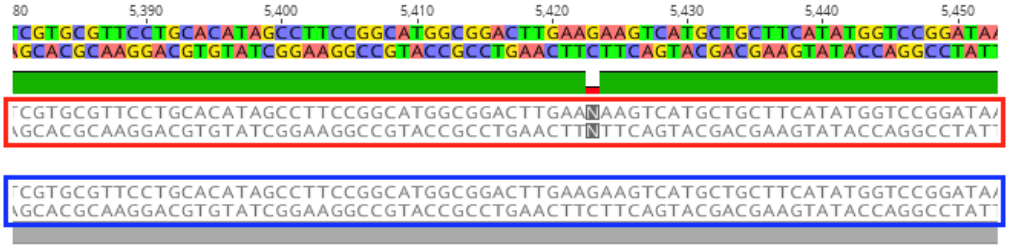
5,390
5,400
5,410
5,420
5,430
5,440
5,450

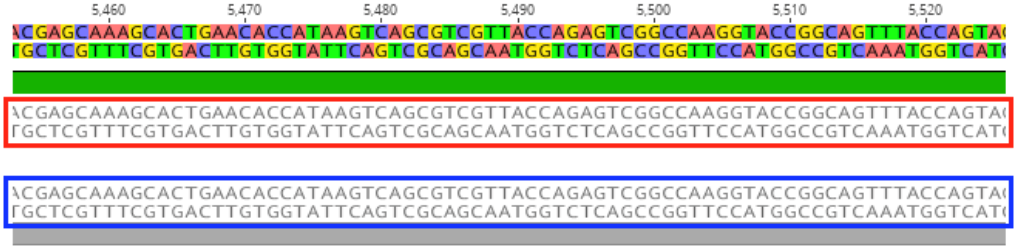
5,460
5,470
5,480
5,490
5,500
5,510
5,520

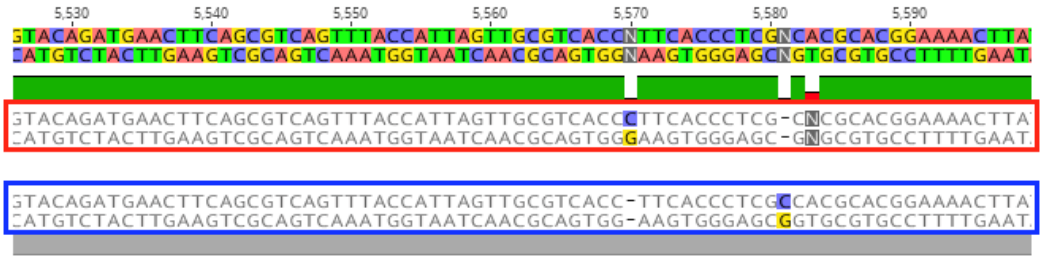
5,530
5,540
5,550
5,560
5,570
5,580
5,590

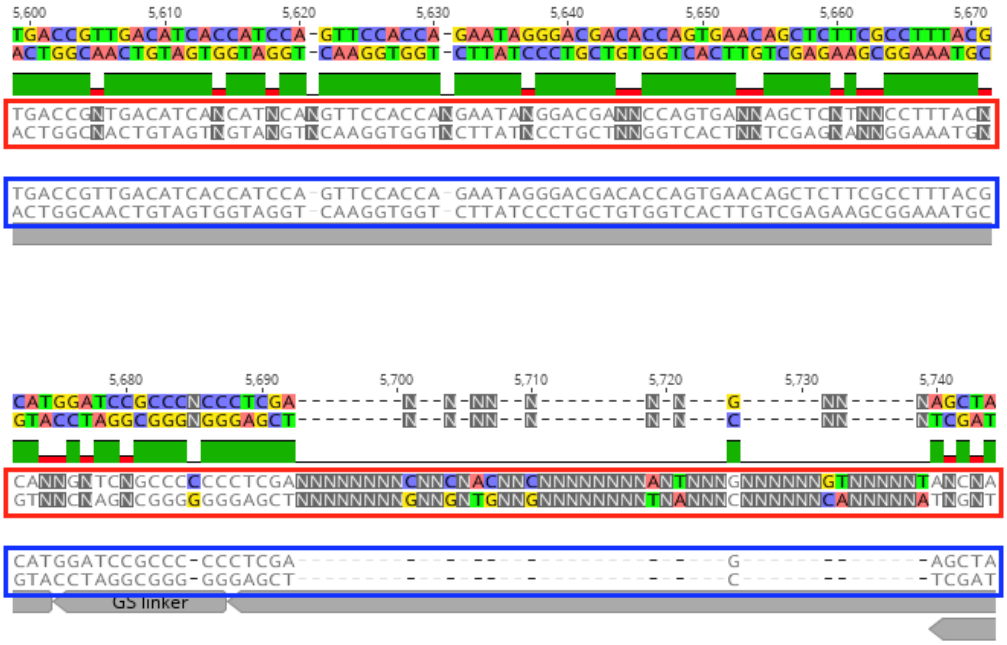

Figure D.5: Sequencing result of sfGFP from pETcon_ Amyloid-β_{42}_sfGFP

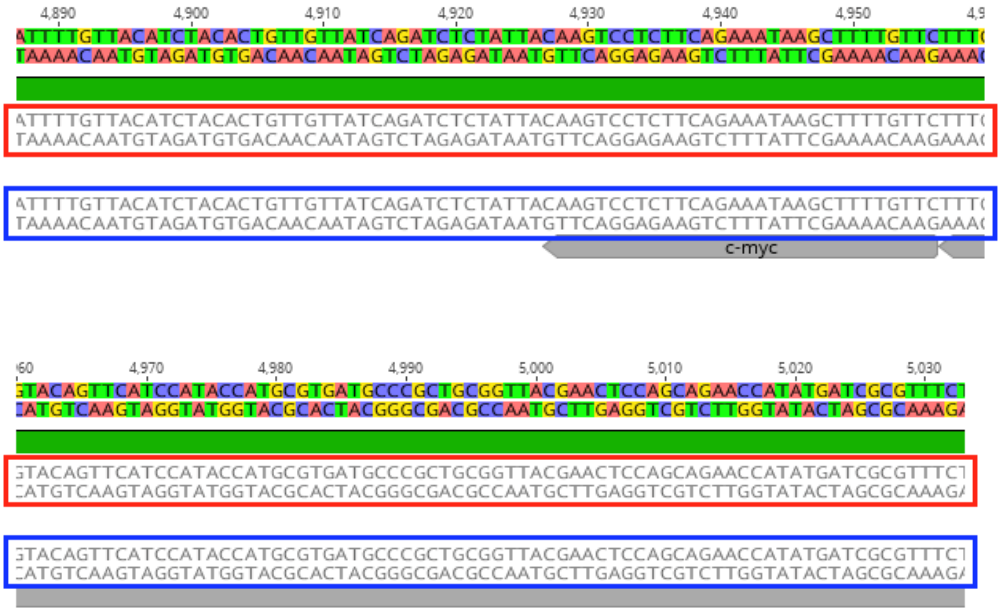

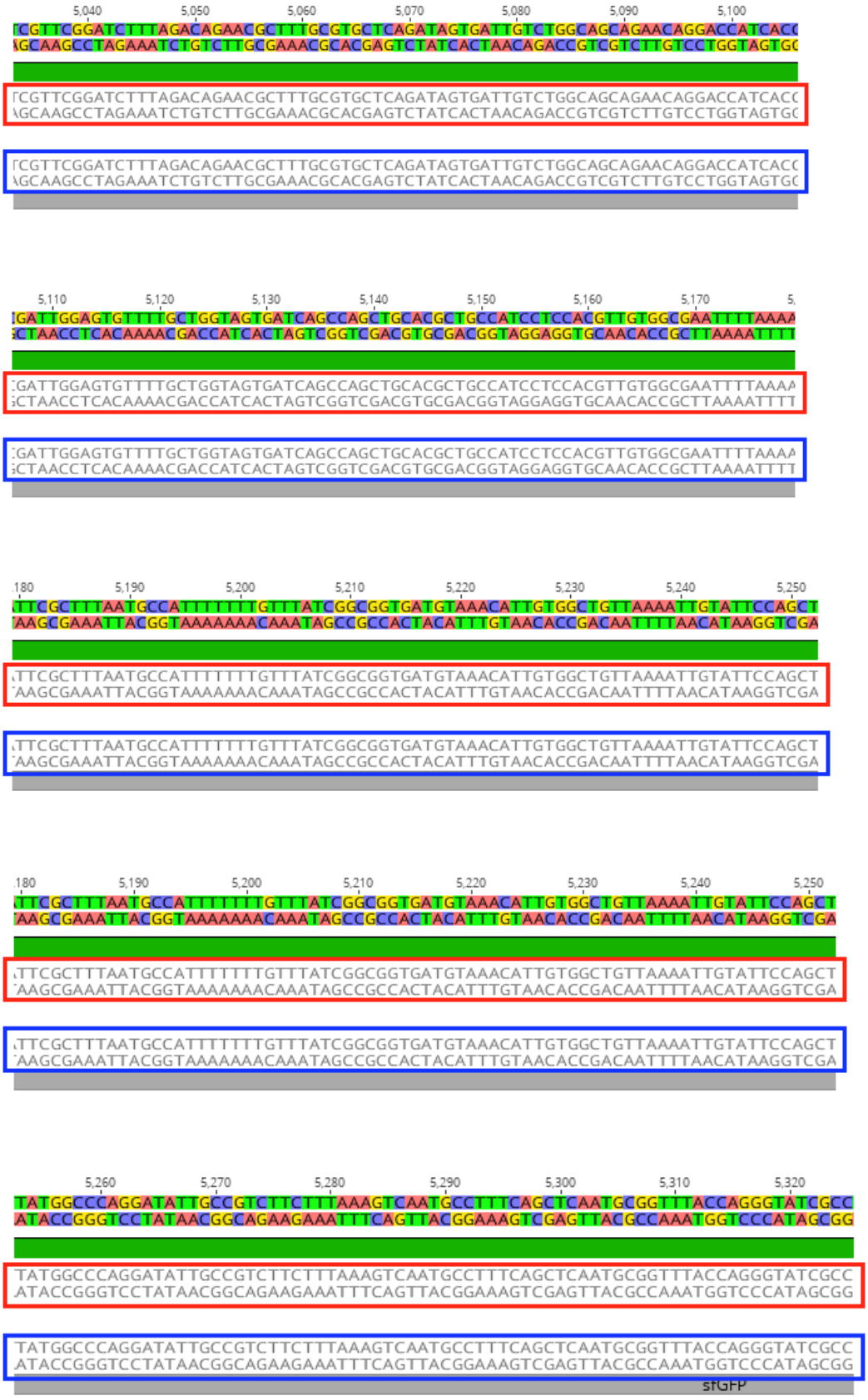
5,040
5,050
5,060
5,070
5,080
5,090
5,100
5,110
5,120
5,130
5,140
5,150
5,160
5,170
5,180
5,190
5,200
5,210
5,220
5,230
5,240
5,250
5,260
5,270
5,280
5,290
5,300
5,310
5,320
sfGFP

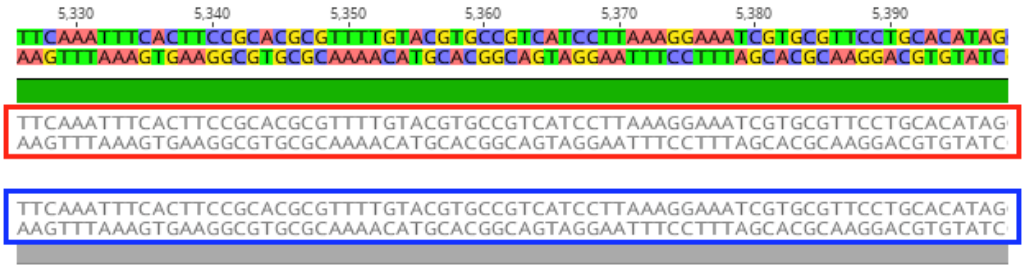
5,330
5,340
5,350
5,360
5,370
5,380
5,390
TTCAAATTTCACTTCCGCACGCGTTTTGTACGTGCCGTCATCCTTAAAGGAAATCGTGCGTTCCTGCACATAG
AAGTTTAAAGTGAAGGCGTGCGCAAAACATGCACGGCAGTAGGAATTTCCTTTAGCACGCAAGGACGTGTATC

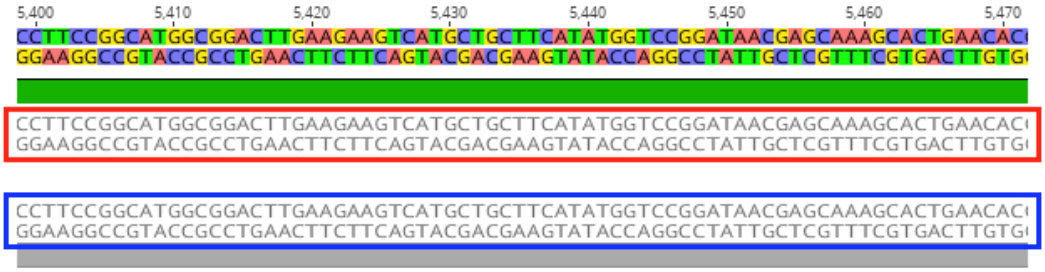
5,400
5,410
5,420
5,430
5,440
5,450
5,460
5,470
CCTTCCGGCATGGCGGACTTGAAGAAGTCATGCTGCTTCATATGGTCCGGATAACGAGCAAAGCACTGAACAC
GGAAGGCCGTACCGCCTGAACTTCTTCAGTACGACGAAGTATACCAGGCCTATTGCTCGTTTCGTGACTTGTG

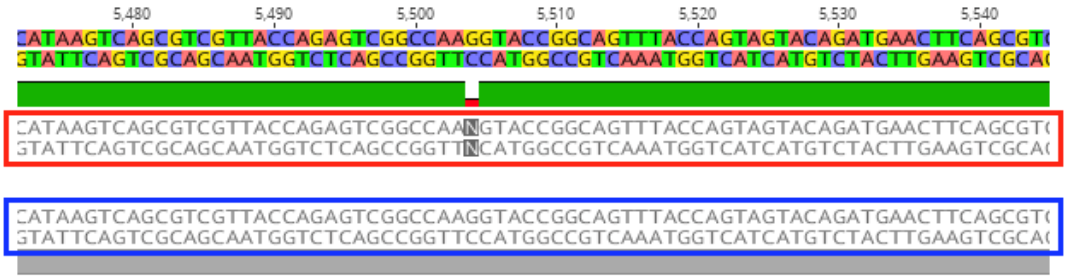
5,480
5,490
5,500
5,510
5,520
5,530
5,540
CATAAGTCAGCGTCGTTACCAGAGTCGGCCAAGGTACCGGCAGTTTACCAGTAGTACAGATGAACTTCAGCGT
GTATTCAGTCGCAGCAATGGTCTCAGCCGGTTCCATGGCCGTCAAATGGTCATCATGTCTACTTGAAGTCGCA

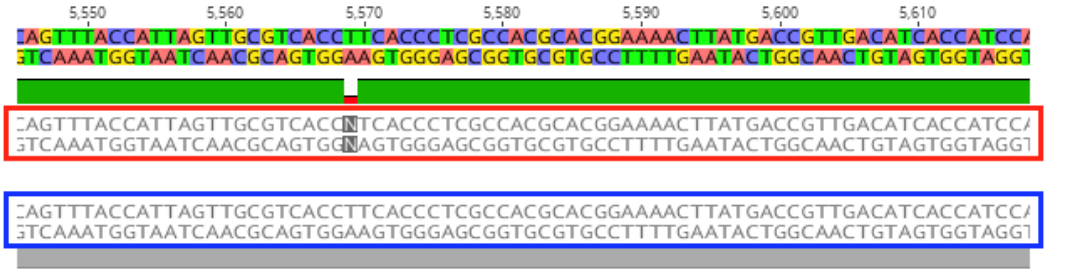
5,550
5,560
5,570
5,580
5,590
5,600
5,610
AGTTTACCATTAGTTGCGTCACCTTCACCCTCGCCACGCACGGAAAACTTATGACCGTTGACATCACCATCC
TCAAATGGTAATCAACGCAGTGGAAGTGGGAGCGGTGCGTGCCTTTTGAATACTGGCAACTGTAGTGGTAGG

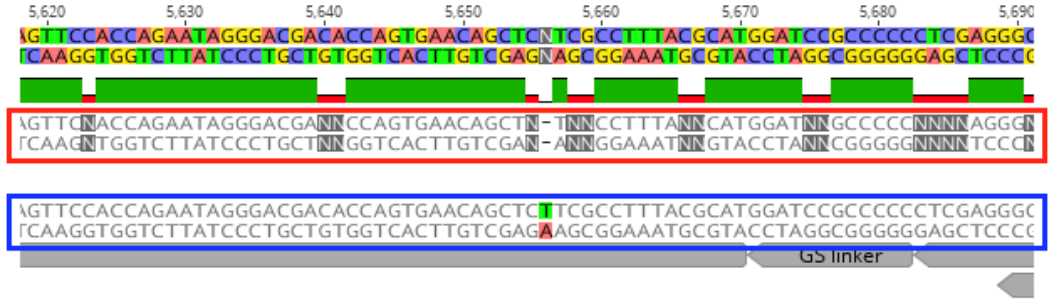

Figure D.6: Sequencing result of sfGFP from pETcon_α-synuclein_sfGFP

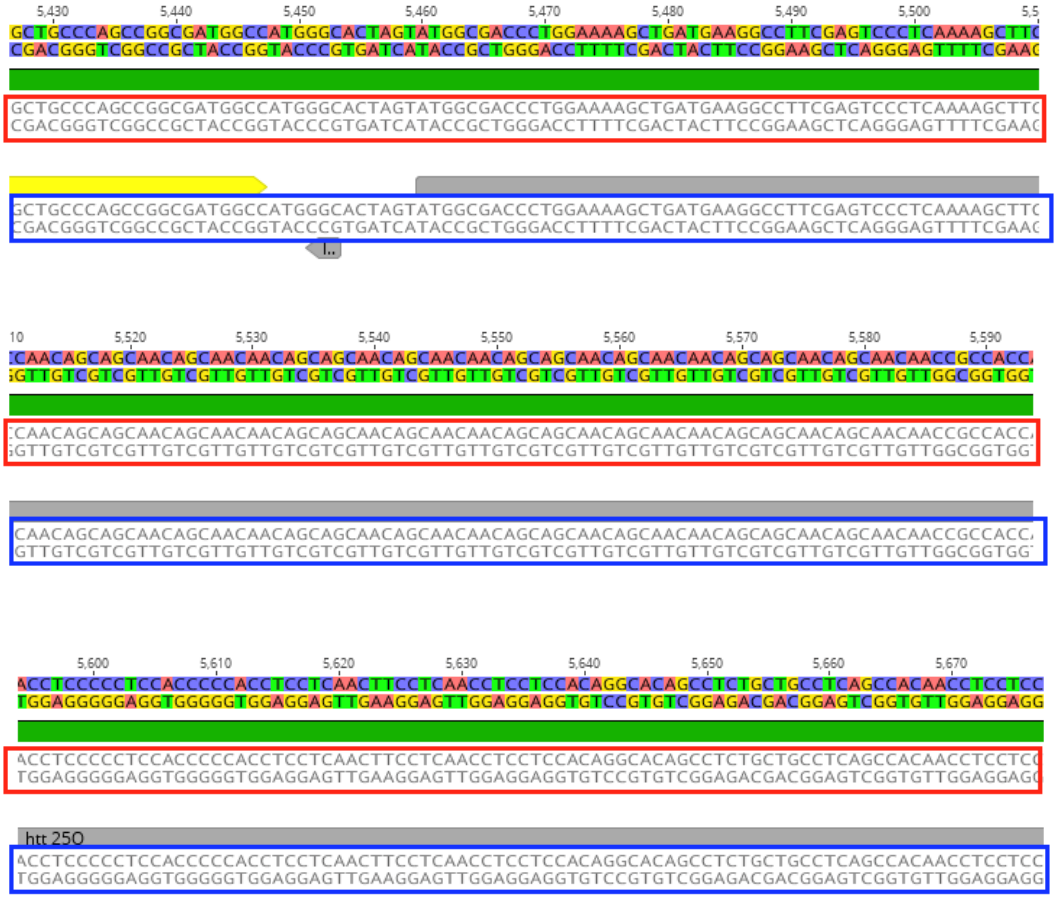

Figure D.7: Sequencing result of 25Q-Htt from pET22b_Ag43_160N_ 25Q-Htt

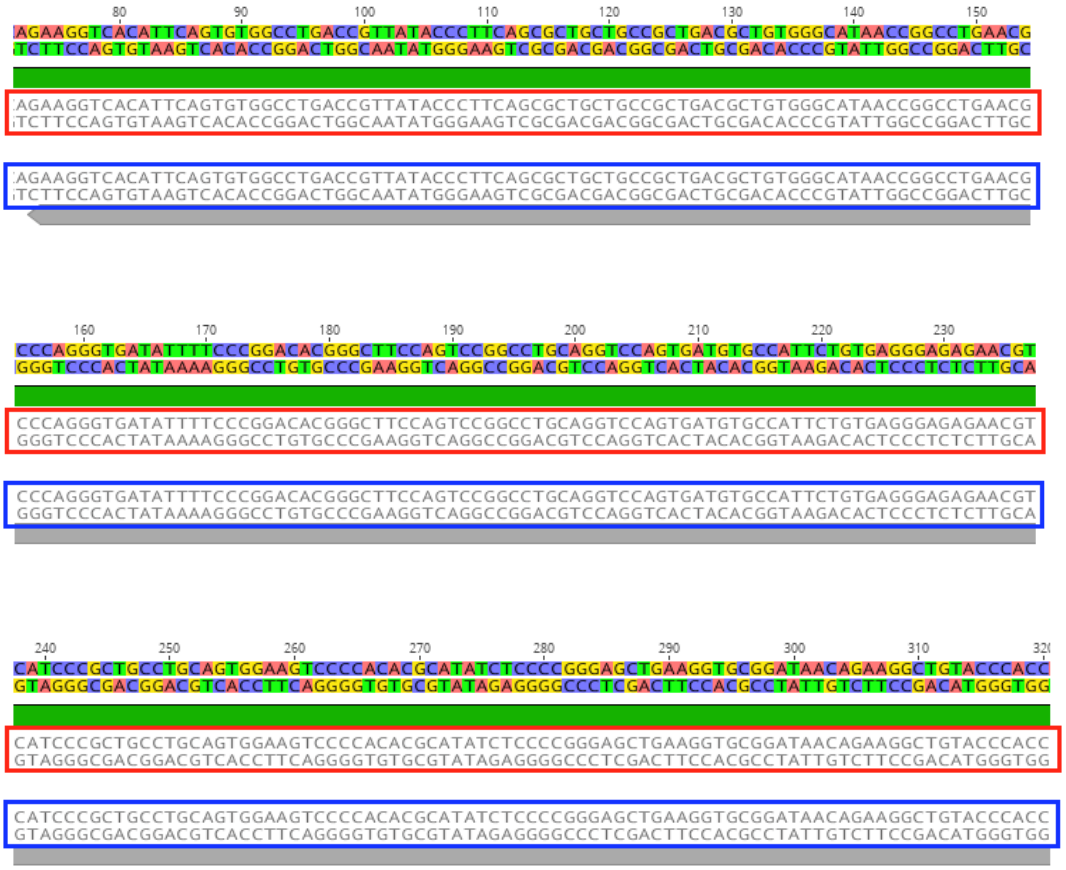

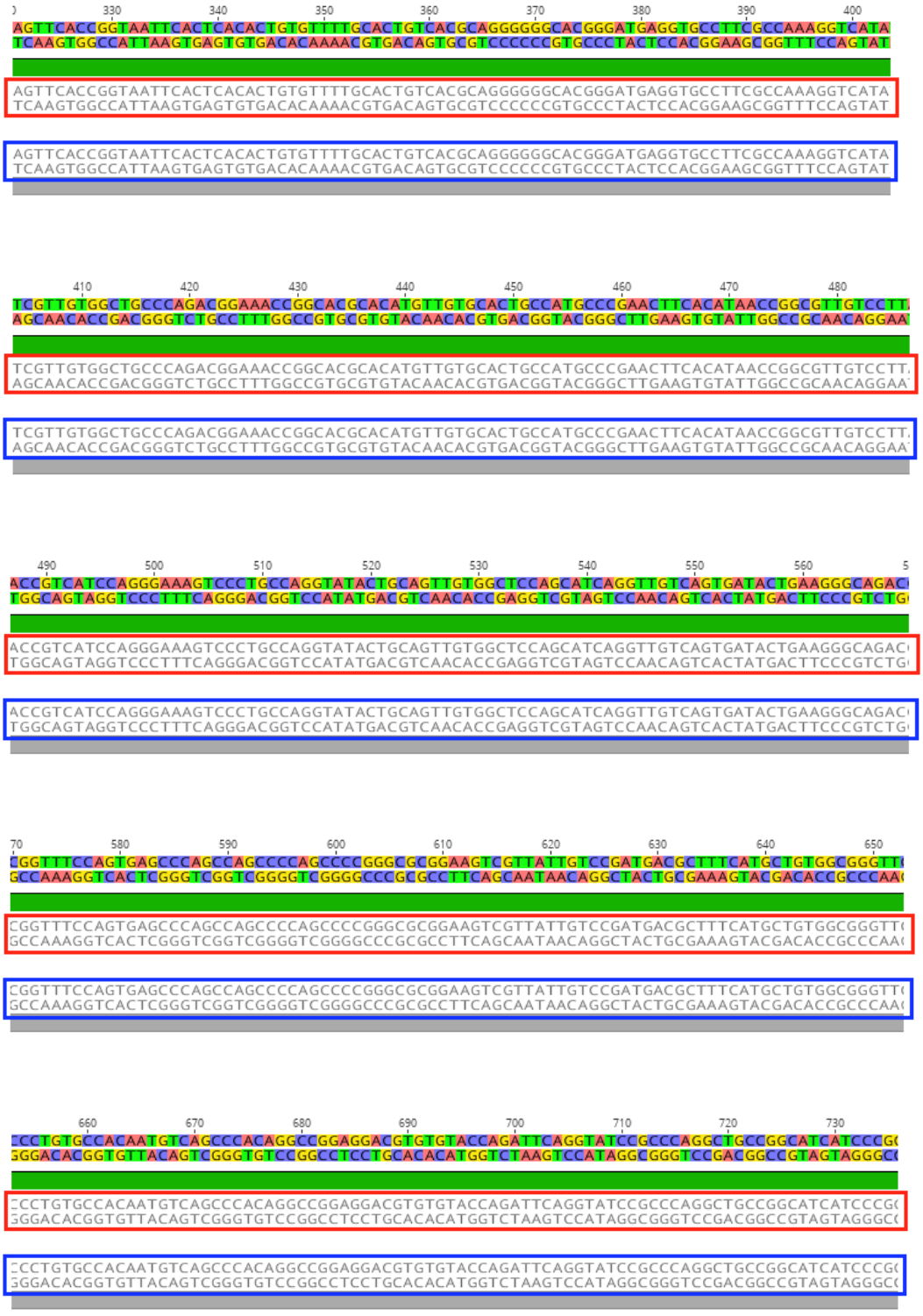
330 340 350 360 370 380 390 400
AGTTCACCGGTAATTCACTCACACTGTGTTTTGCACTGTCACGCAGGGGGGCACGGGATGAGGTGCCTTCGCCAAAGGTCATA
TCAAGTGGCCATTAAGTGAGTGTGACACAAAACGTGACAGTGCGTCCCCCCGTGCCCTACTCCACGGAAGCGGTTTCCAGTAT
410 420 430 440 450 460 470 480
TCGTTGTGGCTGCCCAGACGGAAACCGGCACGCACATGTTGTGCACTGCCATGCCCGAACTTCACATAACCGGCGTTGTCCTT
AGCAACACCGACGGGTCTGCCTTTGGCCGTGCGTGTACAACACGTGACGGTACGGGCTTGAAGTGTATTGGCCGCAACAGGAA
490 500 510 520 530 540 550 560
ACCGTCATCCAGGGAAAGTCCCTGCCAGGTATACTGCAGTTGTGGCTCCAGCATCAGGTTGTCAGTGATACTGAAGGGCAGAC
TGGCAGTAGGTCCCTTTCAGGGACGGTCCATATGACGTCAACACCGAGGTCGTAGTCCAACAGTCACTATGACTTCCCGTCTG
570 580 590 600 610 620 630 640 650
CGGTTTCCAGTGAGCCCAGCCAGCCCCAGCCCCGGGCGCGGAAGTCGTTATTGTCCGATGACGCTTTCATGCTGTGGCGGGTT
GCCAAAGGTCACTCGGGTCGGTCGGGGTCGGGGCCCGCGCCTTCAGCAATAACAGGCTACTGCGAAAGTACGACACCGCCCAA
660 670 680 690 700 710 720 730
CCCTGTGCCACAATGTCAGCCCACAGGCCGGAGGACGTGTGTACCAGATTCAGGTATCCGCCCAGGCTGCCGGCATCATCCCG
GGGACACGGTGTTACAGTCGGGTGTCCGGCCTCCTGCACACATGGTCTAAGTCCATAGGCGGGTCCGACGGCCGTAGTAGGGC

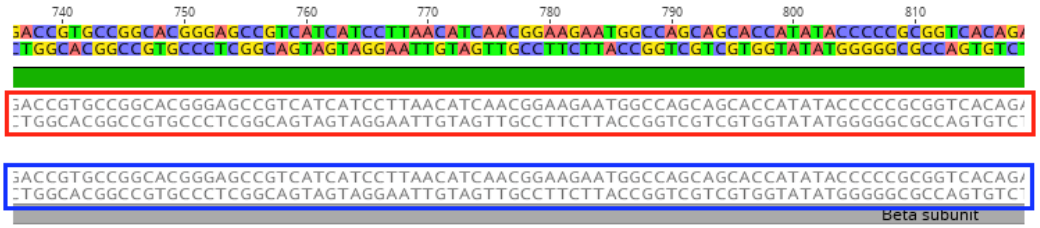
740
750
760
770
780
790
800
810
Beta subunit

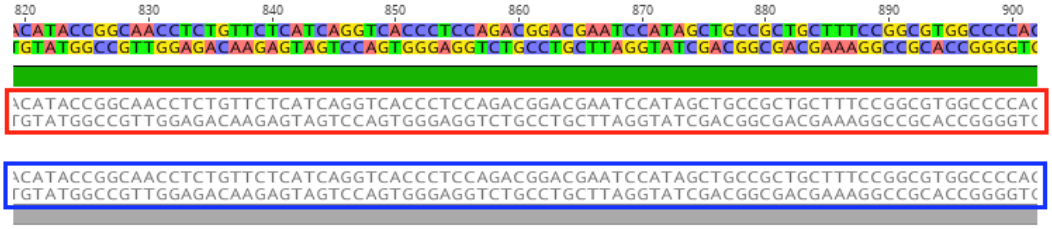
820
830
840
850
860
870
880
890
900

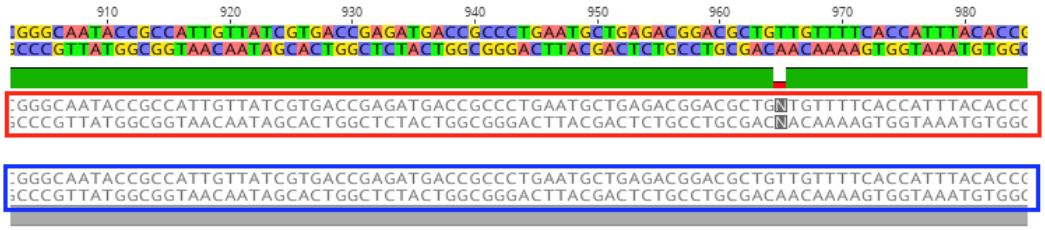
910
920
930
940
950
960
970
980

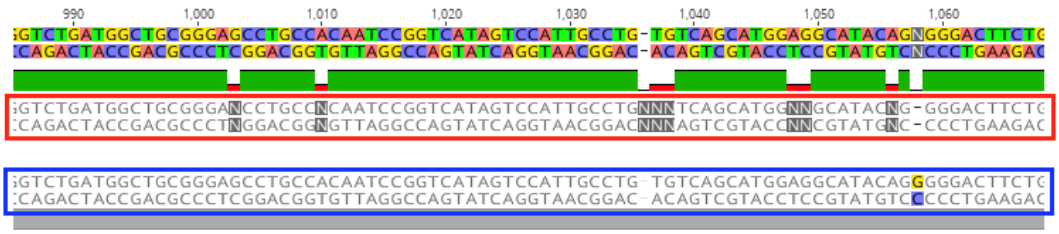
990
1,000
1,010
1,020
1,030
1,040
1,050
1,060

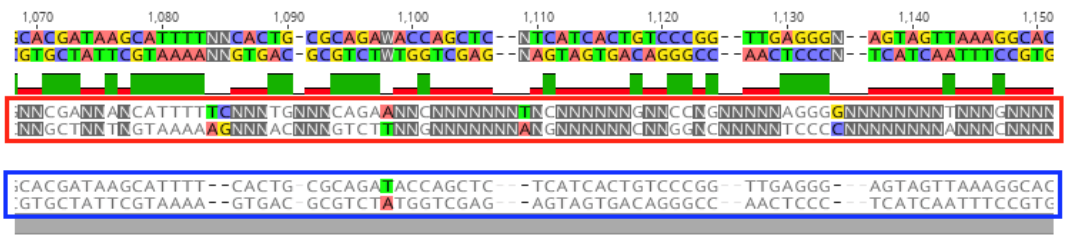
1,070
1,080
1,090
1,100
1,110
1,120
1,130
1,140
1,150

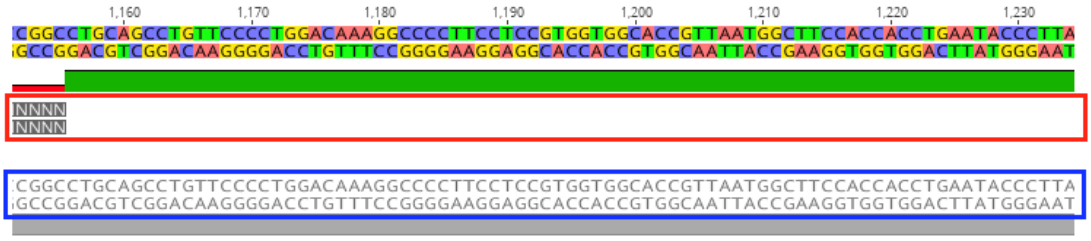

Figure D.8: Sequencing result of β-subunit and α-subunit from pET22b_Ag43_160N_25Q-Htt vector

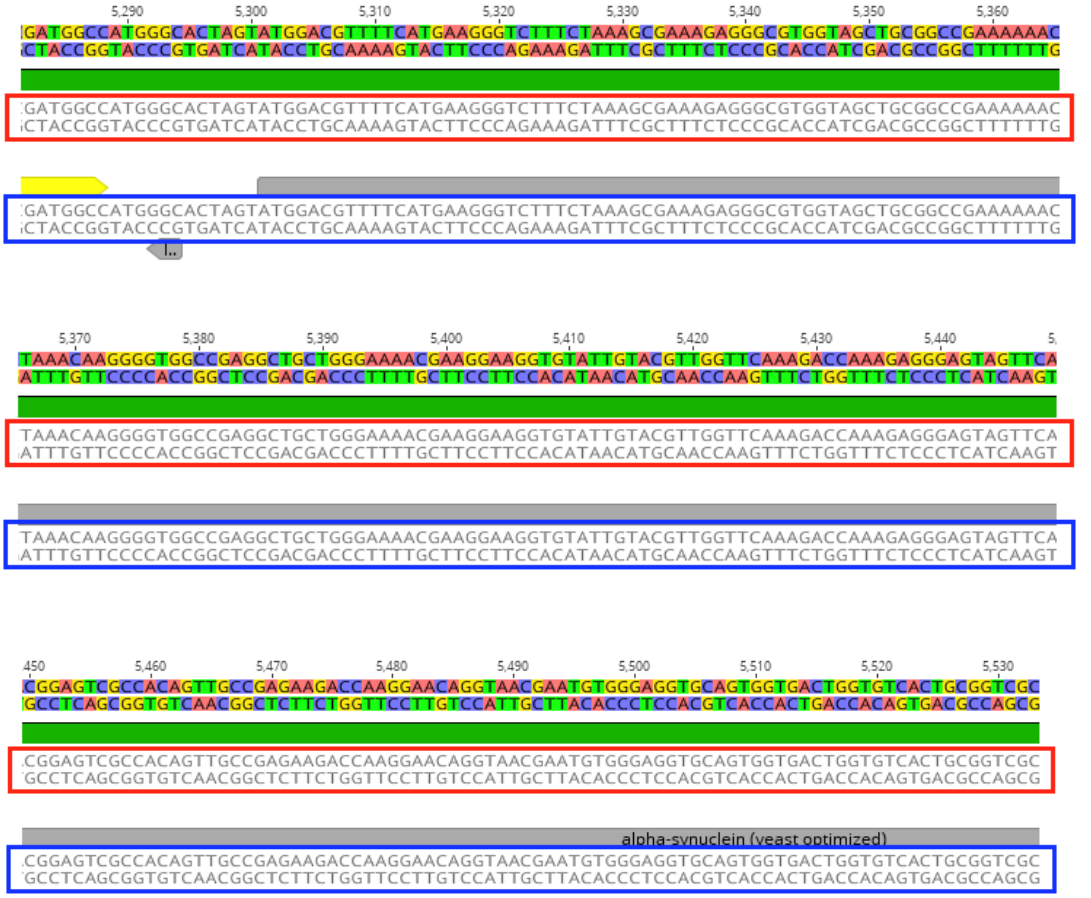

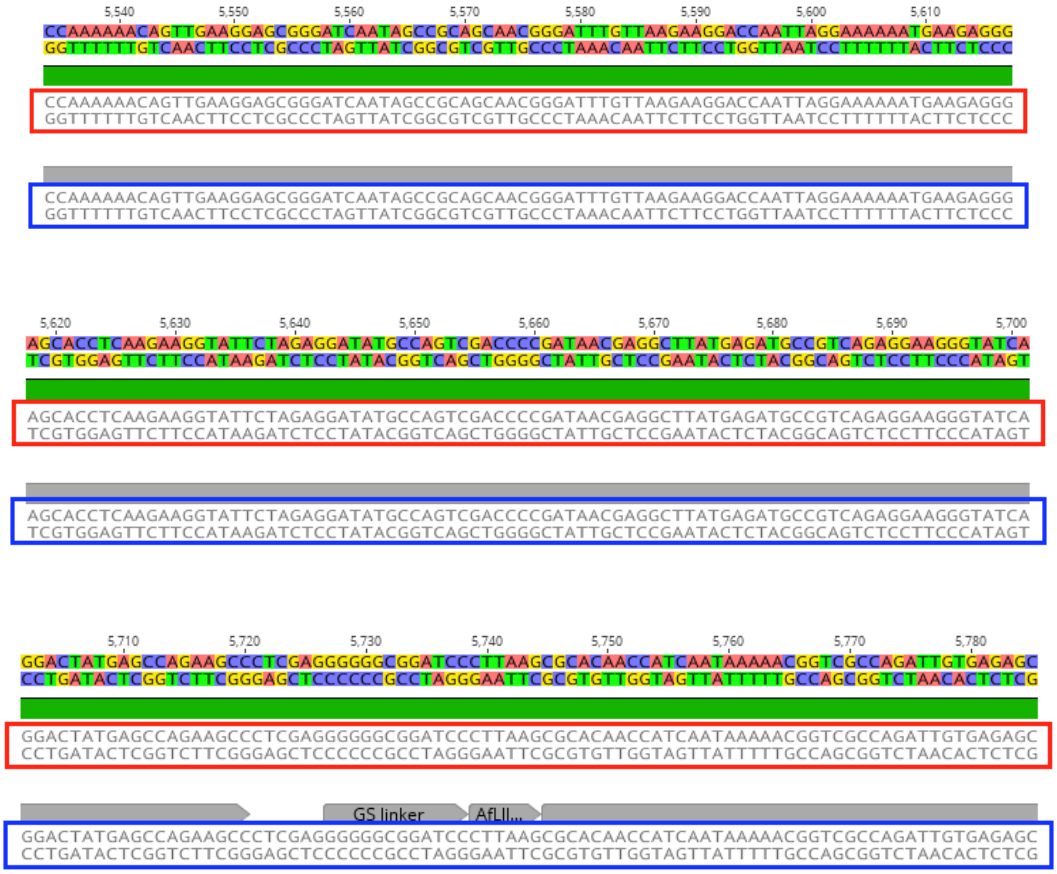

Figure D.9: Sequencing result α-synuclein from pET22b_Ag43_160N_ α-synuclein

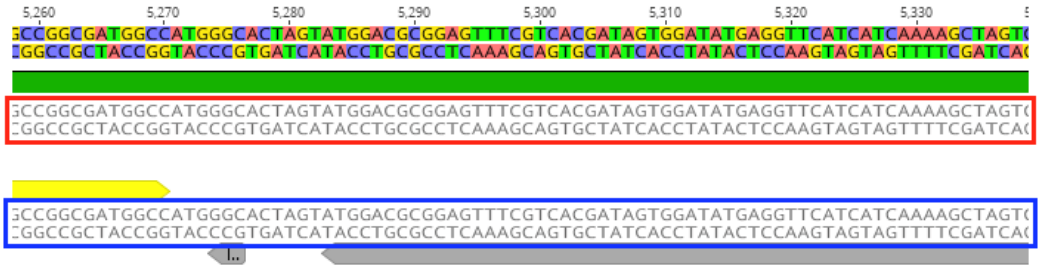

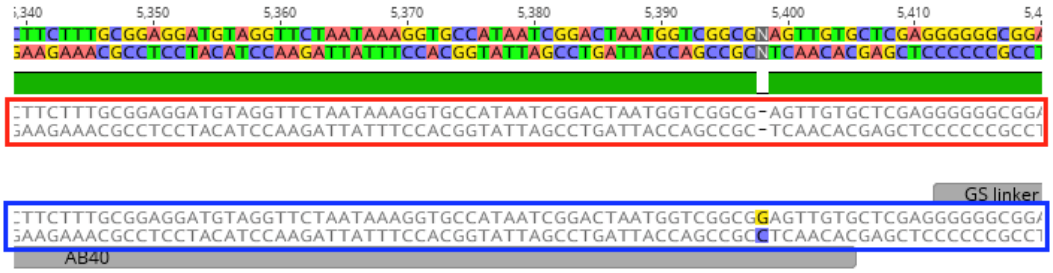

Figure D.10: Sequencing result Amyloid-β_{40} from pET22b_Ag43_160N_ Amyloid-β_{40}

APPENDIX E

Additional reaction recipes and methods

Table E.1: LB growth medium, LB agar and top agar medium recipes

1L of LB Growth Medium Recipe	
H_2O	1000 mL
Tryptone	10 g
Sodium Chloride (NaCl)	5 g
Yeast Extract	5 g
Agar (for Preparing Top Agar)	7 g
Agar (for Preparing LB Agar)	15 g

Table E.2: SOC growth medium recipe

SOC Medium Recipe	
Tryptone	2%
Yeast Extract	0.5%
Sodium Chloride (NaCl)	10 mM
Potassium Chloride (KCl)	2.5 mM
Magnesium Chloride ($MgCl_2$)	10 mM
Magnesium Sulphate ($MgSO_4$)	10 mM
Glucose	20 mM

Table E.3: Selective yeast growth medium recipe

Selective Yeast Growth Medium Recipe	
ddH_2O	50 mL
Yeast Nitrogen Base w/o amino acids	0.335 g
Synthetic Dropout Medium Supplements w/o Trp	0.096 g
Sodium Dihydrogen Phosphate ($NaH_2PO_4.H_2O$)	0.07 M
Disodium Hydrogen Phosphate ($Na_2HPO_4.7H_2O$)	0.07 M
Glucose Monohydrate	0.122 M

Table E.4: Selective yeast induction medium recipe

Selective Yeast Induction Medium Recipe	
ddH_2O	50 mL
Yeast Nitrogen Base w/o amino acids	0.335 g
Synthetic Dropout Medium Supplements w/o Trp	0.096 g
Sodium Dihydrogen Phosphate ($NaH_2PO_4.H_2O$)	0.07 M
Disodium Hydrogen Phosphate ($Na_2HPO_4.7H_2O$)	0.07 M
Galactose	0.1 M

Table E.5: Single restriction enzyme digestion reaction recipe

Restriction Digestion Recipe w/ Single Enzyme	
DNA	500-1000 ng
Restriction Enzyme	1 µL
6X Digestion Buffer	2 µL
Nuclease-Free Water	Completed to 20 µL

Table E.6: Double restriction enzymes digestion reaction recipe

Restriction Digestion Recipe w/ Two Enzymes	
DNA	500-1000 ng
Restriction Enzyme 1	0.4 µL
Restriction Enzyme 2	0.4 µL
6X Digestion Buffer	2 µL
Nuclease-Free Water	Completed to 20 µL

Table E.7: Q5 polymerase PCR recipe

Q5 Polymerase PCR Recipe	
Q5 Polymerase Reaction Buffer	5 µL
GC Enhancer	5 µL
10 µM Forward Primer	1.25 µL
10 µM Reverse Primer	1.25 µL
DNA	10 ng
10 mM dNTP	0.5 µL
Q5 Polymerase	0.25 µL
Nuclease Free Water	Completed to 25µL

Table E.8: Q5 polymerase PCR conditions

Q5 Polymerase Reaction Condition					
Initial Denaturation	**Polymerization (25-35 Cycles)**			**Final Extension**	**Hold**
98ºC	98ºC	50-72ºC	72ºC	72ºC	4-10ºC
30 seconds	5-10 seconds	10-30 seconds	30 seconds/kb	2 minutes	∞

*Tm for polymerization was determined by http://tmcalculator.neb.com/#!/main

Table E.9: Pfu polymerase PCR recipe

Pfu Polymerase PCR Recipe	
Pfu Polymerase Reaction Buffer	2 µL
10 µM Forward Primer	1 µL
10 µM Reverse Primer	1 µL
10 mM dNTP	0.4 µL
DNA	10 ng
Pfu Polymerase	0.2 µL
Nuclease Free Water	Completed to 20µL

Table E.10: Pfu polymerase PCR conditions

Pfu Polymerase Reaction Condition					
Initial Denaturation	**Polymerization (25-35 Cycles)**			**Final Extension**	**Hold**
95ºC	95ºC	42-65ºC	72ºC	72ºC	4-10ºC
2 minutes	30 seconds	30 seconds	2 minutes/kb	5 minutes	∞

*Tm for polymerization was determined by http://tmcalculator.neb.com/#!/main

Table E.11: Gibson assembly reaction recipe

Gibson Assembly Mix Recipe (1.33X)	
Taq Ligase (40 u/µL)	50 µL
5X Isothermal Buffer	100 µL
T5 Exonuclease (1u/µL)	2 µL
Phusion Polymerase (2u/µL)	6.25 µL
Nuclease-Free Water	216.75 µL

Table E.12: T4 ligase reaction recipe

T4 Ligation Reaction Recipe	
T4 DNA Ligase Buffer (10X)	2 µL
Vector DNA (Backbone)	50 ng
Insert DNA	Equal M to vector
T4 DNA Ligase	1 µL
Nuclease-Free Water	Completed to 20 µL

Table E.13: ss-Oligonucleotide annealing recipe for Klenow fragment amplification

Annealing Reaction Recipe for Klenow Reaction	
ssDNA	5 µg
Annealing Primer	3M Equivalents of ssDNA
1X TE/ 100mM NaCl	Completed to 50 µL

Table E.14: Klenow fragment amplification reaction recipe

Klenow Reaction Recipe	
10X NEBuffer2	20 µg
Annealed Duplex	50 µL
10 mM dNTP	8 µL
Klenow Fragment (5u/µL)	3 µL
Nuclease-Free Water	119 µL

Table E.15: 8% nondenaturing polyacrylamide gel recipe

8% Nondenaturing Polyacrylamide Gel Recipe	
30% Acry:Bis	3.2 mL
5X TBE	2.4 mL
10% APS	200 µL
TEMED	10 µL
ddH_2O	6.4 mL